# A Novel Modular Approach to Active Power-Line Harmonic Filtering in Distribution Systems

by

Ramadan A. El Shatshat

A thesis
presented to the University of Waterloo
in fulfillment of the
thesis requirement for the degree of
Doctor of Philosophy
in
Electrical and Computer Engineering

Waterloo, Ontario, Canada, 2001

The University of Waterloo requires the signatures of all persons using or photocopying this thesis. Please sign below, and give address and date.

*DEDICATED TO MY PARENTS,*

*WIFE*

*AND CHILDREN*

.....

# Acknowledgements

First and foremost, I would like to thank and praise Allah almighty for enlightening my way and directing me through each and every success I have or may reach.

I would like to thank my supervisors, Dr. M. M. A. Salama and M. Kazerani, for their guidance and insight throughout the duration of this study. Their enthusiasm and steadfast support were invaluable to me.

My thanks also go to members of the Electrical and Computer Engineering department, especially Wendy Boles for her endless support and help in solving my problems and Gini Ivan-Roth for her everlasting help.

I would also like to thank the educational ministry of Libya for the financial support and continued assistance throughout the course of my studies at the University of Waterloo.

I would like to thank my family for their constant love and encouragement.

Finally, I express my gratitude to my wife for her patience and her moral support through the most difficult periods of this work.

# Abstract

Recently, AC distribution systems have experienced high harmonic pollution due to the wide use of power electronic loads. These non-linear loads generate harmonics which degrade the distribution systems and may affect the communication and control systems. Harmonic filters, in general, are designed to reduce the effects of harmonic penetration in power systems and they should be installed when it has been determined that the recommended harmonic content has been exceeded.

Two approaches have been proposed to reduce the effect of the harmonic distortion, namely active filtering approach and passive filtering approach. Passive filters have the demerits of large size, resonance and fixed compensation. In the active filtering approach, the harmonic currents produced by the nonlinear loads are extracted, and their opposites are generated and injected into the power line using a power converter. Several active filtering approaches based on different circuit topologies and control theories have been proposed. Most of these active filter systems consist mainly of a single PWM power converter with a high rating which takes care of all the harmonic components in the distorted signal. The combination of high power and high switching frequency results in excessive amounts of power losses. Furthermore, the reliability of the existing active filters is a major concern, as the failure of converter results in no compensation at all.

Active power line filtering can be performed in the time domain or in frequency domain. A distinct advantage of the frequency-domain techniques is the possibility of

selective harmonic elimination, thanks to the availability of information on individual harmonic components.

The objective of this research is to develop an efficient and reliable modular active harmonic filter system to realize a cost-effective solution to the harmonic problem. The proposed filter system consists of a number CSC modules, each dedicated to filter a specific harmonic of choice (Frequency-Splitting Approach). The power rating of the modules will decrease and their switching frequency will increase as the order of the harmonic to be filtered is increased. The overall switching losses are minimized due to the selected harmonic elimination and balanced a "power rating"-"switching frequency" product.

Two ADALINEs are proposed as a part of the filter controller for processing the signals obtained from the power-line. One ADALINE (the Current ADALINE) extracts the fundamental and harmonic components of the distorted current. The other ADALINE (the Voltage ADALINE) estimates the line voltage. The outputs of both ADALINEs are used to construct the modulating signals of the filter modules. The proposed controller decides which CSC filter module(s) is connected to the electric grid. The automated connection of the corresponding filter module(s) is based on decision-making rules in such a way that the IEEE 519-1992 limits are not violated. The information available on the magnitude of each harmonic component allows us to select the active filter bandwidth (i.e., the highest harmonic to be suppressed). This will result in more efficiency and higher performance. The proposed controller adjusts the $I_{dc}$ in each CSC module according to the present magnitude of the corresponding harmonic current. This results in optimum dc-side current value and minimal converter losses.

The comparison of the proposed modular active filter scheme and the conventional one converter scheme on practical use in industry is presented. This comparison shows that the proposed solution is more economical, reliable and flexible compared to conventional one.

High speed and accuracy of ADALINE, self-synchronizing harmonic tracking, intelligence and robustness of the controller, optimum $I_{dc}$ value, minimal converter losses, and high speed and low dc energy requirement of the CSC, are the main features of the proposed active filter system.

Simulation results using the EMTDC simulation package are presented to validate the effectiveness of the proposed modular active filter system.

# Table of Contents


**CHAPTER 1 INTRODUCTION** 1

**1.1 POWER QUALITY CONCERNS** 1
**1.2 OBJECTIVES AND CONTRIBUTIONS** 7
**1.3 ORGANIZATION** 10

**CHAPTER 2 BACKGROUND AND LITERATURE REVIEW** 12

**2.1 OVERVIEW** 12
**2.2 HARMONICS AS A POWER QUALITY PROBLEM** 13
2.2.1 HARMONIC DISTORTION INDICES 14
2.2.2 SOURCES OF HARMONICS 17
2.2.3 EFFECTS OF HARMONICS 18
2.2.4 HARMONIC DISTRIBUTION IN DISTRIBUTION SYSTEMS 19
**2.3 HARMONIC MITIGATION TECHNIQUES** 20
2.3.1 PASSIVE HARMONIC FILTERS 21
2.3.2 ACTIVE HARMONIC FILTERS 22
**2.4 LITERATURE REVIEW ON ACTIVE POWER FILTERS** 26
2.4.1 MAGNETIC FLUX COMPENSATION 26
2.4.2 INJECTION OF A SPECIFIC HARMONIC CURRENT 28
2.4.3 ACTIVE HARMONIC FILTERING USING PWM CONVERTERS 28
2.4.4 HYBRID FILTERS 30
2.4.5 UNIFIED POWER QUALITY CONDITIONER (UPQC) 32
2.4.6 CONFIGURATION FOR HIGH POWER APPLICATIONS (MULTI LEVEL CONVERTERS) 33
**2.5 CONCLUDING REMARKS ON EXISTING ACTIVE POWER FILTERS** 35

**CHAPTER 3 HARMONIC ESTIMATION TECHNIQUES** 37

**3.1 OVERVIEW** 37
**3.2 DISCRETE FOURIER TRANSFORM (DFT)** 38
**3.3 HARMONIC ESTIMATION USING KALMAN FILTER** 40
3.3.1 STATE-SPACE MODEL OF A TIME VARYING SIGNAL 41

3.3.2 KALMAN FILTER ALGORITHM 44
**3.4 HARMONIC ESTIMATION USING ARTIFICIAL NEURAL NETWORKS 46**
3.4.1 ADAPTIVE LINEAR NEURON (ADALINE) 48
3.4.1.1 Widrow-Hoff learning rule 50
3.4.2 ADALINE AS HARMONIC ESTIMATOR 50
**3.5 EVALUATION OF THE ESTIMATION TECHNIQUES 52**
3.5.1 SPEED AND CONVERGENCE 52
3.5.2 HARMONIC ESTIMATION IN THE PRESENCE OF NOISE AND DECAYING DC COMPONENTS 54
3.5.3 HIGH SAMPLING RATE 54
3.5.4 SIMPLICITY AND PRACTICAL APPLICABILITY 56
3.5.5 FREQUENCY TRACKING 56
**3.6 SUMMARY 59**

**CHAPTER 4 ACTIVE POWER FILTERING 61**

**4.1 OVERVIEW 61**
**4.2 CONFIGURATION OF THE ACTIVE SOURCE 62**
**4.3 THE SINUSOIDAL-PULSE-WIDTH MODULATION (SPWM) SWITCHING STRATEGY 65**
**4.4 TRI-LOGIC PWM CURRENT SOURCE CONVERTER 69**
**4.5 THE LOSSES IN THE SWITCHING DEVICES 70**
4.5.1 ON-STATE (CONDUCTION) LOSSES 70
4.5.2 SWITCHING LOSSES 71
**4.6 VSC TOPOLOGY VERSUS CSC TOPOLOGY 75**
**4.7 SUMMARY 75**

**CHAPTER 5 THE PROPOSED MODULAR ACTIVE POWER FILTER SYSTEM 77**

**5.1 MOTIVATION 77**
**5.2 A NEW APPROACH TO MODULAR ACTIVE POWER FILTERS 79**
**5.3 THE PRINCIPLE OF THE PROPOSED FILTERING TECHNIQUE 81**
**5.4 SYSTEM CONFIGURATION 82**
**5.5 COMPENSATION PRINCIPLE 83**
**5.6 CONTROL SCHEME 85**
**5.7 MASTER CONTROLLER LOGIC 87**
**5.8 IMPROVED ADALINE-BASED HARMONIC ANALYZER 88**
**5.9 APPLICATION TO 3-PHASE 3-WIRE DISTRIBUTION SYSTEMS 91**

5.9.1 SYSTEM CONFIGURATION AND CONTROL SCHEME 92
**5.10 DIGITAL SIMULATION RESULTS 97**
5.10.1 TRACKING OF THE HARMONIC COMPONENTS AND THE FUNDAMENTAL FREQUENCY VARIATIONS 97
5.10.2 PERFORMANCE OF SINGLE-PHASE MODULAR ACTIVE POWER FILTER 99
5.10.2.1 Steady-State Performance 99
5.10.2.2 Transient Performance 104
5.10.3 PERFORMANCE OF THREE-PHASE MODULAR ACTIVE POWER FILTER 108
**5.11 SUMMARY 112**

**CHAPTER 6 POWER-SPLITTING APPROACH TO ACTIVE HARMONIC FILTERING 115**

**6.1 OVERVIEW 115**
**6.2 SYSTEM CONFIGURATION AND CONTROL SCHEME 116**
**6.3 SIMULATION RESULTS 120**
6.3.1 STEADY-STATE PERFORMANCE 120
6.3.2 TRANSIENT PERFORMANCE 121
**6.4 SUMMARY 124**

**CHAPTER 7 POWER AND CONTROL CIRCUITS DESIGN 125**

**7.1 OVERVIEW 125**
**7.2 DESIGN OF ACTIVE FILTER MODULE 126**
7.2.1 POWER CIRCUIT 126
7.2.2 ENERGY STORAGE ELEMENT 126
7.2.3 OUTPUT FILTER CAPACITOR 128
**7.3 DESIGN EXAMPLE 128**
**7.4 MODULAR ACTIVE POWER FILTER CONTROL 129**
7.4.1 THE SYSTEM EQUATIONS 133
7.4.2 CONTROLLER DESIGN 140
**7.5 SUMMARY 144**

**CHAPTER 8 EVALUATION OF THE PROPOSED MODULAR APPROACH 145**

**8.1 OVERVIEW 145**
**8.2 FREQUENCY SPLITTING VERSUS SINGLE CONVERTER 146**
8.2.1 ECONOMICAL COMPARISON 146

8.2.2 RELIABILITY 149
8.2.3 FLEXIBILITY 149
**8.3 FREQUENCY-SPLITTING APPROACH VERSES POWER-SPLITTING APPROACH 150**
8.3.1 POWER RATING 150
8.3.2 DC TERM: $I_{dc}$ 150
8.3.3 IDENTICAL MODULES 151
8.3.4 CONDUCTION LOSSES 151
8.3.5 SWITCHING LOSSES 152
8.3.6 ECONOMICAL COMPARISON 153
8.3.7 RELIABILITY 155
8.3.8 FLEXIBILITY 156
8.3.9 STEADY-STATE PERFORMANCE 157
**8.4 SUMMARY 158**

**CHAPTER 9 CONCLUSIONS AND FUTURE WORK 160**

**LIST OF PUBLICATIONS 168**

**APPENDIX (A) DISCRETE FOURIER TRANSFORM 170**

**APPENDIX (B) ARTIFICIAL NEURAL NETWORK 172**

**APPENDIX (C) SYSTEM PARAMETERS 178**

**APPENDIX (D) COST OF ELECTRICITY 182**

**APPENDIX (E) CONDUCTION LOSSES AND SWITCHING LOSSES 182**

**REFERENCES 183**

# List of Figures

2.1 A typical distorted waveform and its harmonic content.....20

2.2 Basic configuration of a typical shunt active power filter.....24

2.3 Harmonic voltage compensator.....25

3.1 Some of Harmonic Extraction Methods.....38

3.2 Adaptive linear neuron ( ADALINE ) .....49

3.3 ADALINE as harmonic components estimator.....51

3.4 Estimated magnitude and phase angle of the fundamental, fifth and seventh harmonics (a) using ADALINE (b) using Kalman filter..... 53

3.5 Estimation of fundamental and fifth harmonic components in the presence of noise and decaying dc components (a) using ADALINE (b) using Kalman filter (c) using FFT.....55

3.6 The influence of high sampling rate on the estimation of fundamental and $5^{th}$ harmonic amplitude (a) using ADALINE (b) using Kalman filter (c) using FFT.....57

4.1 (a) Single-phase and three-phase current-source converter (CSC) (b) Single-phase and three-phase voltage-source converter (VSC).....64

4.2 The simplified version of CSC bridge..... 66

4.3 Sinusoidal Pulse-Width Modulation..... 66

4.4 PWM converter as a linear amplifier.....68

4.5Current Source converter with tri-logic PWM control.....70

4.7 Simplified inductive switching circuit.....74

4.7 Instantaneous switch power loss.....74

5.1 The block diagram of the compensation principle of the proposed active filter system.....81

5.2 The proposed modular active power filter system.....84

5.3 The Control Scheme of the modular active filter (The Controller in Fig. 5.2).....86

5.4: The proposed decision-making logic circuit controller.....88

5.5 The modified ADALINE for estimating of $A_l$ and $B_l$, and $\omega$ .....90

5.6 Block diagram of the ADALINE for estimating 3-phase voltages or currents (3-Phase ADALINE).....91

5.7 The proposed 3-phase modular active power filter system.....93

5.8 The Control Scheme of the 3-phase modular active filter (The Controller in Fig. 5.7).....96

5.9 Estimation of the frequency variations and the fundamental and the 3rd components using ADALINE.....98

5.10 Steady state simulation results of the proposed modular active filter.....101

5.11 Test secondary distribution system.....103

5.12 Steady state simulation results of using two modules of the proposed modular active filter for the 3rd and 5th harmonic modules.....104

5.13 Transient simulation results of the proposed modular active filter.....106

5.15 Transient simulation results of the proposed modular active filter subjected to sudden full -load operation and full-load rejection.....107

5.16 Steady state simulation results of the proposed 3-phase modular active filter.....109

5.17 3-phase imbalance distribution system.....111

5.18 Steady state simulation results of the proposed 3-phase modular active filter with the distribution system shown in Fig. 5.17.....112

6.1 Block diagram of power splitting scheme.....117

6.2 The Control Scheme of the proposed power splitting active filter (The Controller in Fig. 6.1).....119

6.3 Steady state simulation results of the proposed power splitting modular active filter.....121

6.4 Transient simulation results of the proposed power splitting modular activefilter.123

7.1 (a) The dc-side voltage of the CSC. (b) The dc-side current ripple.....127

7.2 Control Scheme of the $l^{th}$ CSC module of the proposed active filter.....133
7.3 Single-Phase Current Source Converter.....134
7.4 Equivalent circuit for CSC module given in Fig. 7.3.....135
7.5 Active power control loop for charging the dc-side current.....140
7.6 Bode Diagrams of the open loop transfer function.....142
7.7 Bode Diagrams of the open loop transfer function including the controller.....143
7.8 Unit step response curves for the compensated and uncompensated systems.....143
8.2 Block diagram of the frequency splitting and 1-converter schemes.....146
8.3 Total cost comparison between the 1-converter scheme and frequency splitting converter scheme.....147
8.4 Steady state simulation results of the two modular active filter schemes (a) Distorted current ($i_L$) waveform (b) The filtered current for frequency splitting scheme (c) The filtered current for power splitting scheme.....157

# List of Tables

2.1 Harmonic voltage distortion limits in % at PCC.....15

2.2 Harmonic current distortion limits ( $I_h$ ) in % of load current ( $I_L$ ).....16

2.3 Some active power line conditioning techniques.....27

5.1 Secondary distribution feeder data.....103

5.2 The distribution of the nonlinear loads on the three phases.....110

8.1 Installation costs of 1-converter and frequency splitting schemes.....148

8.2 Operating losses and cost per month of 1-converter and frequency splitting schemes.....148

8.3 Installation costs of frequency-splitting and power-splitting schemes.....154

8.4 Operating losses per month of frequency-splitting and power-splitting schemes...154

# Chapter 1
# Introduction

## 1.1 Power Quality Concerns

In an ideal ac power system, energy is supplied at a single constant frequency and specified voltage levels of constant magnitudes. However, this situation is difficult to achieve in practice. The undesirable deviation from a perfect sinusoidal waveform (variations in the magnitude and/or the frequency) is generally expressed in terms of power quality. The power quality is an umbrella concept for many individual types of power system disturbances such as harmonic distortion, transients, voltage variations, voltage flicker, etc. Of all power line disturbances, harmonics are probably the most degenerative condition to power quality because of being a steady state condition. The Power quality problems resulting from harmonics have been getting more and more attention by researchers [1-15].

The Power quality problem, and the means of keeping it under control, is a growing concern. This is due primarily to the increase in the number and application of nonlinear power electronic equipment used in the control of power apparatus and the presence of sensitive electronic equipment. The non-linear characteristics of these power electronic loads cause harmonic currents, which result in additional losses in distribution system equipment, interference with communication systems, and misoperation of control. Moreover, many new loads contain microprocessor-based controls and power electronic systems that are sensitive to many types of disturbances. Failure of sensitive electronic loads such as data processing, process control and telecommunications equipment connected to the power systems has become a concern as they could result in series economic consequences. In addition, the increasing emphasis on overall distribution system efficiency has resulted in a continued growth in the application of devices such as shunt capacitors for power factor corrections. Harmonic contamination excites resonance in the tank circuit formed by line inductance and power factor correction shunt capacitors, which result in magnification of harmonic distortion levels.

The control or mitigation of the power quality problems may be realized through the use of harmonic filters. Harmonic filters, in general, are designed to reduce the effects of harmonic penetration in power systems and should be installed when it has been determined that the recommended harmonic content has been exceeded [1-3]. Shunt passive filters have been widely used by electric utilities to minimize the harmonic

distortion level [2]. They consist of passive energy storage elements (inductors and capacitors) arranged in such a way to provide a low impedance path to the ground just for the harmonic component(s) to be suppressed. However, harmonic passive filters cannot adjust to changing load conditions; they are unsuitable at distribution level as they can correct only specific load conditions or a particular state of the power system.

Due to the power system dynamics and the random-like behavior of harmonics for a short term, consideration has been given to power electronic equipment known as an active power filter. An active power filter is simply a device that injects equal-but opposite distortion into the power line, thereby canceling the original power system harmonics and improving power quality in the connected power system. This waveform has to be injected at a carefully selected point in a power system to correct the distorted voltage or current waveform. The power converter used for this purpose has been known by different names such as: active power filter and active power line conditioner [19,20]. The rating of the power converter is based on the magnitude of the distortion current and operated at the switching frequency dedicated by the desired filter bandwidth. In addition to its filtering capability, this power converter can be used as a static var compensator (SVC) to compensate for other disturbances such as voltage flicker and imbalance [21].

From a control system point of view, waveform correction on the system bus can be implemented either in the time-domain or frequency-domain. Both have advantages and

disadvantages. The main advantage of a time domain correction technique is its fast response to changes in the power system. Ignoring the periodic characteristics of the distorted waveform and not learning from past experiences are its main drawbacks. The advantage of frequency domain correction lies in its flexibility to select specific harmonic components needed to be suppressed and its main disadvantage lies in the rather burdensome computational requirements needed for a solution, which results in long response times [19].

The concept of active power filtering was first introduced in 1971 by Sasaki and Machida [26] who proposed implementation based on linear amplifiers. In 1976, Gyngyi *et.al,*[30] proposed a family of active power filter systems based on PWM current source inverter (CSI) and PWM voltage source inverter (VSI). These designs remained either at the concept level or at the laboratory level due to the lack of suitable power semiconductor devices.

Due to recent developments in the semiconductor industry, power switches such as the insulated gate bipolar transistor (IGBTs) with high power rating and the capability of switching at high frequency, are available on the market. This makes the application of active power filters at the industrial level feasible. Several active power filter design topologies have been proposed. They can be classified as:

- Series active power filter [19,20,25],
- Shunt active power filter [31-42],

- Hybrid series and shunt active filter [43-47],
- Unified power quality conditioner [48-50]
- Multi level and Multi converter active power filters [51-54]

Almost all of the existing proposed active power filters suffer from one or more of the following shortcomings:

- **High Switching Losses**: Almost all of the recently proposed active power filters utilize PWM switching control strategy due to its simplicity and harmonic suppression efficiency [23]. However, utility companies have been very reluctant in accepting the PWM switching strategy because of the high switching losses incurred in this approach. The power converter used for active filtering is rated based on the magnitude of the distorted current and operated at the switching frequency dictated by the desired filter bandwidth. Fast switching at high power, even if technically possible, causes high switching losses and low efficiency. An important issue in active power filtering is to reduce the power rating and switching frequency. The combinations of active and passive filters as well as employing multi-converter and multi level techniques, have all been attempted to meet the above requirements.
- **Low Reliability**: Most of the active filters connected to distribution systems are mainly a single unit with a high rating taking care of all the harmonic

components in the distorted signal. Any failure in any of the active filter devices will make the entire equipment ineffective. In addition, cascade multi-converter and multi level topology active power filters suffer from low reliability.

- **Control Methodology**: Active power filtering can be performed in time domain or in frequency domain. The waveform correction in time domain is based on extraction of data from the power line. However, in the frequency domain technique, information is extracted rather than data. The main advantage of time domain is fast control response, but, due to lack of information, it cannot control individual harmonics separately or apply various weightings for different harmonic components. Also, ignoring the periodic characteristics of the distorted waveform and not learning from past experiences are additional drawbacks of time domain methods. Correction in frequency domain, which is mainly implemented by FFT, has the advantage of flexible control of individual harmonics (cancel selected harmonics). However, its main disadvantage lies in the rather burdensome computational requirements needed for a solution, which results in longer response times [20].

Nevertheless, increasing needs for high filter performance and economic considerations call for a new active power filter configuration for harmonic cancellation which is suitable for distribution level and can overcome the above limitations.

## 1.2 Objectives and Contributions

The main objective of this research is to develop and design a cost-effective active harmonic power filtering solution capable of enhancing the power quality in distribution systems. The proposed device offers the potential of responding quickly to the changes in the system characteristics and is suitable therefore for on-line applications. This research is motivated by the lack of suitable existing harmonic filtering technique and the demand for high filtering performance and efficiency. The main topics can be outlined as follows:

- Choice of circuit topology based on a modular active filtering approach which is suitable for distribution systems.
- Development of a harmonic filtering strategy which reduces the switching frequency requirements of the active filter system.
- Development of adaptive and active system control by incorporating the adaptive linear neuron (ADALINE), a version of an artificial neural network (ANN), as a part of the controller.
- Complete design of the active filter modules.
- Comparison of the proposed filter with different topologies.

Several aspects of this research work are novel and distinct from previous work done in related areas. Some of the advantages that the proposed modular active power filtering approach offers are as follows:

- **Low switching losses:**

  In the proposed filter, the filtering job is split among a number of active filter modules, each dedicated to eliminate a specific harmonic. The converters dedicated to lower-order harmonics have higher ratings but are switched at lower rates, while those dedicated to higher-order harmonics are of lower ratings but are switched at higher frequencies. The overall switching losses are minimized due to the balanced power rating-switching frequency product and selected harmonic elimination.

- **High reliability:**

  Since the power converter units of the proposed modular active power conditioner are acting as standalone devices, a continuous harmonic cancellation to a distorted waveform is still expected to be provided even if one or more power converters fail to operate. This will result in a better line current spectrum than in an uncompensated one. Note that, in the existing one converter scheme, if due to a fault, the converter is lost, harmonic elimination is not performed at all.

- **High flexibility**

Since each converter is independently connected to the AC system, selected harmonic elimination based on the dominant harmonic component is possible. In order to take advantage of the diversity principle, the proposed filter system can filter a group of harmonics using only one filter module or more by combining them and compensating them in groups. Also, simultaneous multi operation strategies to take care of other disturbances, such as voltage or current imbalance and voltage fluctuations are feasible. This will yield great flexibility and increase the overall performance of the proposed active filter.

- **Enhanced ADALINE-Based Measurement Scheme**

Compared to previous active power filters, the harmonic extraction technique based on an ADALINE has been utilized for the first time in active power filtering. ADALINE is highly adaptive and capable of estimating the variations in the amplitude and phase angle of the harmonic components which will enhance the performance of the proposed active filter. The ADALINE-based measurement scheme has the ability to extract information rather than data from the power system. It has been improved by modifying the original algorithm to track the system frequency variations. This is important for successful charging of $I_{dc}$ of the CSCs and for successful harmonic filtering.

- **Improved Controller**

The controller of the proposed active filter has been improved by utilizing another ADALINE to track the system voltage and extract the fundamental component of the source voltage which is used as a synchronize signal for the $I_{dc}$ regulation loop. This improves the filtering capability of the proposed modular active filter even if the source voltage is harmonics polluted. Making the dc-side current $I_{dc}$ of the converter modules adaptive to the changes in the magnitude of the harmonics to be filtered results in optimum dc-side current value and minimal converter losses.

The information on individual harmonic components allows us not only to reduce the THD but also suppress each harmonic component below the level set by the IEEE 519 standard. Also, the information available on the magnitude of each harmonic component allows us to select the active filter bandwidth (i.e., the highest harmonic to be suppressed). This results in more efficiency and higher performance.

## 1.3 Organization

This thesis includes eight chapters, in addition to this introduction. Background and literature review are presented in Chapter 2. In this Chapter the harmonic problem is addressed and a literature survey of the latest active filtering techniques is reviewed and discussed. Chapter 3 investigates and compares the most common power system

harmonic extraction techniques. The principle of active power conditioning is presented in Chapter 4. Chapter 5 describes and discusses in detail the proposed modular active power filtering technique. The principle and the control scheme of the power splitting approach to active power filtering are introduced in Chapter 6. Chapter 7 details the power and control design of the proposed filter. Comparative evaluation of the proposed active power filter is given in Chapter 8. The conclusions and future research are given in Chapter 9. At the end of the thesis, a list of relevant references, publications and five appendices are given.

# Chapter 2
# Background and Literature Review

## 2.1 Overview

The purpose of this chapter is to familiarize the reader with the harmonic problem in general and to identify its salient features. In this review, special attention is given to harmonic mitigation using active power filters.

Harmonics as a power quality problem is first discussed in Section 2.2. This section highlights the causes and the impact of the harmonics problem as well as its measuring indices. Some background on harmonic mitigation techniques, with emphasis on the active power filtering solution, is given in Section 2.3. The literature review on active power filters, presented in section 2.4 is intended to summarize the main results of the

research work most relevant to the present study. Finally, concluding remarks on existing active filtering techniques are given at the end of the chapter.

## 2.2 Harmonics As A Power Quality Problem

Harmonics are qualitatively defined as sinusoidal waveforms having frequencies that are integer multiples of the power line frequency (50 or 60 Hz); they may be voltages or currents. In power system engineering, the term harmonics is widely used to describe the distortions in the voltage or current waveforms, that is, a steady state deviation from an ideal sine wave of power frequency.

The harmonic problem is not a new phenomenon in power systems. It was detected as early as the 1920s and 30s [6]. At that time, the primary sources of harmonics were the transformers and the main problem was the inductive interference with open-wire telephone systems. Some early work on harmonic filtering in distribution feeders was performed around that time.

Harmonic distortion can have detrimental effects on electrical distribution systems. It can waste energy and lower the capacity of an electrical system; it can harm both the electrical distribution system and devices operating on the system. Understanding the problems associated with harmonic distortion, i.e., its causes and effects, as well as the methods of dealing with it, is of great importance in minimizing those effects and increasing the overall efficiency of the distribution system.

## 2.2.1 Harmonic Distortion Indices

The presence of harmonics in the system is measured in terms of harmonic content (distortion), which is defined as the ratio of the amplitude of each harmonic to the amplitude of the fundamental component of the supply system voltage or current. Harmonic distortion levels are described by the complete harmonic spectrum with magnitude and phase angle of each individual harmonic component. The most commonly used measure of the effective value of harmonic distortion is total harmonic distortion (THD) or distortion factor. This factor is used to quantify the levels of the current flowing in the distribution system or the voltage level at the point of common coupling (PCC) where the utility can supply other customers. THD can be calculated for either voltage or current and can be defined as:

$$THD = \frac{\sqrt{\sum_{h=2}^{\infty} M_h^2}}{M_1} \times 100\% \tag{2.1}$$

where, $M_1$ is the RMS value of the fundamental component and $M_2$ to $M_N$ are the RMS values of the harmonic components of the quantity $M$.

Another important distortion index is the individual harmonic distortion factor (HF) for a certain harmonic $h$. HF is defined as the ratio of the RMS harmonic to the fundamental RMS value of the waveform, i.e., $HF = {M_h}/{M_1} \times 100\%$.

IEEE 519-1992 Standard [3] specifies limits on voltage and current harmonic distortion for 'Low Voltage, Primary and Secondary Distribution, Sub-transmission, and High Voltage transmission systems'. Table 2.1 lists the IEEE 519 recommended harmonic voltage and voltage distortion limits for different system voltage levels.

Table 2.1:Harmonic voltage distortion limits in % at PCC

| Bus Voltage at PCC (V) | Individual Harmonic Voltage Distortion (%) | Total Voltage Distortion – THD (%) |
|---|---|---|
| $V \leq 69kV$ | 3.0 | 5.0 |
| $69kV < V \leq 161kV$ | 1.5 | 2.5 |
| $V > 161kV$ | 1.0 | 1.5 |

IEEE 519 Standard also specifies limits on the harmonic currents from an individual customer which are evaluated at the PCC. The limits are dependent on the customer load in relation to the system short circuit capacity at the PCC. Note that all current limits are expressed as a percentage of the customer's average maximum demand load current (fundamental frequency component) at PCC. The term the *total demand distortion* (TDD) is usually used which is the same as THD except that the distortion is expressed as a percentage of some rated load current rather than as a percentage of the fundamental current magnitude. TDD is defined as:

$$TDD = \frac{\sqrt{\sum_{h=2}^{\infty} I_h^2}}{I_L} \times 100\% \qquad (2.2)$$

where, $I_h$ is the RMS magnitude of an individual harmonic current component, $I_L$ is the maximum RMS demand load current and $h$ is the harmonic order. Note that the term distortion factor is more appropriate when the summations in (2.1) and (2.2) are taken over a selected number of harmonics. Table 2.2 provides limits on every individual harmonic current component as well as limits on total demand distortion (TDD) for different voltage levels.

Table 2.2: Harmonic current distortion limits ($I_h$) in % of load current ($I_L$)

| $V_n \leq 69kV$ | | | | | | |
|---|---|---|---|---|---|---|
| $I_{sc} / I_L$ | $h < 11$ | $11 \leq h < 17$ | $17 \leq h < 23$ | $23 \leq h < 35$ | $35 \leq h$ | *TDD* |
| <20 | 4.0 | 2.0 | 1.5 | 0.6 | 0.3 | 5.0 |
| 20-50 | 7.0 | 3.5 | 2.5 | 1.0 | 0.5 | 8.0 |
| 50-100 | 10.0 | 4.5 | 4.0 | 1.5 | 0.7 | 12.0 |
| 100-1000 | 12.0 | 5.5 | 5.0 | 2.0 | 1.0 | 15.0 |
| >1000 | 15.0 | 7.0 | 6.0 | 2.5 | 1.4 | 20.0 |
| $69kV < V_n \leq 161kV$ | | | | | | |
| <20* | 2.0 | 1.0 | 0.75 | 0.3 | 0.15 | 2.5 |
| 20-50 | 3.5 | 1.75 | 1.25 | 0.5 | 0.25 | 4.0 |
| 50-100 | 5.0 | 2.25 | 2.0 | 1.25 | 0.35 | 6.0 |
| 100-1000 | 6.0 | 2.75 | 2.5 | 1.0 | 0.5 | 7.5 |
| >1000 | 7.5 | 3.5 | 3.0 | 1.25 | 0.7 | 10.0 |
| $V_n > 161kV$ | | | | | | |
| <50 | 2.0 | 1.0 | 0.75 | 0.3 | 0.15 | 2.5 |
| ≤ 50 | 3.5 | 1.75 | 1.25 | 0.5 | 0.25 | 4.0 |

### 2.2.2 Sources of Harmonics

Harmonic distortion results from the nonlinear characteristics of the devices and loads in the power system. The device or equipment is said to be nonlinear when the relationship between the instantaneous voltage and current is not linear. These nonlinear loads primarily generate harmonic currents, which upon passing through the system impedances produce voltage harmonics which distort the system voltage waveform.

Nowadays, modern semiconductor switching devices are employed in a wide variety of domestic and industrial loads. They offer reliable and economical solutions to the control of electric power, from a few watts to many megawatts. However, they are considered as the main cause of an alarming amount of harmonic distortion in electric power systems. The nonlinear characteristic of semiconductor devices as well as the operational function of most power electronic circuits cause distorted current and voltage waveforms in the supply system. These loads are commonly referred to as "power electronics loads", "power system polluters" or "distorting sources" in the relevant literature.

Harmonic sources can be classified into three categories: saturable devices, arcing devices, and power electronic devices. All of the above categories present nonlinear voltage/current characteristics to the power system. Saturable devices, e.g. transformers, [2,7] and arcing devices such as arc furnaces [2,8,9], arc welders and discharge type lighting (fluorescent), are passive, and the nonlinearities are the result of physical

characteristics of the iron core and electric arc. In power electronic equipment, the switching of the semiconductor devices is responsible for the nonlinear characteristic. The power electronic equipment includes adjustable speed motor drives, DC power supplies, battery chargers, electronic ballasts, and many other rectifier/inverter applications [2,10-13].

### 2.2.3 Effects of Harmonics

Harmonics in power systems can result in a variety of unwelcome effects. Harmonics can cause signal interference, overvoltages, and circuit breaker failure, as well as equipment heating, malfunction, and damage.

The IEEE Working Group on Power System Harmonics lists the following areas of harmonic problems [6]:

- Failure of capacitor banks due to dielectric breakdown or reactive power overload;
- Interference with ripple control and power line carrier systems, causing misoperation of systems which accomplish remote switching , load control and metering;
- Excessive losses resulting in heating of induction and synchrouns machines;

- Overvoltages and excessive currents on the system from resonance to harmonic voltages or currents in the network;
- Dielectric breakdown of insulated cables resulting from harmonic overvoltages in the system;
- Inductive interface with telecommunication systems;
- Errors in meter readings;
- Signal interference and relay malfunction, particularly in solid state and microprocessor-controlled systems;
- Interference with large motor controllers and power plant excitation systems;
- Mechanical oscillations of induction and synchrouns machines;
- Unstable operation of firing circuits based on zero crossing detecting or latching.

### 2.2.4 Harmonic Distribution in Distribution Systems

In electric distribution systems, the magnitude of the harmonic current component is often inversely proportional to its harmonic order, $i_{h,peak} \propto \frac{1}{h}$, and $f_h \propto h$, where $i_{h,peak}$ is the peak value of the magnitude of the harmonic current, $h$ is the harmonic order and $f_h$ is the harmonic frequency. Fig. 2.1 displays a real distorted waveform generated by a typical non-linear load and its harmonic spectrum [1].

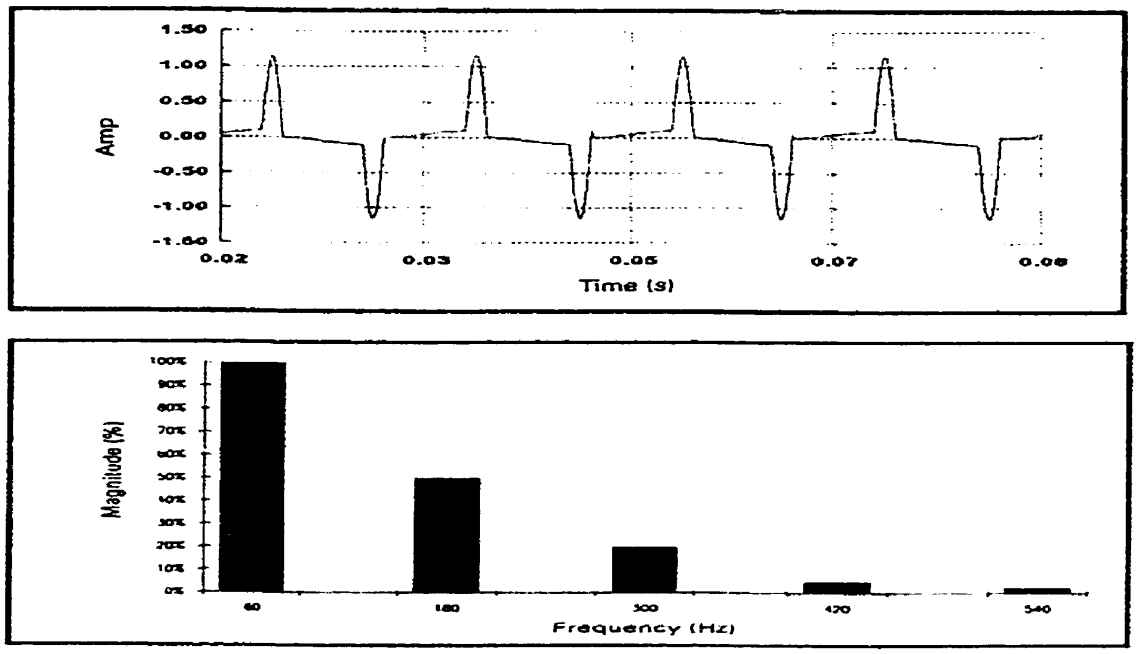


Fig 2.1 A typical distorted waveform and its harmonic content.

## 2.3 Harmonic Mitigation Techniques

As mentioned earlier, due to the increase in the use of nonlinear loads in the distribution systems, large amounts of distorted current and voltage waveforms exit. Therefore, the need to compensate for these distortions is essential in order to minimize their effects on the distribution system and improve its efficiency.

Two approaches have been used to cut the harmonic-related problem and to enhance the performance of the distribution system, namely passive approach and active approach. The two harmonic filtering methods, passive and active are presented and briefly discussed.

### 2.3.1 Passive Harmonic Filters

Passive harmonic filters are made of inductive, capacitive, and resistive elements. They are employed either to shunt the harmonic currents off the line or to block their flow between parts of the system by tuning the elements to create a resonance at a selected harmonic frequency (frequencies). When passive filters are connected in series with the power line, they are designed to have a large impedance at a certain harmonic. This will isolate the harmonics produced by the loads from reaching the supply system. However, when they are connected in parallel with the power line, they provide a low impedance path for selected harmonic currents to pass to ground, thus preventing them from entering the supply system. Passive L-C tuned filters are the most common type of passive filters.

Passive filters are relatively inexpensive compared to other means for eliminating harmonic distortion. However, they are designed to filter specific harmonic components; they are not adaptable to successfully filter varying harmonics.

Passive filters must be carefully sized. Undesirable large bus voltages can result from using an oversized filter. An undersized filter can become overloaded. Filter size can be difficult to gauge, considering that harmonic currents can be drawn from other areas of a distribution system.

The capacitance in passive filters may interact with the system impedance, which, in fact, can result in a system resonance condition [2, 17,18]. In this scenario, harmonic currents can be amplified on the source side and cause significant distortion in the voltage. This resonance condition can persist even with the filter tuned slightly below the system resonant frequency [2,18]. Also, changes in the distribution system can cause the resonant point itself to change.

### 2.3.2 Active harmonic filters

Active power harmonic filtering is a relatively new technology for eliminating harmonics which is based on sophisticated power electronics devices. An active power filter consists of one or more power electronic converters which utilize power semiconductor devices controlled by integrated circuits.

The use of active power filters to eliminate the harmonics before they enter a supply system is the optimal method of dealing with the harmonics problem. While they do not have the shortcomings of the passive filter, active power filters have some interesting features outlined as follows:

- They can address more than one harmonic at a time and can compensate for other power quality problems such as load imbalance and flicker. They are particularly useful for large, distorting loads fed from relatively weak points on the power system.

- They are capable of reducing the effect of distorted current/voltage waveforms as well as compensating the fundamental displacement component of current drawn by nonlinear loads.
- Because of high controllability and quick response of semiconductor devices, they have faster response than the conventional SVC's.
- They primarily utilize power semiconductor devices rather than conventional reactive components. This results in reduced overall size of a compensator and expected lower capital cost in future due to the continuously downward trend in the price of the solid state switches.

However, the active power filter technology adds to complexity of circuitry (power circuit and control). There will also be some losses associated with the semiconductor switches

The concept of the active power filter is to detect or extract the unwanted harmonic components of a line current, and then to generate and inject a signal into the line in such a way to produce partial or total cancellation of the unwanted components. Active power filters could be connected either in series or in parallel to power systems; therefore, they can operate as either voltage sources or current sources. The shunt active filter is controlled to inject a compensating current into the utility system so that it cancels the harmonic currents produced by the nonlinear load. The principle of active filtering for current compensation is shown in Fig. 2.2. The load current is nonlinear

due to the nonlinear load. In this figure, the active filter is controlled to draw (or inject) a current $I_{af}$ such that the source current $I_s = I_L + I_{af}$ is sinusoidal.

The series active filter is connected in series with the utility system through a matching transformer so that it prevents harmonic currents from reaching the supply system or compensates the distortion in the load voltage. The series active filter is the "dual" of the shunt active filter. Fig. 2.3 shows the application of an active power filter in series with a

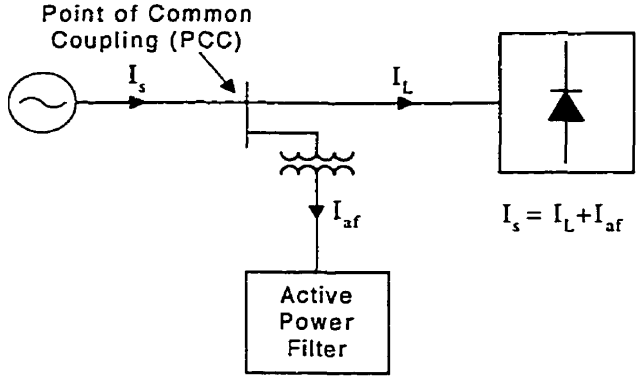


Fig. 2.2: Basic configuration of a typical shunt active power filter

non-linear load. The active power filter in this configuration is referred to in the literature as the series voltage injection type, and it is suitable for compensating the load voltage in a weak AC system. It is controlled to insert a distorted voltage such that the load voltage is sinusoidal and is maintained at a rated magnitude.

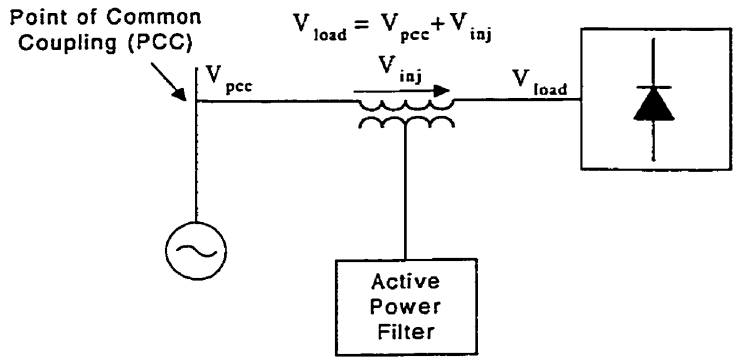


Fig. 2.3: Harmonic voltage compensator.

There are two fundamental approaches for active power filtering: one that uses a converter with an inductor to store up energy to be used to inject current of appropriate magnitude and frequency contents into the system, called a current source converter (CSC), and one that uses a capacitor as an energy storage element, called a voltage source converter (VSC). When the magnitude and the frequency of the AC output voltage or current is controlled by the pulse-width modulation (PWM) of the inverter switches, such inverters are called PWM inverters.

Active power line filtering can be performed in the time domain or in the frequency domain [19]. The correction in the time-domain is based on extracting the fundamental component of the distorted line current using a notch filter, finding the instantaneous error between the distorted waveform and its fundamental component, and compensating for the deviation from the sinusoidal waveform by injecting the computed error into the line. The correction in the frequency-domain, on the other hand, is based

on the extraction of the harmonic components of the line current. A distinct advantage of the frequency-domain techniques is the possibility of selected harmonic elimination.

## 2.4 Literature Review on Active Power Filters

There are many new ideas proposed in the technical literature for harmonic active filtering applied to power systems. This has been motivated by the existing problems associated with the use of passive filters and recent break-throughs in power handling capabilities and speed of power semiconductor switches. Table 2.3 shows a partial summary of some of the latest active power line conditioning techniques. It represents the major trends in harmonic mitigation techniques using active filters.

### 2.4.1 Magnetic Flux Compensation

This method of harmonic elimination is performed using the principle of magnetic flux compensation [26]. This is basically achieved by the use of current to produce a flux to counteract the flux produced by the harmonics. The main drawback of this scheme is its inability to remove the lower order harmonics ($2^{nd}$ ,$3^{rd}$ and $4^{th}$ ) without the need for a very high power feedback amplifier. Also this work illustrates that the rather high cost of the high power amplifier and the circuitry necessary to protect it from high voltages are further drawbacks to this method.

Table 2.3: Some active power line conditioning techniques

| Methods | Author(s) | Features |
|---|---|---|
| Magnetic Flux compensation | Sasaki and Machida [26] | Produce a flux to counteract the flux produced by the harmonics. Computer simulation |
| Injection of Specific Harmonics | Bird, *et al.* [27] | Injected a 3rd harmonic current Computer simulation |
| | A. Ametani [28,29] | Generalization of Bird's method Computer simulation |
| Active Power Filtering Using PWM Inverters | Gyugyi and Strycula [30] | Injection of PWM current using VSC and CSC, results are verified experimentally |
| | Akagi, *et al* [31] | Introduction of *p-q theory* and development of a PWM-VSC for reactive power compensation, results are verified experimentally |
| | Hayashi, et al [32] | Injection of PWM current using CSC, the filter is controlled in frequency domain, results are verified by simulations |
| | Kim, *et al.* [33] | Injection of PWM current, results are verified by simulations |
| | Fisher and Hoft [34] | Three-Phase Power Line Conditioner, results are verified by simulations |
| | Shashani [35] | Static VAR Compensator with GTOs, results are verified by simulations |
| | Moran, Ziogas, and Joos [37] | A Power Factor Compensator and Harmonic Suppression Using a PWM-VSC, results are verified experimentally |
| | Enjeti, Ziogas and Lindsay [38] | Programmed PWM Techniques, results are verified experimentally on 1-phase and 3-phase inverter configs |
| | Choe, Wallace and Park [39] | PWM + Active Power Filters, results are verified by simulations |
| | Williams and Hoft [40] | Power line Conditioners: a GTO Bridge + PWM, results are verified by simulations |
| Combination of Active and Passive Filters (Hybrid filters) | Takeda, Ikeada and Tominaga [45] | Installation of active power filter at Chubu Steel Co., in Japan |
| | Peng, Akagi and Nabea [43] | PWM Active Filter + Passive LC Filter, results are verified experimentally |
| | Fujita and Akagi [44] | PWM Active Filter + Passive Filter, results are verified experimentally |
| | Tokoda et al [45] | Active filter + LC filter, results are verified experimentally |
| | Van Zyl, Enslin and Spee [46,47] | Introduction of power quality manager (PWM-VSC +passive filters), results are verified experimentally |
| Unified Power Quality Conditioner (UPQC) | Akagi [48] | Integration of series and shunt active filters, results are verified experimentally |
| | Fujita [49] | Discussion of the control strategy of the UPQC, results are verified experimentally |
| | Aredes, *et.al.* [50] | UPQC for fundamental frequency compensation and active harmonic mitigation. |
| Multi Level and Multi Converter Approach | Meynard and Foch [51] | Multi level active power conditioner, results are verified by simulations |
| | Lai and Peng [52] | Multi level SVC, results are verified by simulations |
| | Ned mohan [56] | PWM-VSC multi converter, results are verified by simulations |
| | Peng [57] | Modular Topology of Active Power Conditioner, results are verified experimentally |

### 2.4.2 Injection of a Specific Harmonic Current

Bird, *et al.* [27] were among the first to attempt to reduce harmonic distortion, as opposed to the use of conventional passive filters. They proposed that the harmonic currents produced by pulse converters could be eliminated or partially eliminated by injecting a third harmonic current to the rectangular waveform produced by the converter. Bird's experimental results proved that the method is effective in eliminating one harmonic of choice. However, Bird's work was costly and inefficient and its major drawback was that it was impossible to fully eliminate more than one harmonics. Later on, Bird's work was generalized and improved [28,29] to eliminate multiple harmonics. Both of the above methods are predetermined methods, namely, they inject fixed harmonic frequency currents. They have the same disadvantage as passive filters in that the harmonics must be known in advance.

### 2.4.3 Active Harmonic Filtering Using PWM Converters

In 1976 Gyugyi and Strycula presented the concept to compensate for harmonics by the applications of semiconductor switches in the form of PWM inverters. [30]. They presented a switching system, which consisted of a simple bridge circuit of transistors switched in pairs to produce a two-level current waveform using the PWM technique. Two topologies based on CSC and VSC were proposed which were controlled to counteract the flow of harmonic currents from the nonlinear load to the utility system.

The correction of the distorted signal occurs in the time domain which is based on the principle of holding the instantaneous voltage or current within some tolerance of a sine wave. The timing of the switching needed was determined by a control unit which monitored the instantaneous load voltage. The work done by Gyugyi and Strycula was one of pioneering attempts to compensate for harmonic components using the PWM inverters.

However, most of the proposals in active power conditioning presented during the 1970s were in a laboratory stage because the circuit technology was too poor to practically implement the compensation.

In the 1980s, the remarkable progress in power electronic technology (specifically, fast switching devices) encouraged the interest in the study of active power line conditioners for reactive power and harmonic compensations. Akagi and others introduced p-q theory and developed a PWM-voltage type converter topology for instantaneous reactive power compensation [31]. In this work, the authors decomposed the instantaneous voltages and currents into orthogonal components yielding, in the time domain, a component termed the instantaneous reactive power. The active filter is controlled to eliminate this instantaneous reactive power thus resulting in reactive power compensation in the time domain. The notion of "the instantaneous reactive power" is only applicable to 3-phase systems. Hayashi and others reported current-source active filters for harmonic compensation [32]. In this application, the current

compensation control was done in the frequency domain in terms of closed loop control. A research group in Korea presented an active power filter that reduced the magnitude of harmonics by means of the injection of PWM currents made up of sine and cosine terms of a compensating current [33]. Enjeti [38] provides an evaluation of several PWM techniques to eliminate harmonics for single phase and three phase inverters. Guidelines to choose the appropriate topology for each application are also presented.

The main problem with the schemes, which utilized the PWM switching technique, is the high switching losses involved due to the fast switching rates.

### 2.4.4 Hybrid Filters

In order to reduce the ratings of active power filters, designs that combine active filters and passive filters have been implemented by many researchers [36,43-47]. Peng *et.al.* [43] proposed the use of a small capacity series active filter to operate in parallel with a traditional bank of passive filters. This technique is different from the previous method in that it does not use the active filter for harmonic current compensation, but rather to improve the filtering characteristics of the passive filters.

The objective of this series filter is to exhibit zero impedance at the fundamental frequency and a high impedance at the harmonic frequencies created due to a parallel resonant situation between the passive filters and the source impedance. The

determination of the harmonic currents to be injected by the active filter is based on p-q theory developed by Akagi[31].

The main drawback of this topology, in addition to the switching losses associated with the PWM control method, is the series transformer that would require a high basic insulation level to withstand the large switching transients and lightning surges. Another significant point is that the current carried by the active filter will also include the fundamental component of the load current and the fundamental leading power factor current of the shunt passive filter.

In order to avoid the problems associated with the active filter in parallel with passive filters topology, another combined system of active filters and passive filters or LC circuits was proposed by Fujita and Akagi[44] and Tokuda *et.al.* [45]. Again, the aim is to reduce the required size of the active filter. In these schemes, the active filters are connected in series with either a shunt passive filter or an LC tuned filter. The difference between these topologies and the one presented in reference [43] is that the single-phase PWM inverters are replaced by one three-phase inverter and the DC-side voltage source is regulated by a feedback loop. In another work, VanZyle *et al* [46-47] proposed a relocatable converter to be used in series with a passive filter that is permanently installed on the line and is called the Power Quality Manager (PQM). The passive filter consists of tuned filters for fifth and seventh order harmonics. The PQM is

used to as SVC to improve the voltage regulation and has the capability to work as a harmonic isolator.

The weakness of these schemes is that the active filter always carries the capacitive fundamental component of the current through the shunt passive filter or the LC tuned filter.

### 2.4.5 Unified Power Quality Conditioner (UPQC)

The unified power quality conditioners (UPQC) are a new family of active power filters, which consist of two 3-phase VSC, connected back to back with a common dc coupling capacitor [48]. One inverter is shunt connected with the power line and the other is connected in series through a transformer. The main objective of the series active filter in the UPQC is harmonic isolation between a sub-transmission system and a distribution system. In addition, the series active filter has the capability of voltage–flicker/imbalance compensation as well as voltage regulation and harmonic compensation at the point of common coupling (PCC). The main purpose of the shunt filter is to absorb harmonic currents, compensate for reactive power and negative sequence current and regulate the dc-link between both active filters.

Later, Fujita [49] provided experimental results obtained from the UPQC laboratory model and discussed the control strategy of the UPQC with the focus on the flow of the instantaneous active and reactive powers inside the UPQC.

Recently, a generalized and improved work has been introduced by Aredes et.al. [50], in which a generic control concept based on the instantaneous and imaginary power theory for UPFC (UPQC) is presented. They proposed a device, called Universal Active Power Line Conditioner (UPLC) that incorporates both a fundamental frequency compensation and active harmonic mitigation.

The UPQC (UPLC) consists of two IGBT dc-ac power inverters and their switching strategies are based on a PWM control technique. The main limitation of the proposed UPQC (UPLC) besides the high switching losses and control complexity is the inability of the proposed device to perform simultaneous jobs. This is because of the limitations of the PWM to include all the functions within the same time window, which results in over modulation.

### 2.4.6 Configuration for High Power Applications (Multi level converters)

For low-power applications, such as industrial applications, the active power filter can be realized by one PWM converter [31,32,43,46]. The required voltage-withstand and current-carrying capabilities can be achieved by series and parallel connections of semiconductor switches. However, in high- power applications, the filtering job cannot be performed by one converter alone, due to the power rating and switching frequency limitations of semiconductor switches, as well as the problems associated with

connecting a large number of switches in series or in parallel to attain the necessary ratings.

To overcome the above-mentioned restrictions, the concept of multi level and multi converter topologies has been introduced [51,56-60]. The general structure of the multilevel converters is to synthesize a staircase voltage waveform (sinusoidal wave for an infinite number of levels) from different levels voltages, typically obtained from capacitor voltage sources.

Menard and Foch [51] propose a multi-level active current filter suitable for HV networks. They present a simulation of a case study for a 20 kV power system. In this study, the compensation of the current harmonics was up to $19^{th}$ order. The main limitations of the multi-level configuration are the switching frequency and neutral voltage fluctuation.

Cascade multi-converter active power filters based on VSC topology have been proposed recently [56-60]. They have neither the switching frequency and neutral voltage fluctuation limitations of multi-level configuration [56] nor the problems associated with the parallel and series connection of switches of the single-converter scheme. The main drawbacks of cascade multi-converter active power filters are low reliability and control circuit complexity.

Another multi-converter active filtering approach is proposed by Huang and Wu [60]. This approach is an extension of the fundamental filtering concepts introduced by

the author of this thesis [59], but using 3-phase voltage source converters. In this work, a test result obtained from the laboratory prototype was provided.

## 2.5 Concluding Remarks on Existing Active Power Filters

Based on the literature survey on the subject of active power filters and active filtering techniques, one finds:

- Almost all of the recently proposed active power filters utilize PWM switching control strategy. However, the conventional PWM inverter based active power filtering schemes suffer from high-switching losses incurred in the PWM switching technique.
- Most of the recent existing active power filters are realized by one unit of single-phase or three-phase bridge converter of voltage- or current-source topology [20,21]. However, there are some other attempts, which are based on multi-converter and multi level topologies. The advantage of single-phase topology lies in its capability of capturing the unbalanced load conditions. The CSC based active power filtering receives more attention in power quality control applications due to the recent developments in semiconductor industry.

Therefore, it is expected to outperform VSC topology specifically in single-phase applications.

- Most of the existing active filter systems are suffering from low reliability. They mainly consist of a single unit with a high power rating to take care of all the harmonic components in the distorted signal. Any failure in any of the active filter devices will make the entire equipment ineffective.

- The correction of the distorted waveform can be performed in the time domain or in the frequency domain. Correction in the time domain has the advantages of fast control response but it does not have dynamic information on the harmonic spectrum. Therefore, active power filters utilizing time domain control will be switched at high switching rate to cover the whole bandwidth of the harmonic to be filtered. Various time domain control techniques are proposed in the literature, but instantaneous reactive power based on p-q theory is the most common control method utilized in active power filters. However, it is only applicable to 3-phase systems and its performance is degraded if the source voltage is distorted. On the other hand, correction in the frequency domain, which is mainly implemented by the FFT, has the advantage of flexible control of individual harmonics (cancel selected harmonics) due to the availability of the information on the harmonic components. However, its main disadvantage is its high computational requirement.

# Chapter 3
# Harmonic Estimation Techniques

## 3.1 Overview

One important issue that assesses and evaluates the quality of the delivered power is the estimation or extraction of harmonic components from distorted current or voltage waveforms. In order to provide high-quality electricity, it is essential to accurately estimate or extract time varying harmonic components, both the magnitude and the phase angle, to mitigate them using active power filters.

There are several harmonic estimation techniques reported in the literature [62-78] among which the discrete Fourier transform (DFT), the Kalman filter (KF) and

Artificial Neural Networks (ANN) are the most popular. Fig. 3.1 displays some of these estimation technique references.

A comprehensive simulation analysis will be conducted in this chapter to select the most suitable estimation technique for the proposed active power filter. The final conclusion will be based on a performance analysis under different operating condition.

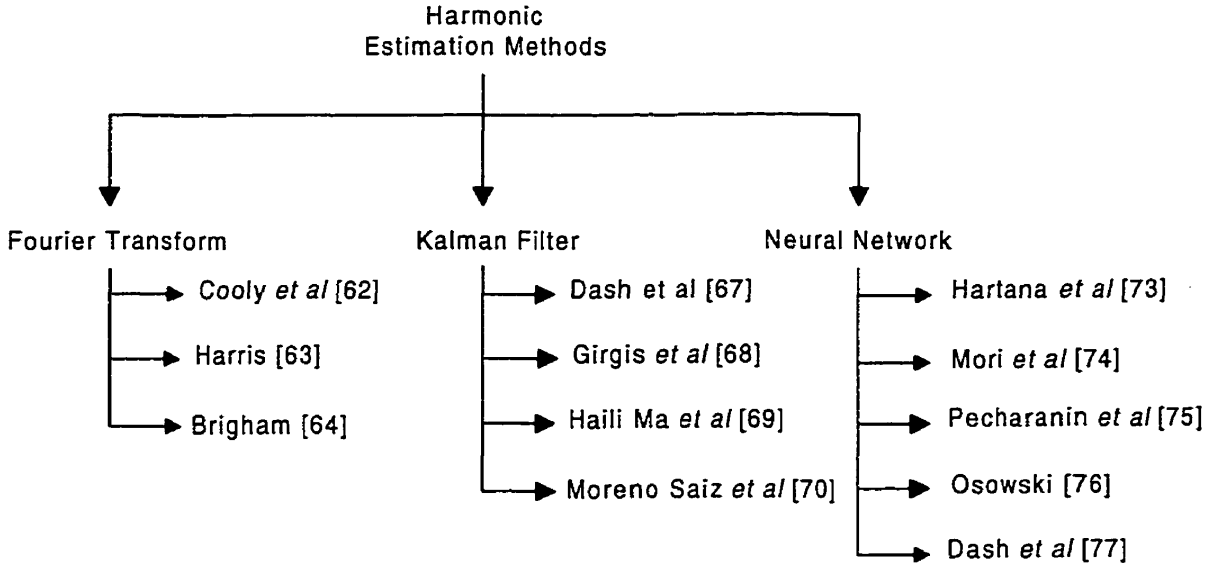


Fig. 3.1: Some of harmonic estimation methods

## 3.2 Discrete Fourier Transform (DFT)

The DFT-based algorithm (fast Fourier transform (FFT)) for harmonic measurement and analysis is a well-known technique and is widely used due to its low computational requirement. In this approach [62-64], the coefficients of individual harmonics are

computed by implementing fast Fourier transform on digitized samples of a measured waveform in a time window. The description of the algorithm is well documented in many references [62-64] and the equations used for calculating the amplitude and phase angle of the harmonic using DFT are briefly described in Appendix (A).

There are several performance limitations inherent in the FFT application. These limitations are [64]:

1) the waveform is assumed to be of a constant magnitude during the window size considered (stationary),
2) the sampling frequency must be greater than twice the highest frequency of the signal to be analyzed, and
3) the window length of data must be an exact integer multiple of power-frequency cycles.

It has been reported in [68] that failing to satisfy these conditions will result in leakage and picket fence effects and hence inaccurate waveform frequency analysis. Moreover, the DFT-based algorithm can cause computational error and may lead to inaccurate results if the signal is contaminated by noise and/or the dc component is of a decaying nature [77].

As far as the active filters are concerned, and because the transformation process takes time, the harmonic compensation will be delayed by two cycles if the FFT is used

as an estimation tool [75]. This will influence the performance of active filtering in case that the load current is in fluctuated state.

## 3.3 Harmonic Estimation Using Kalman Filter

In the Kalman filter approach [67-70], a state variable mathematical model of the signal, including all possible harmonic components, is used. Dash and Sharaf [67] were among the first who utilized the Kalman filter technique to estimate the stationary harmonic components of known frequency from unknown measurement noise. Girgis *et.al* [68] generalized the work in reference [67] to predict time-varying harmonics too. However, it was pointed out in reference [68] that the Kalman filter scheme requires more computational process to update the state vector when estimating the time varying harmonics compared to the stationary.

Later, Haili Ma and Girgis [69] utilized the Kalman filter approach to identify and track the harmonic sources in power systems. A hardware implementation of the Kalman filter to track power system harmonics based on the work done by Girgis [68] was presented by Moreno Saize *et. al* [70].

In the following sub-sections a state space model of a time varying signal and a brief description of the Kalman filter algorithm will be explained.

### 3.3.1 State-Space Model of a Time Varying Signal

Consider the following time-varying sinusoidal signal

$$y(t) = Z(t)\sin(\omega t + \varphi(t)) \tag{3.1}$$

or,

$$y(t) = A(t)\cos(\omega t) + B(t)\sin(\omega t) \tag{3.2}$$

where,

$$Z(t) = \sqrt{A^2(t) + B^2(t)} \qquad \text{and} \qquad \varphi(t) = \tan^{-1}\left(B(t)/A(t)\right)$$

Assume that we are interested in estimating the variables $x_1 = A(t)$ and $x_2 = B(t)$ which represent the in-phase and quadrature-phase components of the signal given in equation (3.2). These variables represented by the vector X are often denoted by the term state variables and are governed by the state equations

$$\begin{bmatrix} x_1 \\ x_2 \end{bmatrix}_{k+1} = \begin{bmatrix} 1 & 0 \\ 0 & 1 \end{bmatrix}\begin{bmatrix} x_1 \\ x_2 \end{bmatrix}_k + \begin{bmatrix} w_1 \\ w_2 \end{bmatrix}_k \tag{3.3}$$

where, $w_1$ and $w_2$ allow the state variables for random walk (time variation) and the subscripts on the vectors represent the time step. The measurement equation would include the signal and noise and can be represented as:

$$z_k = \begin{bmatrix} \cos\omega t_k & \sin\omega t_k \end{bmatrix}\begin{bmatrix} x_1 \\ x_2 \end{bmatrix}_k + V_k \tag{3.4}$$

where $V_k$ represents random measurement noise and $t_k = k^{th}$ sampling time

The state space mathematical model can be expanded to a time-varying signal that includes N-harmonics. Consider the distorted signal $f(t)$ with the Fourier series expansion:

$$f(t) = \sum_{l=1}^{N} Z_l(t) \sin(l\omega t + \phi_l(t)) \tag{3.5}$$

where, $Z_l(t)$ and $\phi_l(t)$ are the amplitude and the phase angle of the $l^{th}$ harmonic, respectively and N is the total number of harmonics.

The discrete-time representation of $f(t)$ will be:

$$f(t_k) = \sum_{l=1}^{N} A_l(t_k) \sin l\omega(t_k) + \sum_{l=1}^{N} B_l(t_k) \cos l\omega(t_k) \tag{3.6}$$

where, $A_l(t_k) = Z_l(t_k)\cos\phi_l(t_k)$, $B_l(t_k) = Z_l(t_k)\sin\phi_l(t_k)$.

Each frequency component requires two state variables. These state variables are defined by equation (3.7) and represent the components in phase and quadrature of each harmonic.

$$\begin{aligned} x_1(t_k) &= A_1(t_k) & \qquad x_2(t_k) &= B_1(t_k) \\ &\vdots & &\vdots \\ x_{2n-1}(t_k) &= A_n(t_k) & x_{2n}(t_k) &= B_n(t_k) \end{aligned} \tag{3.7}$$

The state variable equation (3.7) can be expressed as

$$\mathbf{X}_{k+1} = \mathbf{\Phi}_k \mathbf{X}_k + \mathbf{W}_k \tag{3.8}$$

where, $\mathbf{X}_{k+1}$ is the $(2n\times 1)$ state vector at time $t_{k+1}$, $\mathbf{X}_k$ is the $(2n\times 1)$ state vector at time $t_k$, The $(2n\times 2n)$ transition matrix $\mathbf{\Phi}_k$ in the equation (3.8) relates the state at time step $t_k$ to the state at step $t_{k+1}$. The random variable $\mathbf{W}_k$ is a $(2n\times 1)$ vector assumed to be uncorrelated and of known covariance and represents the discrete variation of the state variables due to an input white noise sequence.

In expanded form, equation (3.8), can be expressed as

$$\begin{bmatrix} x_1 \\ x_2 \\ \cdots \\ x_{2n-1} \\ x_{2n} \end{bmatrix}_{k+1} = \begin{bmatrix} 1 & 0 & \cdot & \cdot & 0 \\ 0 & 1 & \cdot & \cdot & 0 \\ \cdot & \cdot & \cdot & \cdot & \cdot \\ \cdot & \cdot & \cdot & \cdot & \cdot \\ 0 & \cdot & \cdot & \cdot & 1 \end{bmatrix} \begin{bmatrix} x_1 \\ x_2 \\ \cdots \\ x_{2n-1} \\ x_{2n} \end{bmatrix}_k + \mathbf{W}_k \tag{3.9}$$

The Measurements of this process are made at discrete instants of time according to the linear relation given by the equation:

$$z_k = \mathbf{H}_k\mathbf{X}_k + V_k = \begin{bmatrix} \cos(\omega t_k) \\ \sin(\omega t_k) \\ \cdot \\ \cos(n\omega t_k) \\ \sin(n\omega t_k) \end{bmatrix}^T \begin{bmatrix} x_1 \\ x_2 \\ \cdots \\ x_{2n-1} \\ x_{2n} \end{bmatrix}_k + V_k \tag{3.10}$$

where, $z_k$ is the measurement at time $t_k$. The $(1\times 2n)$ vector $\mathbf{H}_k$ in the measurement equation (3.10) relates the state vector $\mathbf{X}_k$ to the measurement $z_k$ at time $t_k$. The $V_k$ is the measurement noise assumed to be a white sequence and not correlated with the sequence $\mathbf{W}_k$.

### 3.3.2 Kalman Filter Algorithm

The Kalman filter is a recursive data processing algorithm that combines all available measurement data, plus priori knowledge about the system and measuring device, to produce an estimate of the desired variables in such a manner that the error is minimized statistically.

In the implementation of a Kalman filter, a mathematical model of signals in state space form is used. Consider the state space model given by equation (3.8) and (3.10). Both of the equations are repeated here for convenience

State variable equation:

$$\mathbf{X}_{k+1} = \mathbf{\Phi}_k \mathbf{X}_k + \mathbf{W}_k \tag{3.11}$$

Measurement equation:

$$z_k = \mathbf{H}_k \mathbf{X}_k + V_k \tag{3.12}$$

The variance of the measurement noise $V_k$ is equal to $R_k$ and the covariance matrix for the $\mathbf{W}_k$ vector is mathematically given by:

$$E\left[\mathbf{W}_k \mathbf{W}_i^T\right] = \begin{cases} \mathbf{Q}_k, & i = k \\ 0, & i \neq k \end{cases} \tag{3.13}$$

where $E\left[\mathbf{W}_k \mathbf{W}_i^T\right]$ is the expected value of $\left(\mathbf{W}_k \mathbf{W}_i^T\right)$.

The design objective of Kalman filter is to determine the optimal estimate $\hat{\mathbf{X}}_k$ based on the $\{z_i\}(0 \le i \le k)$ such that $\mathbf{P}_k = E\lfloor e_k e_k^T \rfloor$ is minimum. The estimation error $e_k$ is defined by the equation

$$e_k = \mathbf{X}_k - \hat{\mathbf{X}}_k \tag{3.14}$$

where, $\{z_i\}$is a sequence of samples of $z_k$ and $\mathbf{P}_k$ is the covariance matrix of the estimation error.

The Kalman filter estimation process is performed in two stages: time update stage and measurement update stage. In the first stage, the Kalman filter projects forward in time the current state and error covariance estimates to obtain the *a priori* estimates for the next time step. The measurement update stage is responsible for incorporating a new measurement into *a priori* estimate to obtain an improved *a posteriori* estimate.

Starting from initial estimate of the system $\hat{\mathbf{X}}_0^-$ and associated covariance matrix $\mathbf{P}_0^-$, we can use the measurements $z_k$ to improve this first estimate. Therefore, using the state space model given by equations (3.11) and (3.12) the measurement update stage can be mathematically represented by:

$$\mathbf{K}_k = \mathbf{P}_k^- \mathbf{H}_k^T \left(\mathbf{R}_k + \mathbf{H}_k \mathbf{P}_k^- \mathbf{H}_k^T\right)^{-1} \tag{3.15}$$

$$\hat{\mathbf{X}}_k = \hat{\mathbf{X}}_k^- + \mathbf{K}_k \left(z_k - \mathbf{H}_k \hat{\mathbf{X}}_k^-\right) \tag{3.16}$$

$$\mathbf{P}_k = \left(\mathbf{I} - \mathbf{K}_k \mathbf{H}_k\right) \mathbf{P}_k^- \tag{3.17}$$

where $\hat{\mathbf{X}}_k$ is the estimate updated at $t_k$, $\mathbf{K}_k$ is a Kalman filter gain at the instant $t_k$, $\mathbf{P}_k^- = E\left[(\mathbf{X}_k - \hat{\mathbf{X}}_k^-)(\mathbf{X}_k - \hat{\mathbf{X}}_k^-)^T\right]$ is an *a priori* error covariance matrix, $\mathbf{P}_k = E\left[(\mathbf{X}_k - \hat{\mathbf{X}}_k)(\mathbf{X}_k - \hat{\mathbf{X}}_k)^T\right]$ is an *a posteriori* error covariance matrix, and $\mathbf{I}$ is a $(2n \times 2n)$ identity matrix.

Making use of the state transition matrix, we can project the filter ahead and use the measurement at instant $t_{k+1}$. Therefore, the estimate for the instant $t_{k+1}$ and the error covariance matrix associated with this estimate will be:

$$\hat{\mathbf{X}}_{k+1}^- = \mathbf{\Phi}_k \hat{\mathbf{X}}_k \tag{3.18}$$

$$\mathbf{P}_{k+1}^- = \mathbf{\Phi}_k \mathbf{P}_k \mathbf{\Phi}_k^T + \mathbf{Q}_k \tag{3.19}$$

## 3.4 Harmonic Estimation using Artificial Neural Networks

There are many available algorithms for estimation of power system harmonic components based on learning principles. Some of ANN algorithms are based on the backpropagation learning rule [73-75] while others utilized the LMS (Widrow-Hoff) learning rule [76-78]. Hartana and Richards[73] were among the first who used backpropagation ANN to track harmonics in large power systems, where it is difficult to locate the magnitude of the unknown harmonic sources. In their method, an initial estimation of the harmonic source in a power system was made using neural networks.

They used a multiple two-layer feedforward neural network to estimate each harmonic amplitude and phase. The scheme was trained to identify the harmonic sources in a 14-bus system. Mori *et. al.*[74] have provided a basic ANN model to estimate the voltage harmonics from real measured data. In their paper, a comparison between the conventional estimation methods for predicting the $5^{th}$ harmonic is given. Pecharanin et.al [75] presented an ANN topology, based on the backpropagation learning rule, for harmonic estimation to be used in active power filters. They taught the neural network to map the amplitude of the $3^{rd}$ as well as the $5^{th}$ harmonic from a half cycle of a distorted current waveform. This method has a limited applicability in active filtering since it does not consider the detection of the harmonic phase angles in which it may increase the distortion and make the case worse if the injected signal is of the wrong phase.

The main drawback of the backpropagation ANN is the requirement of the huge data set required for training. Also, the backpropagation ANN may lead to inaccurate results because of the random-like behavior and the large variations in the amplitude and the phase of the harmonic components and/or in the presence of random noise [78].

Osowski [76] provided an ANN that is based on the least mean square (LMS) learning principle to estimate the harmonic components in a power system. He built electronic circuitry that minimizes the error between the desired (measured) samples of

the line voltage and the output of the neural network in an adaptive way. The Osowski method makes the hardware implementation of harmonic estimation using ANN visible.

Later, Dash et.al [77] utilized the ADALINE, a version of an ANN, as a new harmonic estimation technique. The learning rule of the method is based on the LMS introduced by Widrow-Hoff. ADALINE is an adaptive technique. Its main advantages are speed and noise rejection [77-78]. It proves to be superior to the Kalman Filter technique in finding the magnitudes and phases of the harmonics [77].

### 3.4.1 ADAptive LInear NEuron (ADALINE)

The ADALINE is a two layered feed-forward perceptron, (see Appendix B), having $N$ input units and a single output unit. The ADALINE is described as a combinatorial circuit that accepts several inputs and produces one output. Its output is a linear combination of these inputs. An ADALINE in block diagram form is depicted in Fig. 3.2.

The input to the ADALINE is $\mathbf{X} = (x_0, x_1, x_2, \cdots, x_n)^T$, where $x_0$, is called a bias term or bias input, is set to 1. The ADALINE has a weighted vector $\mathbf{W} = (w_0, w_1, w_2, \cdots, w_n)^T$, and its output is simply $y = \mathbf{W}^T \cdot \mathbf{X} = w_0 + w_1 x_1 + w_2 x_2 + \ldots\ldots\ldots + w_n x_n$.

In a digital implementation, this element receives at time $k$ an input signal vector or input pattern vector $\mathbf{X}(k) = [x_{0k} \quad x_{1k} \quad x_{2k} \quad \cdot \quad \cdot\cdot \quad \cdot \quad x_{nk}]^T$ and a desired response $y_d(k)$,

a special input used to affect learning. The components of the input vector are weighted by a set of coefficients, the weight vector $\mathbf{W}(k)=[w_{0k} \quad w_{1k} \quad w_{2k} \quad \cdots \quad w_{nk}]^T$. The sum of the weighted inputs, i.e., $\mathbf{y}(k) = \mathbf{W}(k)^T \mathbf{X}(k)$ is then computed. The weights are essentially continuous variable, and can take on negative as well as positive values.

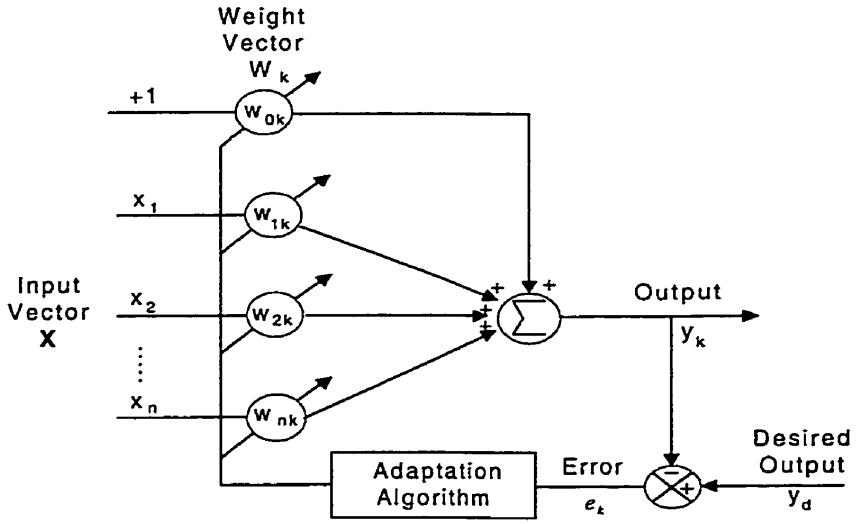


Fig. 3.2. Adaptive linear neuron ( ADALINE )

During the training process, input patterns and corresponding desired responses are presented to the ADALINE. An adaptation algorithm, usually the Widrow-Hoff LMS algorithm, is used to adjust the weights so that the output responses of the input patterns become as close as possible to their respective desired responses. This algorithm minimizes the sum of squares of the linear errors over the training set. The linear error $e(k)$ is defined to be the difference between the desired response $y_d(k)$ and the linear output $y(k)$, at time or sample $k$.

#### 3.4.1.1 Widrow-Hoff learning rule

The Widrow-Hoff learning delta rule calculates the changes to weights of ADALINE to minimize the mean square error between the desired signal output $y_d(k)$ and the actual ADALINE output $y(k)$ over all k. The weight adjustment, or adaptation, equation can be written as [79]

$$\mathbf{W}(k+1) = \mathbf{W}(k) + \alpha \frac{e(k)\mathbf{X}(k)}{\mathbf{X}^T(k)\mathbf{X}(k)} \tag{3.20}$$

where $k$ = time index of iteration, $\mathbf{W}(k)$ = weight vector at time $k$, $\mathbf{X}(k)$ = input vector at time $k$, $e(k) = y_d(k) - y(k)$ = error at time $k$, and $\alpha$ = reduction factor.

### 3.4.2 ADALINE as Harmonic Estimator

The ADALINE has been used to estimate the time-varying magnitudes and phases of the fundamental and harmonics in a distorted waveform [77-78], Fig 3.3. Consider a distorted signal $f(t)$ with the Fourier series expansion:

$$f(t) = A_{dc}e^{-\beta t} + \sum_{l=1}^{N} Z_l \sin(l\omega t + \varphi_l) \tag{3.21}$$

where, $A_{dc}e^{-\beta t}$ is the decaying dc component, $\beta$ =decaying coefficient, $Z_l$ and $\varphi_l$ are the amplitude and the phase angle of the $l^{th}$ harmonic, respectively, and N is the total number of harmonics. In the literature [77-78], $\omega$ is assumed to be known in advance. The discrete-time representation of $f(t)$ will be:

$$f(t_k) = A_{dc}(1-\beta kT_s) + \sum_{l=1}^{N} A_l \cdot \sin l\omega t_k + \sum_{l=1}^{N} B_l \cdot \cos l\omega t_k \tag{3.22}$$

where, the term $A_{dc}(1-\beta kT_s)$, represents the first two terms of the Taylor series expansion of the decaying dc component, $T_s = 2\pi/\omega N_s$, $N_s$ is the sampling rate, $A_l = Z_l \cos\varphi_l$, $B_l = Z_l \sin\varphi_l$, and $t(k) = k^{th}$ sampling time.

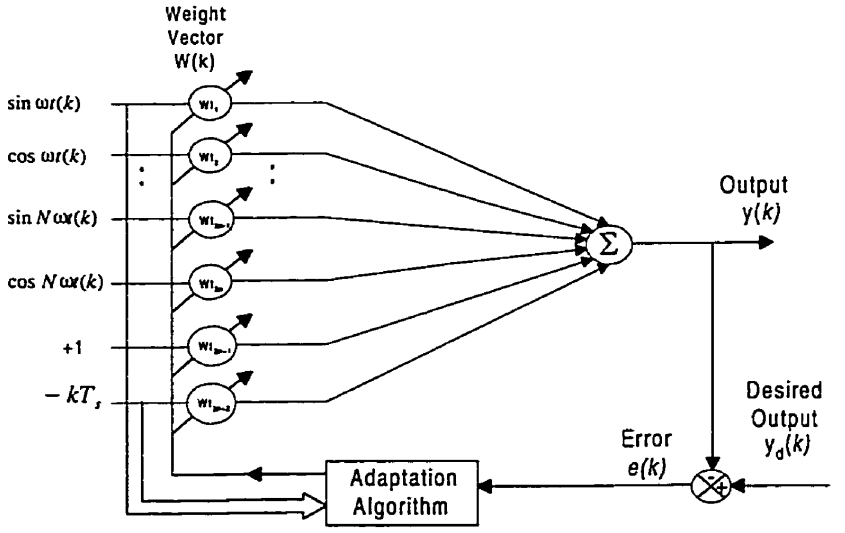


Fig. 3.3 ADALINE as harmonic components estimator.

To extract the fundamental and harmonic components from $f(k)$, the ADALINE input vector, $\mathbf{X}(k)$, is chosen to be:

$$\begin{aligned}\mathbf{X}(k) = [&\sin\omega t(k) \quad \cos\omega t(k) \quad \sin 2\omega t(k) \quad \cos 2\omega t(k), \\ &\cdots\cdots, \sin N\omega t(k) \quad \cos N\omega t(k) \quad 1 \quad -kT_s]^T\end{aligned} \tag{3.23}$$

and its desired output $y_d(k)$ is set to be equal to the actual signal, $f(k)$.

Perfect tracking is attained when the tracking error $e(k)$ is brought to zero ( or below a pre-specified value). Then

$$y(k) = y_d(k) = f(k) = \mathbf{W}_o^T \mathbf{X}(k) \tag{3.24}$$

where $\mathbf{W}_o$, the weight vector after final convergence is attained, is:

$$\mathbf{W}_o = [A_1 \quad B_1 \quad \cdots\cdots \quad A_N \quad B_N \quad A_{dc} \quad \beta A_{dc}] \tag{3.25}$$

The estimated magnitudes and phases of the harmonics ($Z_l$ and $\varphi_l$, $l$ =1,...., N) can be readily calculated from the elements of $\mathbf{W}_o$, i.e., the Fourier coefficients. Therefore,

$$Z_l = \sqrt{w_o^2(2l-1) + w_o^2(2l)} \tag{3.26}$$

$$\phi_l = \tan^{-1}\left\{ w_o(2l) \Big/ w_o(2l-1) \right\} \tag{3.27}$$

# 3.5 Evaluation of The Estimation Techniques

In this section, both of the harmonic estimation techniques (ADALINE and Kalman filter) are investigated and compared against each other from different points of view using computer simulations. FFT is used as a reference for this comparison. The diagonal elements of the process covariance matrix Q and the measurement noise variance R of the Kalman filter algorithm are chosen to be 0.01 and 0.001, respectively [77].

## 3.5.1 Speed and Convergence

To test the speed and convergence of the estimation techniques (ADALINE and Kalman filter), a waveform of known harmonic contents is taken for estimation. The waveform

consisting of the fundamental, third, fifth, seventh, eleventh, thirteenth and nineteenth harmonics is simulated using MATLAB. The waveform is described as

$$f(t) = 1.0\sin(\omega t + 10^{o}) + 0.2\sin(3\,\omega t + 20^{o}) + 0.08\sin(5\,\omega t + 30^{o}) + 0.05\sin(7\omega t + 40^{o}) + 0.06\sin(11\,\omega t + 50^{o}) + 0.05\sin(13\,\omega t + 60^{o}) + 0.03\sin(19\,\omega t + 70^{o}) \quad (3.28)$$

The sampling frequency was selected to be 64x60 Hz.

Fig.3.4 shows the estimation of the magnitude and phase of the fundamental, fifth and seventh harmonics, respectively. Both of the estimation algorithms estimate the harmonic parameters correctly in the time interval corresponding to approximately one period (T) of the fundamental frequency.

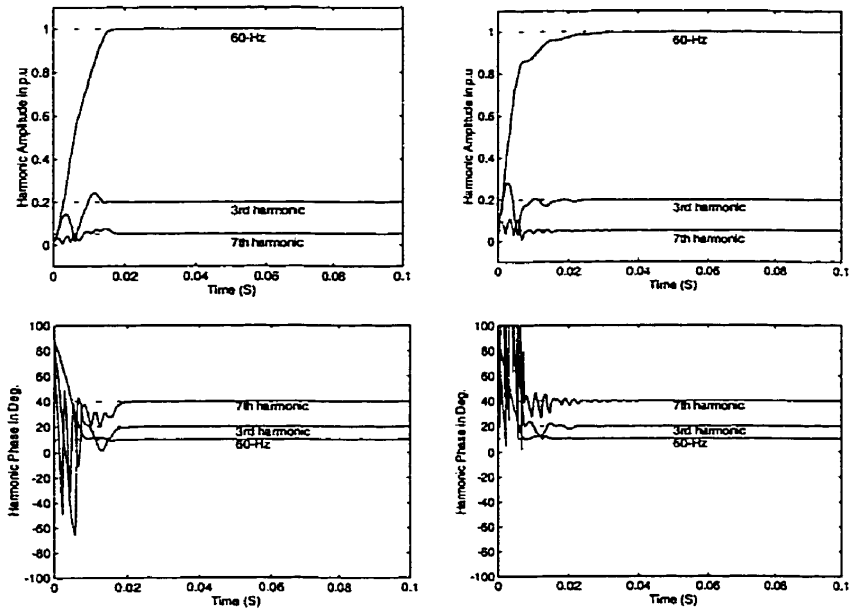


(a) (b)

Fig. 3.4: Estimated magnitude and phase angle of the fundamental, fifth and seventh harmonics
(a) using ADALINE (b) using Kalman filter

### 3.5.2 Harmonic Estimation in the Presence of Noise and Decaying dc Components

Further investigations have been made to check the ability of the above-mentioned algorithms in tracking the waveform harmonic components in the presence of random noise and decaying dc component. A random noise of variance 0.02 and an exponentially decaying dc component represented as $(0.1\exp(-5t))$ were added to the measured samples of the waveform given by equation (3.28).

Fig 3.5(a), Fig. 3.5(b) and Fig. 3.5(c) display the results of estimation of the fundamental and the fifth harmonic using ADALINE, 12-state tuned Kalman filter and FFT, respectively.

On comparison of Fig. 3.5(a), Fig. 3.5(b) and Fig. 3.5(c), one can observe that the ADALINE has a better performance in terms of convergence speed and noise rejection compared with the Kalman filter and FFT in the presence of random noise and decaying dc component.

### 3.5.3 High Sampling Rate

In order to investigate the performance of the estimation algorithm signals with high sampling rate, the sampling points of the signal given by equation (3.28) are increased. Fig. 3.6(a), Fig. 3.6(b) and Fig. 3.6(c) present the influence of increasing the sampling

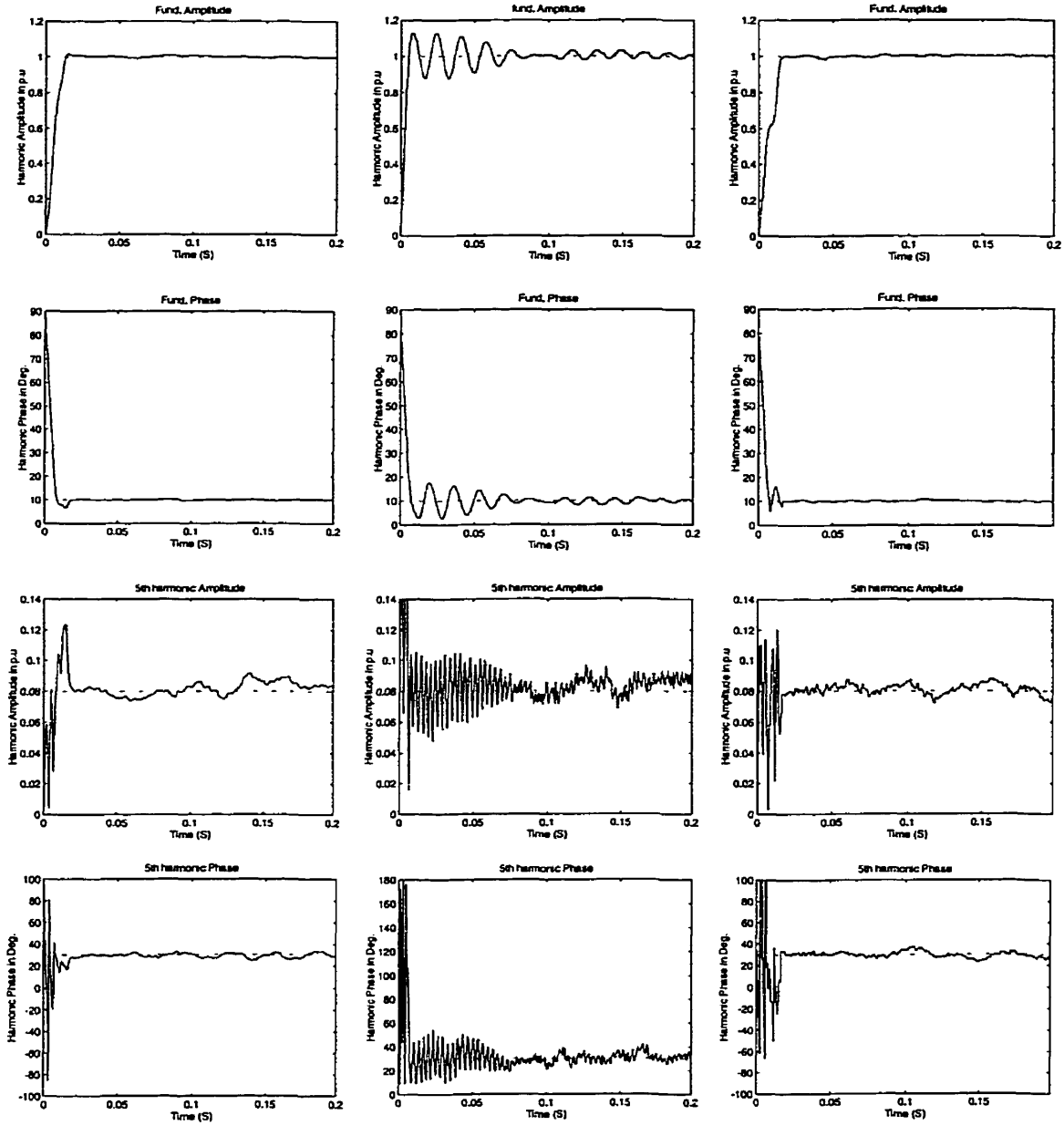


(a) (b) (c)

Fig. 3.5: Estimation of fundamental and fifth harmonic components in the presence of noise and decaying dc components

(a) using ADALINE
(b) using Kalman filter
(c) using FFT

rate on the results of the estimation of the magnitudes and phases given in Fig. 3.5(a), Fig. 3.5(b) and Fig. 3.5(c). The figures show the performance of ADALINE is improved dramatically compared with the Kalman filter and that the error *e(k)* between the measured waveform and the output of ADALINE is reduced by increasing the number of samples.

### 3.5.4 Simplicity and Practical Applicability

The algorithm for ADALINE is simple and computationally efficient compared to Kalman filter algorithms that require high amounts of computation due to transcendental function evaluation and matrices inversion in real time. This makes ADALINE more suitable for on-line applications specifically when it is used for estimating time-varying signals.

### 3.5.5 Frequency Tracking

One of the common problems with FFT is the spectral leakage effect resulting from the deviation in the fundamental frequency. A fundamental frequency offset of 0.4 Hz produces an error of 10% in the amplitude of the fifth harmonic [80]. To overcome this problem, a variety of numerical algorithms have been developed for frequency measurement, such as the zero crossing technique. This technique is simple and reliable

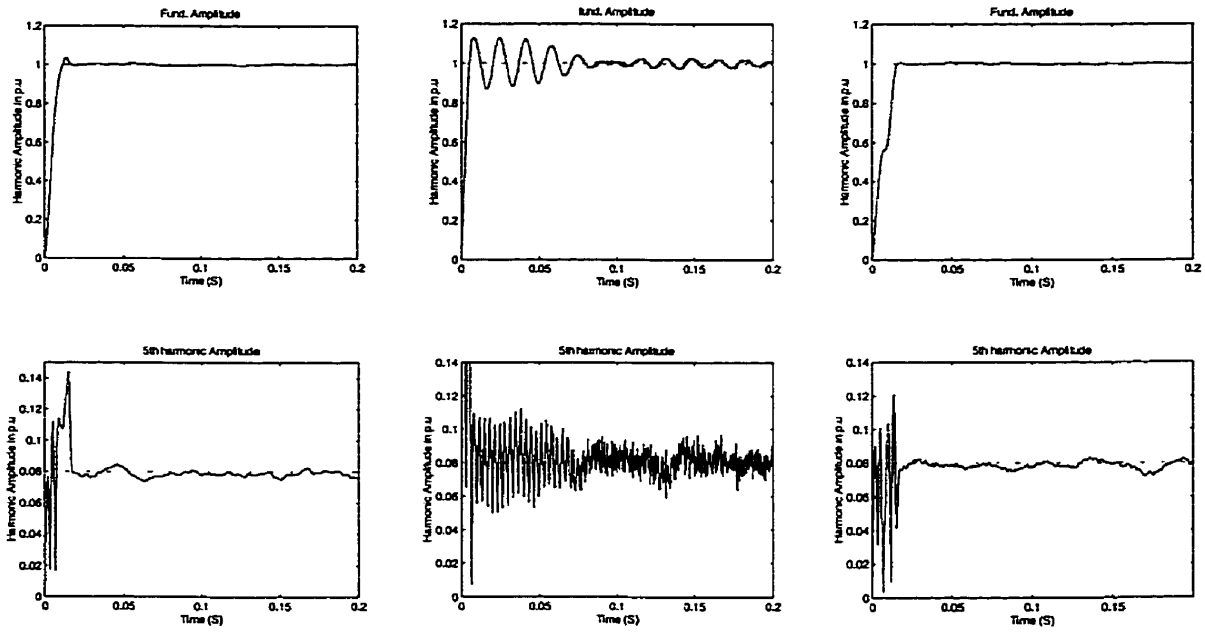


Fig. 3.6: The influence of high sampling rate on the estimation of fundamental and 5$^{th}$ harmonic amplitude
(b) using ADALINE
(c) using Kalman filter
(d) using FFT

but its performance has a cost: long measurement times (generally more than 3 cycles of the fundamental). Both the Kalman filter and FFT may use zero crossing as an external algorithm to measure the fundamental frequency. However, the ADALINE algorithm is modified by combining the fundamental frequency tracking with ADALINE-based harmonic analyzer as proposed in Chapter 5.

The fundamental frequency tracking capability is an important feature for successful active harmonic filtering. An unregulated dc-side of the CSC module is expected if the fundamental frequency drifts from its nominal value.

From the above comparison, one can observe the following:

1. Both of the estimation algorithms (ADALINE, Kalman filter) have similar performance and the convergence achieved within one cycle of fundamental frequency when the analyzed signal is not contaminated with noise and decaying dc component.
2. The ADALINE produces faster convergence and noise rejection in the presence of noise and decaying dc components compared with the Kalman filter and FFT.
3. As the number of samples of a measured waveform corrupted by a dc component, harmonic and noise is increased, the ADALINE exhibits better performance compared with the Kalman filter. As the value of the decaying dc component increases, the performance of the Kalman filter and FFT got worse. Note that the results shown in Fig. 3.5 and Fig. 3.6 happen to be case dependent and the performance of the Kalman filter would be improved by the proper selection of the filter parameters $\mathbf{Q}$ and $R$.
4. The Kalman filter technique estimates the harmonic components by utilizing a smaller number of samples and in relatively shorter time as compared to FFT

[77]. But, its main problem is the high computational demand due to transcendental function evaluations. This makes the Kalman filter approach unfit for on-line applications, specifically for extracting time-varying harmonics.

## 3.6 Summary

In this chapter, three different harmonic estimation approaches (ADALINE, Kalman filter and FFT) were discussed. The harmonic estimation methods presented throughout this work can be evaluated as follows:

- The ADALINE and Kalman filter are recursive techniques, and they are faster than the FFT method and they have a noise rejection capability. However, the Kalman filter is computationally burdensome because of the evaluation of the transcendental functions and the involved matrices inversion.
- The estimation algorithms exhibit similar performance when the analyzed signal is not corrupted with noise and decaying dc component.
- The ADALINE has better overall performance compared with the Kalman filter and FFT algorithms especially if the signal is corrupted by noise and a decaying dc component. However, the performance could be improved by proper tuning of the Kalman filter parameters.

- The speed and accuracy in estimating the time-varying harmonic components in a noisy environment, automatic tuning to the system frequency, and the adaptive feature are the main advantages of ADALINE over the other estimation algorithms.

The analytical expectation has been verified in this chapter by extensive simulation results using the MATLAB simulation package.

Since ADALINE outperforms the other harmonic estimation techniques in terms of simplicity and practical applicability as well as noise rejection capability, it is well suited as an estimation tool for the modular harmonic filtering approach presented in this proposal.

# Chapter 4
# Active Power Filtering

## 4.1 Overview

The objective of this chapter is to study the base configuration of the active source used in active filters and how the active sources behave as a linear amplifier using PWM switching strategy. Emphasis is given to the losses due to the PWM technique.

The configuration of the active source is first given in section 4.2 to highlight the basic power converter topologies used in active power filters. Section 4.3 details the PWM switching technique and how high-power amplifiers are formed using PWM technique. The calculation of the conduction and switching losses in the active power

filters are explained in details in section 4.4. Finally, the comparison between single-phase CSC and VSC followed by the summary are given at the end of the chapter.

## 4.2 Configuration of the Active Source

As seen in Chapter 2, active power filtering based on the injection method is basically performed by replacing the portion of the sine wave that is missing in the current drawn by a nonlinear load. This can be accomplished in two stages. The first stage consists of detecting the amplitudes and phases of the AC harmonic currents (or any system quantity associated with them) which are present in the AC line. The second stage is the injection of the appropriate harmonic currents (or insertion of appropriate harmonic voltages) at the appropriate frequency so as to supply the AC harmonic currents required by the nonlinear load.

The active harmonic source within the filtering network is basically a static converter connected to a DC source. The converter must be controlled to provide the proper filtering harmonic currents or voltages. This is accomplished by shaping the DC input source into an output waveform of appropriate magnitude and frequency through modulation of semiconductor switches [20].

The harmonic converter can use either a DC voltage source or a DC current source. The DC source of a voltage converter consists of a capacitor that resists voltage changes, while that of a current converter consists of an inductor that resists current

changes. In both cases, the DC source receives its power from the AC power system. Converters are referred to as either voltage-fed or current-fed according to the type of DC-side source. The basic voltage and current source converter topologies are displayed in Fig. 4.1. In the current-source converter, a diode is placed in series with every switch to avoid reverse breakdown of the switch when the voltage across the switch during the OFF-period is negative. In voltage-source converter, an inverted diode is placed across each switch to provide a path for the current when the current cannot pass through the switch.

The power electronic circuits and devices used in both types of converter are quite similar. Most of the existing active power filters utilize switching devices such as gate turn-off thyristor (GTO), bipolar junction transistor (BJT) and insulated gate bipolar transistor (IGBT) for switching speeds up to 50 kHz. However the most attractive device is the IGBT. It has the merit of fast switching capability and requires very little drive power at the gate. Recently, a new generation of the IGBTs family called Non-Punch-Through (NPT) IGBT has emerged in the market. The distinct advantage of this device over its predecessor in IGBTs family is its ability to block the same voltage in both directions.

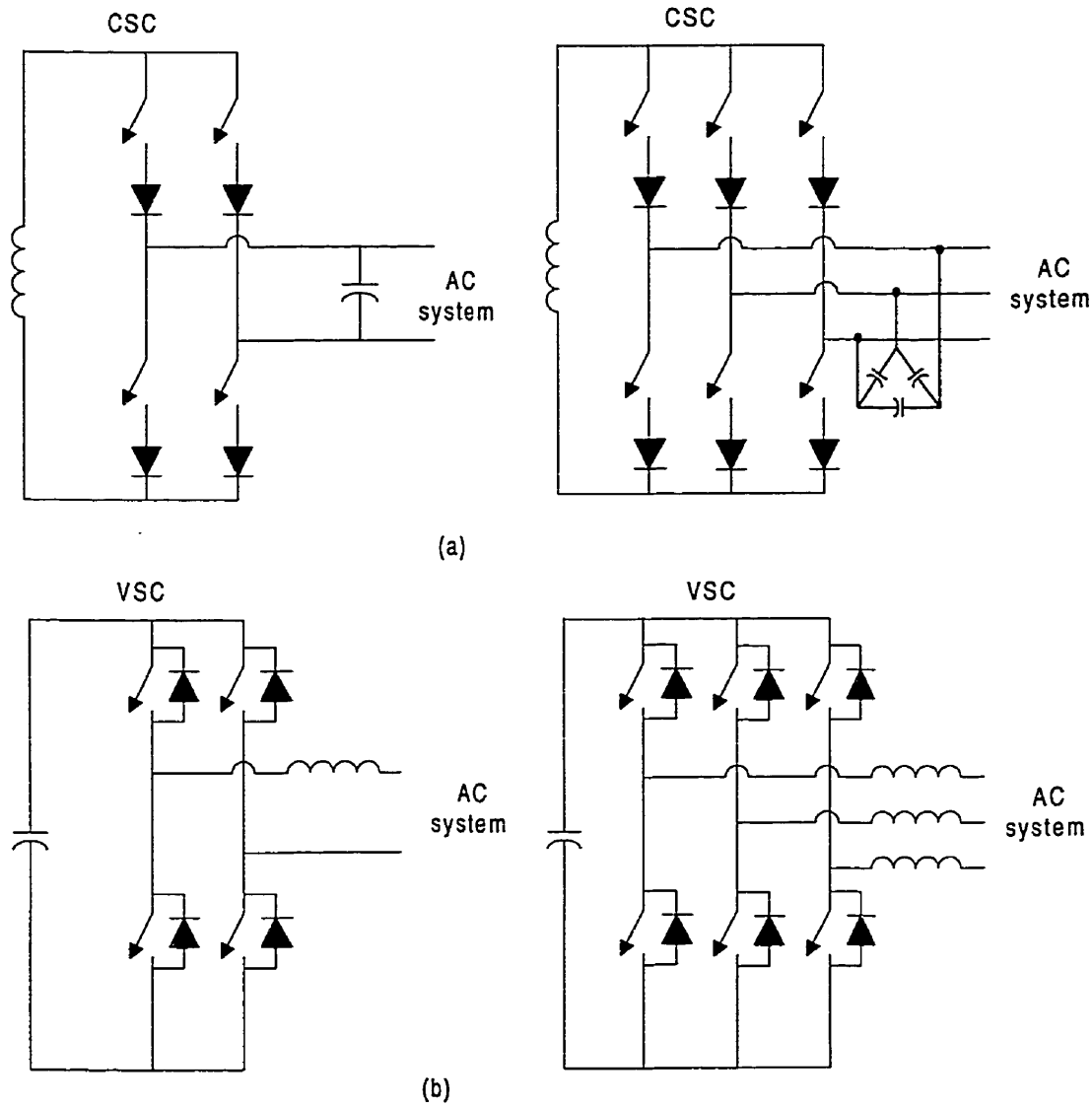


Fig. 4.1: (a) Single-phase and three-phase current-source converter (CSC)
(b) Single-phase and three-phase voltage-source converter (VSC)

# 4.3 The Sinusoidal-Pulse-Width Modulation (SPWM) Switching Strategy

PWM is a simple switching technique to control power converters. It employs switching at a constant frequency (a constant switching time) to control the output voltage or current. It generates control-switching signals to control the state (on or off) of the switch(s). This is achieved by comparing a control voltage signal ($v_{control}$) with a repetition waveform of a frequency higher than the fundamental frequency. The output of the comparator controls the switches. The output voltage or current of the converter, Fig. 4.2, is in the form of pulse trains having the same frequency as the generated switching signals. The pulse train is modulated so that the local average value of each pulse is equal to the instantaneous value of the required signal at the time of its occurrence. If the control signal is a sinusoidal waveform, the method is called the sinusoidal pulse width modulation (SPWM).

In order to obtain a sinusoidal current waveform at a desired frequency, a sinusoidal control (modulating) signal at the desired frequency is compared with a repetitive switching frequency triangular (carrier) waveform, as shown in Fig. 4.3. Whenever the value of the modulating signal ($v_{control}$) is higher than that of the carrier signal ($v_{tri}$), the power switches pair ($S_3$, $S_4$) is turned OFF and, immediately, the other pair ($S_1$, $S_2$) is turned ON. Contrarily, whenever $v_{control}$ is lower than $v_{tri}$, the pair of switches ($S_1$, $S_2$)

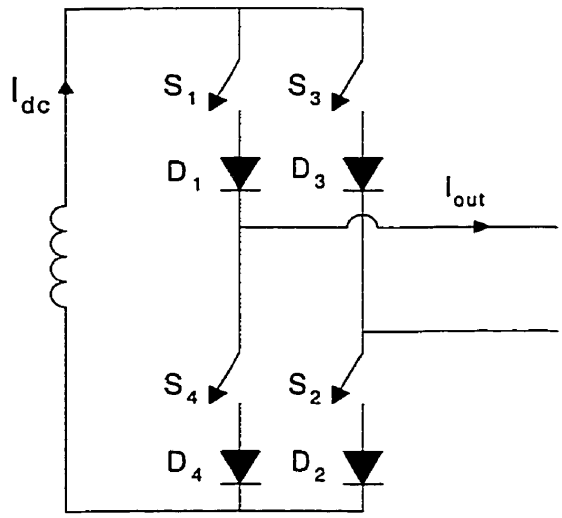


Fig. 4.2: The simplified version of CSC bridge

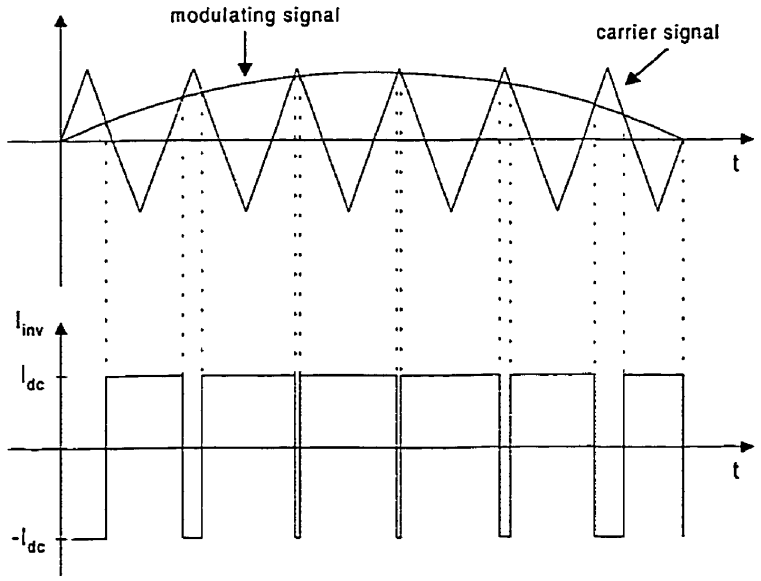


Fig. 4.3: Sinusoidal Pulse-Width Modulation

is switched on and hence the other pair is switched off. The converter output current ($I_{out}$) is a train of variable duration pulses that fluctuates between ± $I_{dc}$, which will reproduce the modulated signal when averaged.

The ratio of the peak of the amplitude of the modulating signal ($\hat{V}_{control}$) to the amplitude of the triangular waveform ($\hat{V}_{tri}$) is defined as the "amplitude modulation index"

$$m_a = \frac{\hat{V}_{control}}{\hat{V}_{tri}} \tag{4.1}$$

The amplitude of the desired fundamental component of the output current $(\hat{I}_{Ao})_d$, provided that $m_a \leq 1$ and that the frequency of the triangular waveform ($f_s$) is much larger than the frequency of the modulated signal ($f_d$), is given by

$$(\hat{I}_{Ao})_d = m_a I_{dc} \tag{4.2}$$

Therefore, the PWM converter behaves like a linear amplifier, as long as the amplitude of the carrier signal is greater than that of the modulating signal and its frequency is much greater than the of that modulating signal.

It should be noted that the frequency of the triangular waveform ($f_s$) decides the frequency bandwidth of the converter and is generally kept constant along with its amplitude.

PWM converter can be considered as a linear power amplifier because it has the ability to generate compensating harmonic currents or voltages corresponding to a small control signal. Fig. 4.4 shows a block diagram of PWM converter operating as a linear amplifier. In this diagram, all the properties of the signal $c(t)$ are maintained in the fundamental component of the output waveform, except for the magnitude which is multiplied by the gain of the amplifier (k). This is always true as long as the switching frequency is sufficiently high such that $c(t)$ can be considered constant during one switching period [54].

The performance of the pulse width modulation (PWM) technique is very promising when it is applied to active power filtering. It is capable of obtaining harmonic suppression to less than 1% of the fundamental [25]. Also this method can be programmed to eliminate specific harmonics.

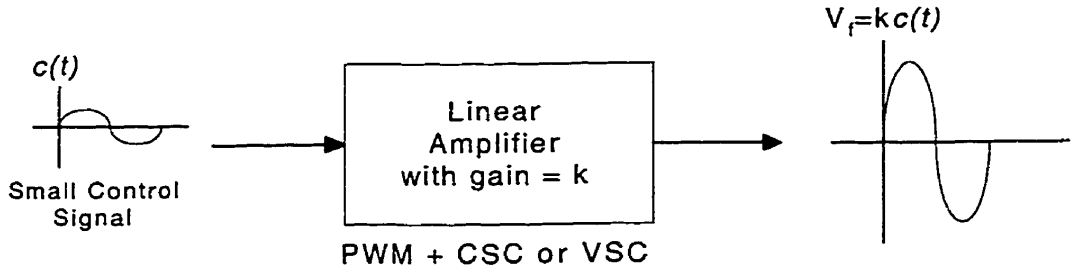


Fig. 4.4: PWM converter as a linear amplifier

## 4.4 Tri-Logic PWM Current Source Converter

In this section, CSC configuration under the tri-logic PWM switching technique which is used in the proposed modular active filter is presented. Fig. 4.5 shows the CSC bridge which consists of 6 IGBT switches, a dc-side reactor and a 3-phase ac-side capacitive filter for filtering the switching harmonics.

For the CSC to operate properly, one and only one of the upper switches and one and only one of the lower switches must operate at any moment of time. The dynamic tri-logic PWM technique [55] has been developed to satisfy the above requirement and to provide independent control on the ac-side currents of the CSC, based on three control signals $S_{ma}, S_{mb}$, *and* $S_{mc}$, with the condition that $S_{ma}+S_{mb}+S_{mc}=0$. The tri-logic PWM control block, shown in Fig.4.5, produces 3-level signals to control the three legs of the CSC independently.

For the case of 3-phase 3-wire ac systems, the sum of the three phase currents is equal to zero. Therefore, the sum of the compensating currents to be injected in the lines will be equal to zero and as a result, $S_{ma}+S_{mb}+S_{mc}=0$. It can be shown [55] that

$$\begin{bmatrix} i_a \\ i_b \\ i_c \end{bmatrix} = k \cdot I_{dc} \cdot \begin{bmatrix} S_{ma} \\ S_{mb} \\ S_{mc} \end{bmatrix} \tag{4.3}$$

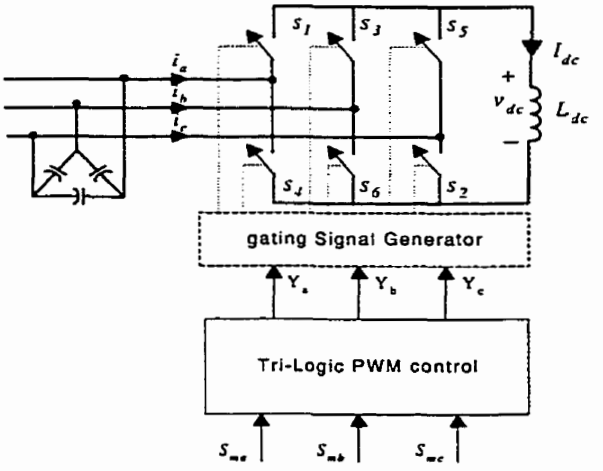


Fig. 4.5: Current Source converter with tri-logic PWM control

where, $k$ is a proportionality constant. From the above relation, one can observe that the CSC under the Tri-Logic PWM operates as three independent linear amplifiers, one amplifier for each phase.

# 4.5 The Losses in the Switching Devices

Two distinct types of power losses can be attributed to the switching devices.

## 4.5.1 On-state (conduction) losses

When the semiconductor switch is in the on-state, there is a finite voltage across the device. The current through the device ($i_{sw}$) and the on-state voltage drop across the device ($V_{ON}$), contribute to the conduction loss ($P_{cond}$).

$$P_{cond} = i_{sw,ON} V_{ON} \tag{4.4}$$

## 4.5.2 Switching losses

During the turn-ON and the turn-OFF process of the semiconductor switch, some power is dissipated due to the presence of finite current through the switch and finite voltage across it at the same time. The duration of the simultaneous presence of the current and the voltage, i.e. the length of cross-over period, depends on the nature of the load being switched. The worst case happens when a pure inductive load is switched (Fig. 4.6).

The turn-ON and turn-OFF processes of the switch in Fig. 4.6, can be explained using Fig. 4.7. When the switch is OFF, the load current is freewheeling through the diode. The voltage drop across the switch can be approximated by

$$v_{sw,OFF} = V_d$$

Also,

$$i_{sw,OFF} = 0$$

When the switch receives an ON- command, after a short delay, its resistance starts to drop providing a path for a part of $I_L$, and $i_{sw}$ start rise to $I_L$ during the $t_r$, the switch current rise-time. But as long as the diode is conducting, the voltage across the switch will be equal to $V_d$. When the load current is completely transferred to the switch, the voltage across the diode starts to rise until all $V_d$ is placed across the reverse

biased diode. The switch will conduct the load current $I_L$ and the voltage across the switch will be $V_{ON}$.

During $t_{on}$, since there is a voltage across the switch and a current through it, some power will be lost. Assuming linear variations, the current through the switch $i_{sw}$ is given by:

$$i_{sw} = \frac{I_L t}{t_r} \tag{4.5}$$

$I_L$, the load current, is assumed to be constant during one switching period.

The power loss is shown as a function of time in Fig. 4.6. The energy loss during $t_{on}$ will be:

$$E_{on} = \frac{I_L V_d t_{on}}{2} \tag{4.6}$$

When the switch receives an OFF- command, after a short delay, its resistance starts to grow, increasing $v_{sw}$. But as long as $v_{sw}$ has not reached $V_d$, the diode can not be forward biased and all the load current $I_L$ passes through the switch. When $v_{sw} = V_d$, the diode become forward biased, and the current is transferred gradually from the switch to the diode, during $t_f$, the switch current fall time, till all the load current starts freewheeling through the diode and $i_{sw} = 0$.

From the graph of power loss vs. time, the energy loss during $t_{off}$ can be found as:

$$E_{off} = \frac{I_L V_d t_{off}}{2} \tag{4.7}$$

Therefore, the total energy loss due to switching can be given by:

$$E_{sw} = (E_{on} + E_{off}) = \frac{I_L V_d (t_{on} + t_{off})}{2} \tag{4.8}$$

If the switch is turned ON and OFF at a rate $f_{sw}$, $E_{sw}$ will be the energy loss due to switching in $T_{sw} = \frac{1}{f_{sw}}$ seconds. The average power lost due to the switching, $P_{sw}$, is given by:

$$P_{sw} = \frac{E_{sw}}{T_{sw}} = E_{sw} f_{sw} = \frac{1}{2} I_L V_d (t_{on} + t_{off}) f_{sw} \tag{4.9}$$

As seen, as the $t_{on}$ and $t_{off}$ (i.e, the switching times of the device) and $f_{sw}$ (the switching frequency of the device) are increased, the switching losses are increased as well.

In a converter unit with a number of switches, the total losses (conduction and switching) will be determined by the number of switches and the voltage and current levels that they are exposed to.

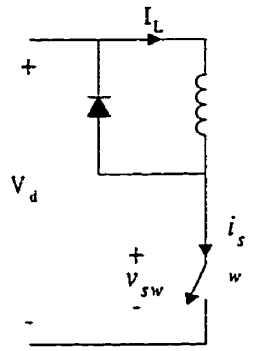


Fig. 4.6: Simplified inductive switching circuit

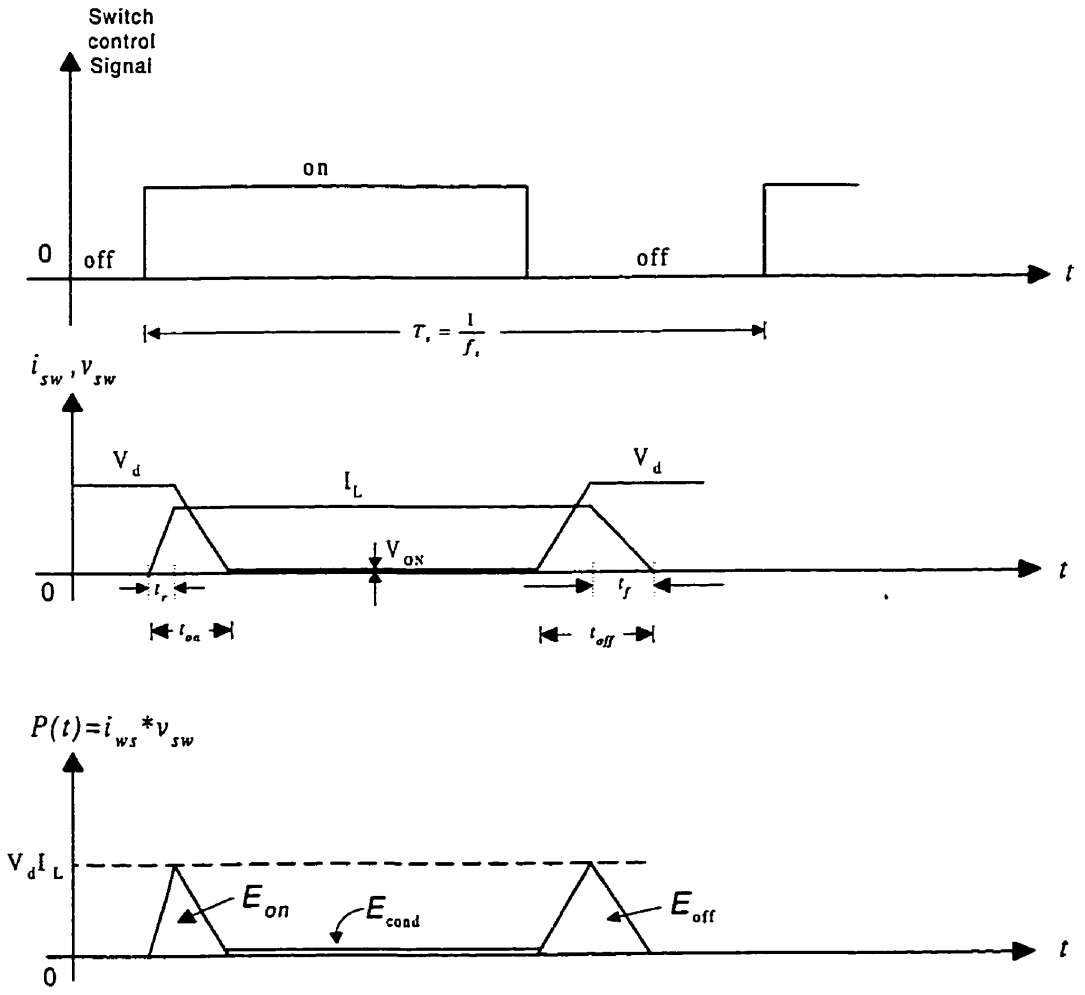


Fig. 4.7: Instantaneous switch power loss.

## 4.6 VSC Topology Versus CSC Topology

For a long time, VSC topology was preferred to CSC topology due to the higher conduction losses in the latter. With the availability of (NPT) IGBT switches, capable of bi-directional blocking, the series diodes are no longer required in the CSC topology and high conduction losses and low efficiency will no longer be an issue [24]. In applications such as active power filtering, the CSC topology proves to be advantageous over the VSC topology on two counts: (1) In CSC, the output current is controlled directly, resulting in fast dynamic response, while in VSC, the control on the output current is indirect, resulting in a rather sluggish response. (2) In CSC, the DC-link current to be maintained depends on the output current demand, while in VSC, the DC-link voltage to be maintained, depends on the line voltage level. As a result, the CSC is more likely to perform a specific filtering job with lower DC energy storage requirement [24]. Due to the above favorite characteristics, CSC topology is receiving more and more attention in power quality control applications.

## 4.7 Summary

In this chapter, the basic principles of active harmonic filtering have been presented. The device switching losses as well as the converter topologies used in active filtering were discussed. The advantages of using PWM control strategy for power converters

and how they work as a linear amplifier were presented. A comparison between the single-phase CSCs and VSCs showed the advantages of using CSC in active filters over its counterpart.

# Chapter 5
# The Proposed Modular Active Power Filter System

## 5.1 Motivation

As seen in Chapter 2, the need for a better overall system performance than that provided by AC passive filters prompted power electronics and power system engineers to develop a new dynamic solution to the harmonic problem, namely, the active power filter. Almost all of the recently proposed active power filters utilize the PWM switching control strategy due to its simplicity and harmonic suppression efficiency. However, they suffer from one or more of the following shortcomings:

- Active power filters that are based on PWM switching strategy are not welcome by utility companies because of the high switching losses produced by the PWM

approach. The power converter used for this purpose is rated based on the magnitude of the distortion current and operated at the switching frequency dictated by the desired filter bandwidth. Fast switching at high power, even if technically possible, causes high switching losses and low efficiency.

- A serious shortcoming for proposing active power filters in electric power systems is the large converter size (rating). As seen in Chapter 2, the combinations of active and passive filters as well as employing multi-converter and multi level techniques are among the attempts in order to reduce the rating of converter.

- Most of the active filters connected to distribution systems are mainly a single unit with a high rating adequate for handling all harmonic components in the distorted waveform. Any failure in any of the active filter devices will make the whole equipment ineffective.

From the above discussion, the need for new equipment that can overcome all or some of the above drawbacks is evident. This equipment should have minimum switching losses, be highly reliable and flexible and have a low rating power converter. The proposed equipment should have fast response, adapt to the load variations and be appropriate for on-line applications.

## 5.2 A New Approach to Modular Active Power Filters

In low-voltage distribution system applications, almost all of the existing active power filters are realized by one unit of a single-phase or three-phase bridge converter [19-22]. The required voltage-withstand and current-carrying capabilities can be achieved by series and parallel connections of semiconductor switches. However, in high-power applications, the filtering job cannot be performed by one converter alone, due to the power rating and switching frequency limitations of semiconductor switches, as well as the problems associated with connecting a large number of switches in series or in parallel to attain the necessary ratings.

To overcome the above-mentioned restrictions, different multi-converter (modular) topologies have been proposed [56-58]. In these modular approaches, the filtering job is split among a number of pulse width modulated (PWM) voltage source converters (VSC) or current source converters (CSC) connected in series or in parallel. In the modular approach, the filtering load is distributed equally among active filter modules of identical power circuit and control circuit design. The power rating and switching frequency of each module is equal to the power rating and switching frequency required for the filtering task, divided by the number of modules. This makes it possible to use

the present gate-turn-off switch technology to realize high-power active filters of desirable performance.

In this thesis, a novel active filtering technique, based on CSC modules, which is appropriate for harmonic mitigation in electric distribution systems, is proposed. This active filter system is composed of the extraction, computation and mitigation stages. First, the information on the line current and the bus voltage are extracted very accurately by linear adaptive neurons (ADALINEs) from the power-line signals. Then, the required corrective signals are calculated and finally, the information is passed to the controller which activates the CSC modules to produce the compensating currents and inject them into the power line. Fig. 5.1 shows the block diagram of the operating stages of the proposed system. The proposed filter consists of several filter modules, each dedicated to eliminate a specific harmonic of choice. Low conduction and switching losses, high reliability and flexibility, fast response, self-synchronization and accuracy of ADALINE and fast response and high efficiency of CSC are the main advantages of the proposed system. The performance of the proposed active power filter is found to be excellent in eliminating the line harmonics.

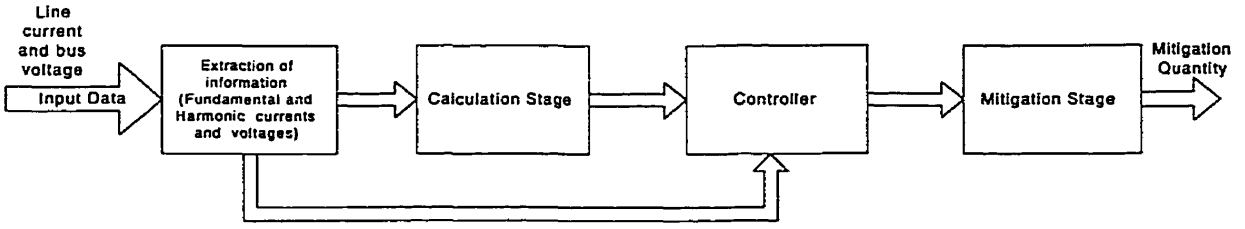


Fig. 5.1: The block diagram of the compensation principle of the proposed active filter system.

## 5.3 The Principle Of The Proposed Filtering Technique

The basic principle of the proposed filtering method is based on:

1. the extraction of the fundamental and individual harmonic current components of interest using one ADALINE and estimating the fundamental component of the line voltage by another ADALINE and,
2. injecting equal-but-opposite of each harmonic component of each phase into the corresponding phase using a CSC module dedicated to that specific harmonic (for eliminating the harmonics).

As seen in Chapter 2, in distribution systems, the magnitudes of the harmonic currents decrease and their frequencies increase with harmonic order. Therefore, in this proposed filter, the power converters dedicated to lower-order harmonics have higher ratings but are switched at lower rates, while those dedicated to higher-order harmonics

are of lower ratings but are switched at higher rates. As a result, the overall switching losses are considerably reduced due to balanced "power rating"-"switching frequency" product and selected harmonic elimination. The control system utilizes two (ADALINEs) to process the signals obtained from the power-line. The ADALINEs' outputs are used to construct the modulating signals of the filter modules. For each phase, the two ADALINEs continuously track the line current harmonics and line bus voltage as well as the system frequency and turn over this information to the controller of the CSC modules. The ADALINEs have the ability to predict accurately the fundamental and harmonics of the distorted signal in case of frequency drifting. In this method, a sophisticated software (the ADALINE-based controller) is developed to reduce the operating cost and increase the flexibility of the proposed filter system. The current and voltage ADALINEs are realized by calling a common subroutine, the ADALINE algorithm which is explained in section 5.8.

## 5.4 System Configuration

The basic blocks of the proposed modular active filter system connected to the electric distribution system are shown in Fig. 5.2. The system consists of a number of single-phase current-source converter (CSC) modules connected in parallel for each phase. Each filter module is dedicated to suppress a specific low-order harmonic of choice. The proposed active filter system uses two ADALINEs to process the signals obtained

from the power line. The method is based on estimating the discrete Fourier coefficient of a distorted current by one module of ADALINE (the current ADALINE) and predicting the phase bus voltage by another module (the voltage ADALINE). The output of the current ADALINE is used to generate the modulating signals for the CSC modules. The power rating of the modules will decrease and their switching frequency (bandwidth) will increase as the order of the harmonic to be filtered increases. As a result, the overall switching losses are reduced due to selected harmonic elimination and balanced power rating-switching frequency product. The information made available by the current ADALINE allows for selected harmonic elimination. The output of the second ADALINE (the voltage ADALINE) is the fundamental component of the line voltage signal. It is used as the synchronizing signal for the regulation of the $I_{dc}$ of the CSC modules.

## 5.5 Compensation Principle

The basic function of the proposed active filter is to suppress selected low-order harmonics. The method is based on extracting individual harmonic components using the current ADALINE and injecting equal, but opposite of the summation of these harmonic currents into the power line using the corresponding filter modules. With $i_L = i_1 + \sum i_h$ ($h$ being the harmonic order), $i_{inj} = \sum i_h$ is injected by the active filter system so that $i_s = i_1$, only (where $i_1$ = fundamental current).

As shown in Fig. 5.2, for each phase, the line current signal ($i_L$) is obtained through a current transformer (CT) and fed to the current ADALINE which adaptively and continuously estimates the fundamental and harmonic components of the line current signal. The phase voltage signal is obtained by a potential transformer (PT) and processed by another ADALINE (voltage ADALINE) to extract the fundamental component of the phase voltage waveform. The output of the current ADALINE is used to generate the PWM switching signals for the CSC units which inject the corresponding distortion in order to suppress the harmonic components in the line current ($i_L$). The output of the second ADALINE is used as a synchronization signal in the control loop that maintains the dc-side average current ($I_{dc}$) of each CSC module at

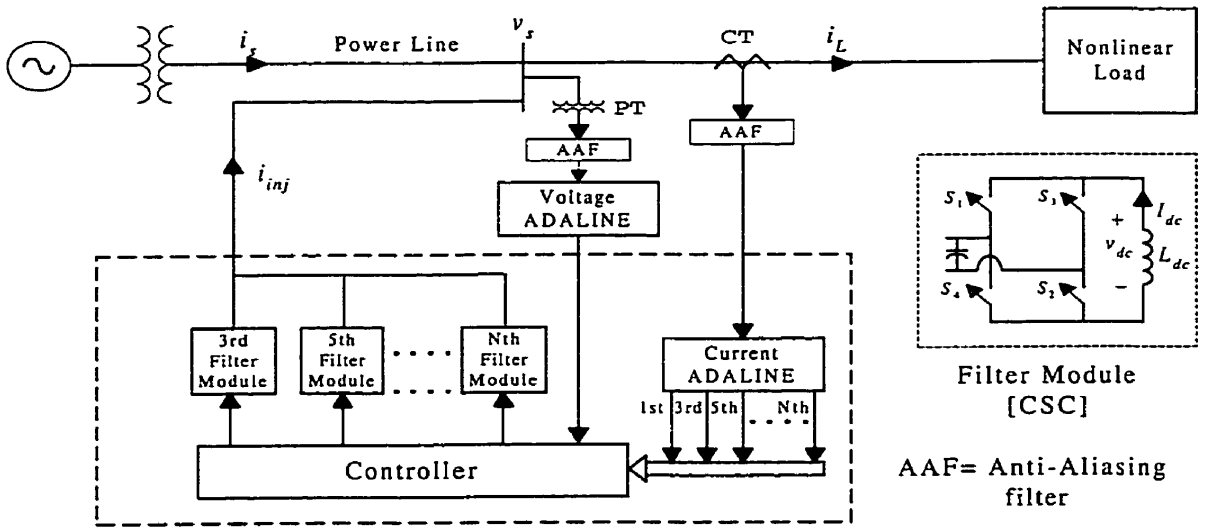


Fig.5.2: The proposed modular active power filter system.

a desired value. The output currents of all the CSCs are added at a junction point and injected into the power line. The total injected current, $i_{inj}$, is equal, but opposite to the sum of the harmonic components to be eliminated ($\sum i_h$).

## 5.6 Control Scheme

Fig. 5.3 shows the control scheme for the proposed active filter. In this controller, the $l^{th}$- harmonic signal $A_l \sin(l\omega t + \varphi_l)$ is reconstructed from the output of the current ADALINE and compared to a triangular waveform to create the PWM switching pattern for the switches of the CSC module dedicated to that particular harmonic. Note that a CSC under the PWM strategy behaves as a linear amplifier. The gain of this amplifier is equal to $I_{dc}/V_{tri}$, where $I_{dc}$ is the dc-side current of the CSC and $V_{tri}$ is the peak value of the triangular waveform. In order to achieve a linear amplifier, the $I_{dc}$ of each CSC must be regulated to a constant value.

The converter losses and system disturbances, such as sudden load fluctuations, affect the dc-side currents of the CSC modules. For successful operation of CSCs as linear power amplifiers, $I_{dc}$ of each module must be regulated by means of a feedback control loop. The control loop adjusts the amplitude of a sinusoidal template, synchronized with the system voltage ($v_s$) obtained from the voltage ADALINE. The above signal will be used as a part of the modulating signal of the CSCs, as shown in

Fig.5.3. It results in drawing a small current component at fundamental frequency in phase with the system voltage (for charging up the $L_{dc}$ or increasing $I_{dc}$) or out of phase by 180° with respect to the system voltage (for discharging the $L_{dc}$ or decreasing $I_{dc}$). This action involves only real power transfer between the system and CSC modules in contrast with harmonic current injection that involves only reactive power transfer.

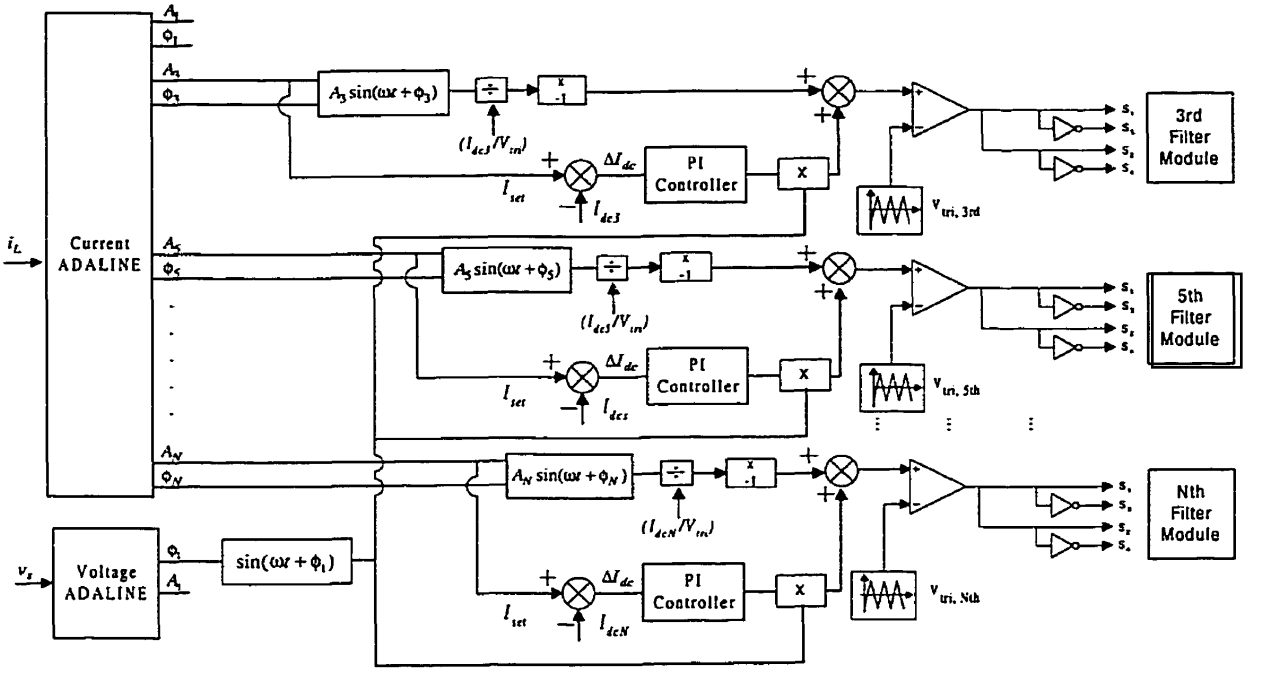


Fig. 5.3: The Control Scheme of the modular active filter (The Controller in Fig. 5.2)

In contrast to the other dc-regulation algorithms, the proposed filter controller regulates the value of the dc-side current based on the present peak value of the harmonic current available from the Current ADALINE. In other words, $I_{set}$ of each CSC is set to be equal to the amplitude of the corresponding harmonic to be filtered by

the CSC module. This will reduce the conduction and switching losses, which are proportional to dc-side current, and enhance system performance thanks to the adaptive nature of the ADALINE.

## 5.7 Master Controller Logic

The proposed active filter system suppresses selected low-order harmonics by connecting the corresponding CSC modules to the electric grid. The master controller connects the filter module(s) based on an automated decision-making algorithm, which is shown in Fig. 5.4. In this algorithm, the current total harmonic distortion ($THD_i$) and the harmonic current factors (HF) are calculated from the magnitudes of the harmonic components obtained from the output of the current ADALINE. Then $THD_i$ and each HF are compared with reference values to create a switching signal for connecting the corresponding filter module to the grid. The intelligent controller activates the active filter module when both the $THD_i$ and the corresponding HF exceed the limits set by the IEEE 519-1992 standard. For harmonics of low magnitudes, a single CSC can be assigned to filter two or more harmonics. Also, a CSC which is not being used to its full capacity, can be assigned the responsibility of reactive power control, i.e., behaving as a static VAR compensator (SVC) while performing the filtering job.

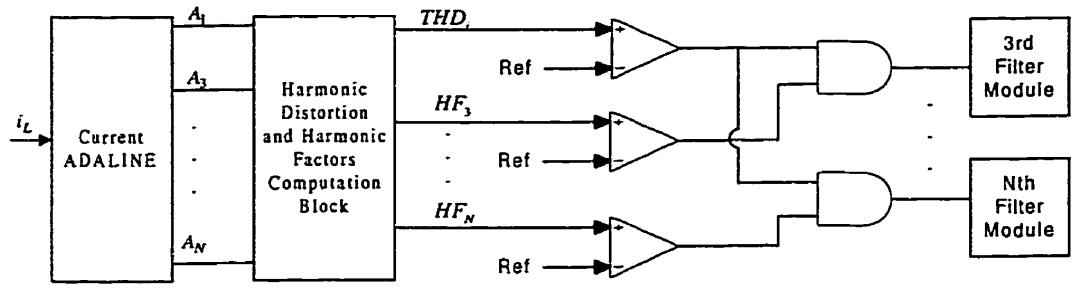


Fig.5.4: The proposed decision-making logic circuit controller

The information available on individual harmonic components allows us not only to reduce the THD but also to suppress each harmonic component below the level set by the IEEE 519 standard. Also, the information available on the magnitude of each harmonic component allows us to select the active filter bandwidth (i.e., the highest harmonic to be suppressed). This will result in more efficiency and higher performance.

Finally, the output currents of all the CSCs are added at a junction point and injected into the power line. The total injected current, $i_{inj}$, is equal, but opposite to the sum of the harmonic components to be eliminated. The higher-order harmonics are taken care of by a passive low-pass filter.

## 5.8 Improved Adaline-Based Harmonic Analyzer

In the original ADALINE algorithm given in Chapter 3, it is assumed that the fundamental frequency of the distorted waveform is known in advance [77,78]. In this research, the ADALINE algorithm has been modified to track the system frequency

variations to take care of the above problem. The frequency-tracking feature is essential specifically when ADALINE is used in conjunction with active power filtering. If the fundamental frequency drifts from its nominal value, then dc-side of the active filter module cannot be maintained which will result in unsuccessful elimination of harmonics. Let's assume that the instantaneous mean square error is given by [76]

$$\varepsilon(k) = 0.5\left(\sum_{l=1}^{N}\left(A_l \cdot \sin l\omega t(k) + B_l \cdot \cos l\omega t(k)\right) - y_d(k)\right)^2 \tag{5.1}$$

The derivative of mean square error with respect to the angular frequency ($\omega$), i.e. the change in $\omega$, can be found as [67]

$$\Delta\omega = -\alpha_\omega \cdot e(k) \cdot \left(\sum_{l=1}^{N}\left(l \cdot t(k) \cdot A_l \cos l\omega t(k) - l \cdot t(k) \cdot B_l \cos l\omega t(k)\right)\right) \tag{5.2}$$

where, $\alpha_\omega$ is a reduction factor.

To find the change in the angular frequency, $\omega$ is initially set to the nominal value. To guarantee the convergence of the algorithm, the reduction factor for updating the frequency should be several times lower than the reduction factor for the adaptation of $A_l$ and $B_l$ (the ratio $\alpha_\omega : \alpha$ was 1:100). Fig.5.5 represents the ADALINE with the modified adaptive algorithm for estimating $A_l$, $B_l$ and $\omega$.

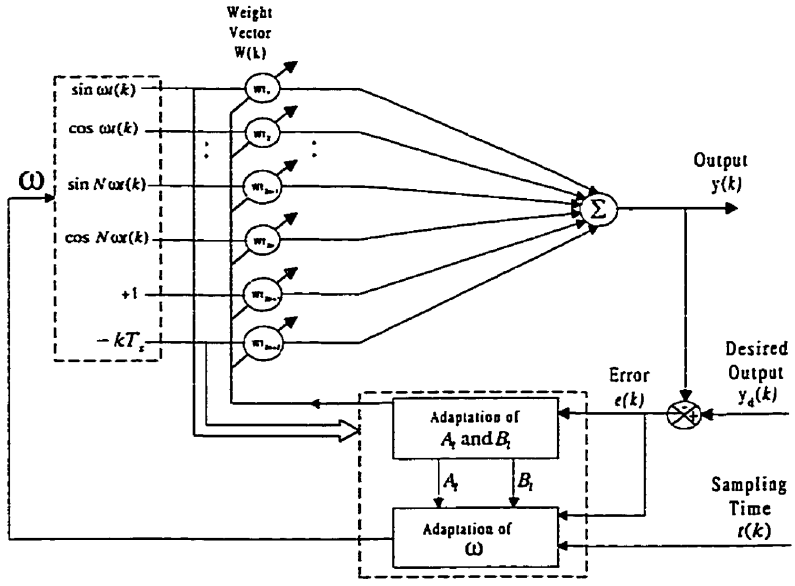


Fig. 5.5: The modified ADALINE for estimating $A_l$ and $B_l$, and $\omega$.

Also, the algorithm given has been modified to estimate the 3-phase voltages or currents simultaneously using ADALINE consisting of 3 neurons in total (one neuron per phase), as shown in Fig. 5.6. The output from the neural estimator for phase-a is:

$$\hat{V}_a(t) = W_a^T X \tag{5.3}$$

where $W_a$ denotes the weight vector for the a-phase voltage or current and **X** is the input vector given by equation (3.23) .

After final convergence is reached, the three phase Fourier coefficients for the estimated signals are computed as:

$$A_{l,j} = \sqrt{w_{o,j}^2(2l-1) + w_{o,j}^2(2l)}$$
$$\varphi_{l,j} = tan^{-1}\left[\frac{w_{o,j}(2l)}{w_{o,j}(2l-1)}\right] \qquad for\ j = a,b,c \tag{5.4}$$

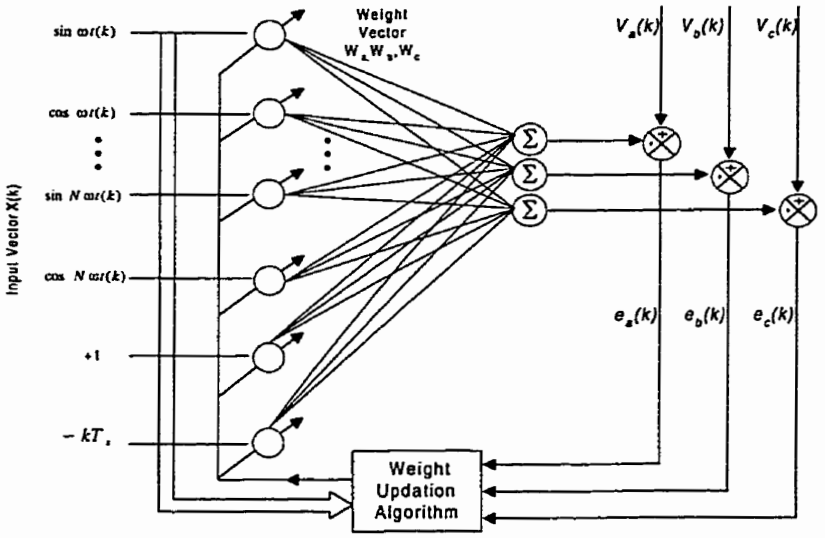


Fig. 5.6: Block diagram of the ADALINE for estimating 3-phase voltages or currents (3-Phase ADALINE)

## 5.9 Application to 3-Phase 3-Wire Distribution Systems

The proposed active power filter system explained is introduced to improve the electric power quality through harmonic mitigation in electric distribution systems. The proposed system is based on the per-phase treatment of the line current harmonics in 3-

phase 4-wire AC distribution system. In such systems, three single-phase CSC filter modules will be required for filtering a specific harmonic in the three power lines.

However, in 3-phase 3-wire distribution systems, instead of using three single-phase CSC modules, only one 3-phase module is required to suppress a specific harmonic of choice in the three lines. The proposed filter is based on 3-phase 6 switches PWM-controlled current-source converter (CSC) modules, where each filter module is dedicated to eliminate a specific harmonic and/or balance the line currents. Based on the information extracted from the line by the ADALINE, each leg of every CSC module is independently controlled to perform the balancing or/and harmonic filtering in a 3-phase 3-wire distribution system. The power ratings of the modules will decrease and their switching frequencies (bandwidth) will increase as the order of the harmonic to be filtered increases. As a result, the overall switching losses are reduced due to selected harmonic elimination and balanced power rating-switching frequency product.

## 5.9.1 System Configuration And Control Scheme

Fig. 5.7, shows the block diagram of the proposed 3-phase modular active filter connected to the electric distribution system. It is composed of several parallel power converter modules, each dedicated to suppress a specific harmonic component of choice. One module is assigned to correct the current imbalances. Each module is a standard 3-phase CSC bridge. The basic function of the proposed 3-phase active filter is

to suppress selected low-order harmonics in the unbalanced 3-phase 3-wire distribution system. Each phase is controlled independently. The method is based on extracting individual harmonics and negative sequence components using the current ADALINE and injecting equal, but opposite of the summation of these harmonic and negative sequence currents into the power line using the corresponding filter modules. The controller generates tri-logic PWM switching patterns for controlling the filter modules to eliminate selected harmonics and to balance the unbalanced currents. With the line current, $i_{L,j} = i_{1p,j} + i_{1n,j} + \sum i_{h,j}$ ($h$ being the harmonic order, $i_{1p,j}$ and $i_{1n,j}$, the fundamental positive and negative sequence currents of phase $j$, and $j = a,b,c$), $i_{inj,j} = i_{1n,j} + \sum i_{h,j}$ is injected by the active filter system so that the source current $i_{s,j} = i_{1p,j}$, only.

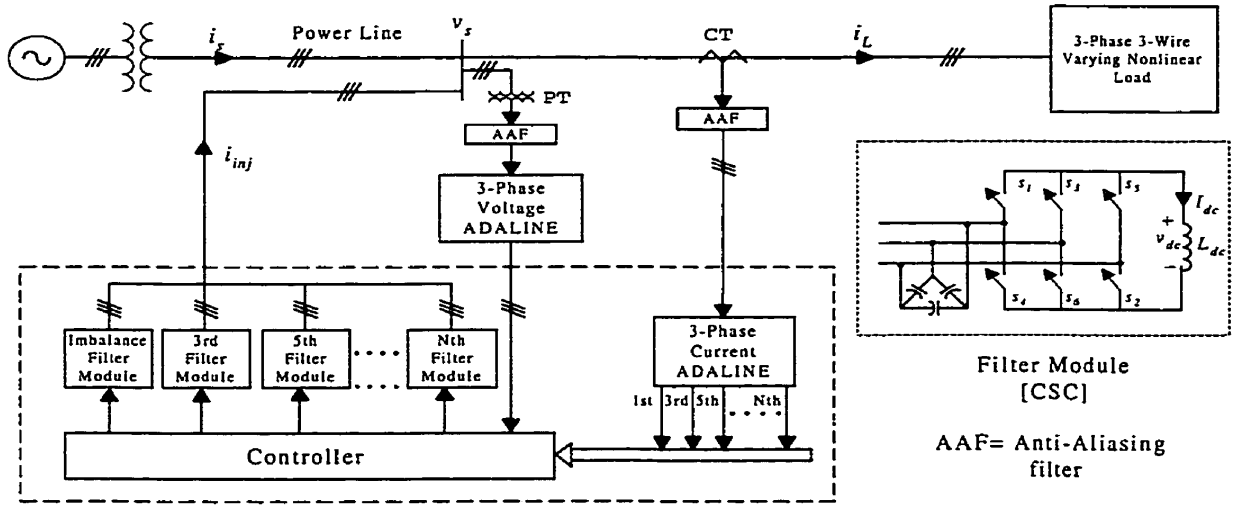


Fig. 5.7: The proposed 3-phase modular active power filter system

The 3-phase line current signals ($i_{L,j}, j=a,b,c$) are obtained through three current transformers (CT) and are fed to the 3-phase current ADALINE which adaptively and continuously estimates the fundamental and harmonic components of the line current signals. The negative sequence components are constructed from the fundamental current components obtained from the current ADALINE. The line voltage signals ($v_{s,j}, j=a,b,c$) are obtained by three potential transformers (PT) and processed by another 3-phase ADALINE (voltage ADALINE) to extract the fundamental components of the line voltage waveforms. The output of the current ADALINE is used to generate the tri-logic PWM switching signals for the CSC units which inject the corresponding distortion in order to suppress the harmonic components and correct the unbalanced current in the lines. The output of the second ADALINE is used as synchronization signal in the control loop that maintains the dc-side average current ($I_{dc}$) of each CSC module at a desired value. The compensated currents of all the CSCs are added at a junction point and injected into the power line. The total injected current, $\sum i_{inj,j}, j=a,b,c$, is equal, but opposite to the sum of the harmonic components to be eliminated plus the negative sequence currents ($i_{ln,j} + \sum i_{h,j}$).

Fig. 5.8 shows the control scheme for the proposed 3-phase modular active power filter. In this controller, the $l^{th}$ harmonic signal $A_{l,j} sin(l\omega t + \varphi_{l,j}), j=a,b,c$ is reconstructed from the output of the current ADALINE and is used as control signal for

tri-logic PWM block, to create the PWM switching pattern for the switches of the CSC module dedicated to the $l^{th}$ harmonic. The control scheme also includes the control of one of the filter modules assigned for balancing the unbalanced currents. The instantaneous 3-phase negative sequence components are constructed from the fundamental components of the line currents and are used to control the CSC module to inject the desired negative sequence currents. Note that the output current of each phase of each filter module is independently controlled to eliminate harmonic currents or to correct the current imbalances provided that the instantaneous fundamental currents as well as their multiples in the three phases add up to zero. As seen in Chapter 4, the CSC under the tri-logic PWM strategy behaves as a linear amplifier. The gain of this amplifier is equal to $I_{dc}/\sqrt{3}V_{tri}$, where $I_{dc}$ is the dc-side current of the CSC and $V_{tri}$ is the peak value of the triangular waveform. Note that in order to achieve a linear amplifier, the $I_{dc}$ of each CSC must be constant. This can be accomplished by regulating the dc-side current of each CSC by means of a feedback control loop. The converter losses and system disturbances such as sudden fluctuation of the load create a need for a dc current regulator that is always active. In this feedback loop, the modulating signal for charging the dc-side inductor is synchronized with the line voltages ($v_s$) obtained from the voltage ADALINE. The above signal will be used as a part of the modulating signal of the CSCs, as shown in Fig.5.8. It results in drawing a small current at fundamental frequency contributing only to active power required for

the regulation of $I_{dc}$. The regulation of the dc-side current is based on the present peak value of the harmonic current which will result in low conduction and switching losses.

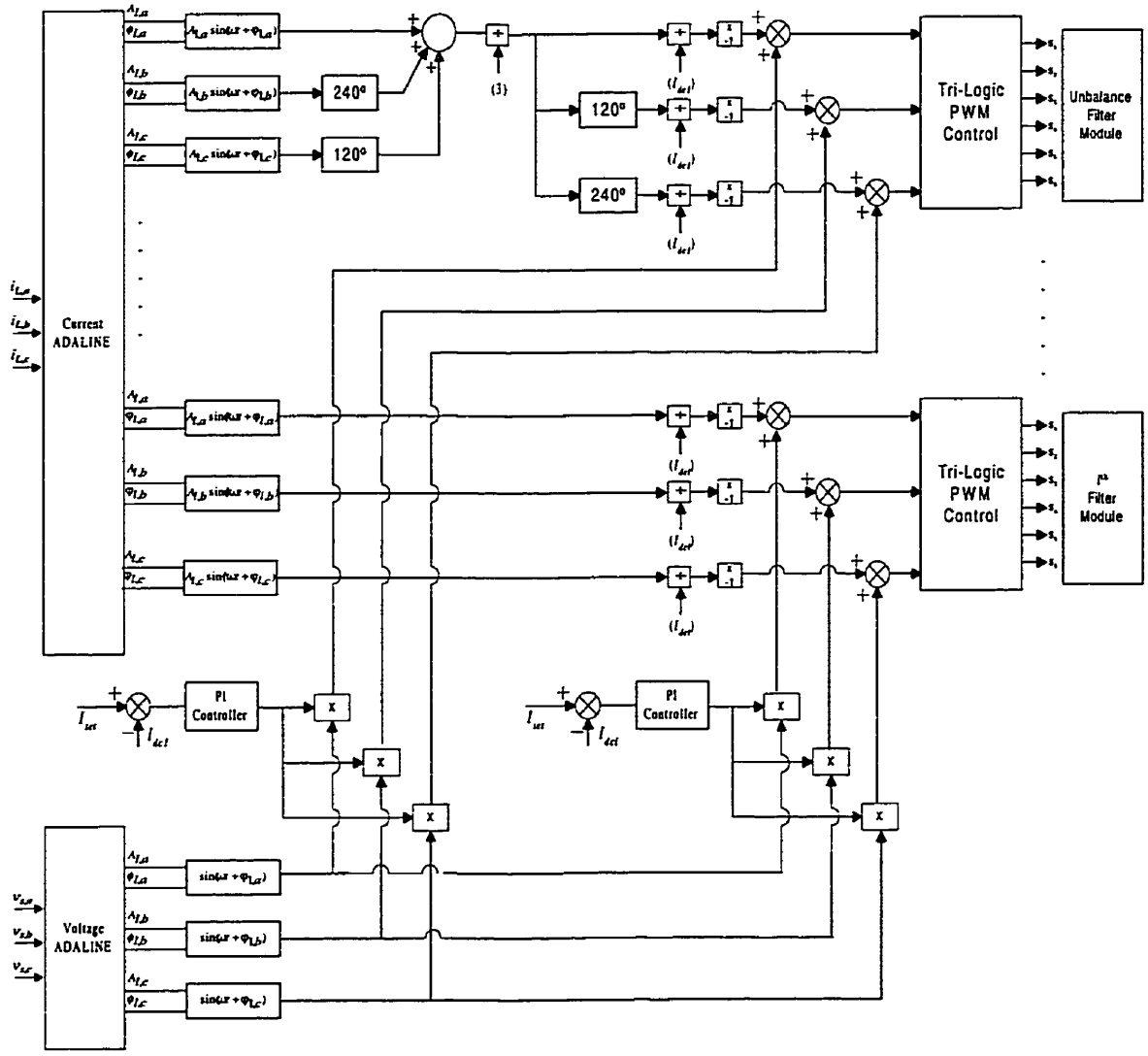


Fig. 5.8: The Control Scheme of the 3-phase modular active filter
(The Controller in Fig. 5.7)

# 5.10Digital Simulation Results

Since the ADALINE constitutes the main part of the proposed active filter controller, its performance in tracking the harmonic components and the fundamental frequency variation will be checked and evaluated first. The steady state and the transient performances of the whole active power filter system will be investigated next.

## 5.10.1 Tracking of the Harmonic Components and the Fundamental Frequency Variations

This section illustrates the ability, verifies the validity and checks the performance of the ADALINE in estimating the time-varying harmonic components and fundamental frequency variations. This will be demonstrated through a practical example.

A time-varying distorted voltage waveform of known harmonic contents and frequency variations is considered. The distorted waveform consists of the fundamental component and the $3^{rd}$ harmonic with the fundamental frequency varying between 59.8 and 60.2 Hz. Fig. 5.9 displays the distorted voltage waveform, the fundamental frequency variations and the magnitudes of the fundamental and the $3^{rd}$ harmonic embedded in the distorted waveform as detected by the ADALINE.

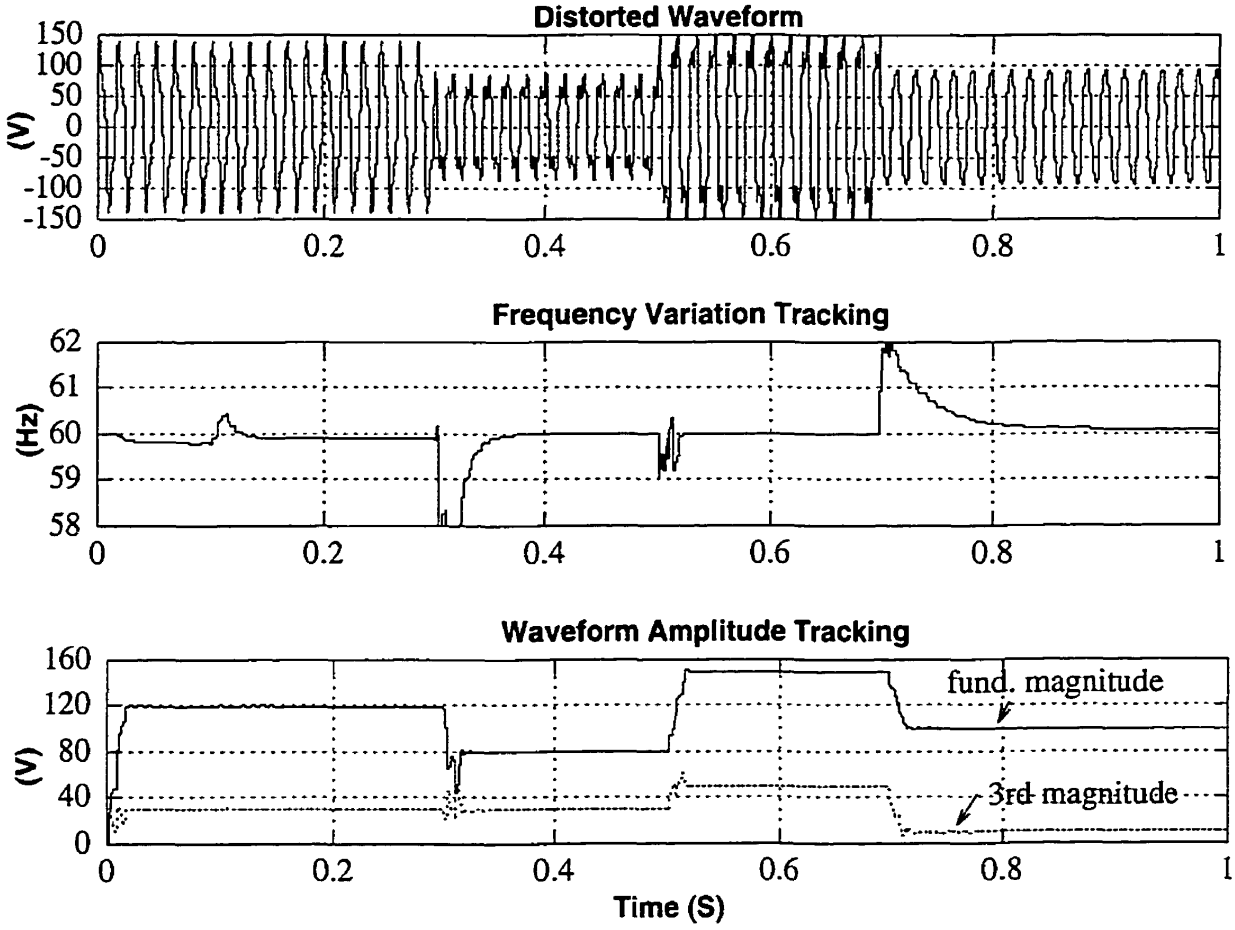


Fig.: 5.9 Estimation of the frequency variations and the fundamental and the 3rd components using ADALINE.

From the plots on Fig. 5.9, it appears that the ADALINE output is accurately tracking the fundamental and the 3rd harmonic magnitudes in an adaptive way. The ability of ADALINE to estimate accurately the new state of the fundamental frequency can also be seen.

## 5.10.2 Performance of single-phase modular active power filter

### 5.10.2.1 Steady-State Performance

**Case 1:**

To test the performance of the proposed modular active filter in steady-state, the system of Fig. 5.2 was simulated using the EMTDC simulation package. The parameters of the system under study are given in Appendix (C). The nonlinear load is a single-phase full bridge diode rectifier. This is the worst-case scenario, as 3-phase nonlinear loads cause much less harmonic distortion in the line current. The harmonics are extracted from the line current signal ($i_L$) using the Current ADALINE. The ADALINE module subroutine has been written and interfaced with the EMTDC simulation package (shown as ADALINE block in Fig. 5.2). The first 6 dominant harmonics are selected to be suppressed. The harmonics are extracted from the line current signal ($i_L$) using the current ADALINE. The distorted signal is composed of fundamental component (127A), $3^{rd}$, $5^{th}$, $7^{th}$, $9^{th}$, $11^{th}$, and $13^{th}$ harmonics (33.3%, 20%, 14.3%, 11.1%, 9% and 7.7% of the fundamental, respectively). Control signals for the $3^{rd}$, $5^{th}$, $7^{th}$, $9^{th}$, $11^{th}$, and $13^{th}$ harmonics are obtained. Each is used to generate the PWM switching pattern for one CSC dedicated to suppress the corresponding harmonic. In this case, 6 CSC's are used.

Fig.5.10 shows the waveforms of the phase-a distorted current, $i_L$, the total injected current into the line by the active filter modules, $i_{inj}$, and the filtered current at the interface of the ac system, $i_s$. The waveforms clearly demonstrate an excellent performance in eliminating the selected harmonics from the line current. The total harmonic distortion (THD, up to 3 kHz) of the filtered current is 6.9%, down from 44.5% in the distorted line current.

Fig. 5.10 also shows how quickly the ADALINE estimates the magnitude and phase of one of the harmonics ($5^{th}$) embedded in the distorted waveform ($i_L$). It appears that the proposed active filter system starts performing the filtering job within one cycle of the fundamental frequency in an adaptive way, compared to other systems that utilize the FFT technique and require almost two cycles to compensate for the harmonics [74]. This is the result of incorporating the ADALINE as a part of the control scheme.

**Case 2:**

In this section, the proposed modular active conditioner was tested with a realistic example of a three-phase distribution system, which is shown in Fig. 5.11 and its feeder section data are listed in Table 3. This system supplied a mixture of non-linear and linear loads and it is loaded until it reaches its rated capacity. The load sharing percentage will be equal to [61]:

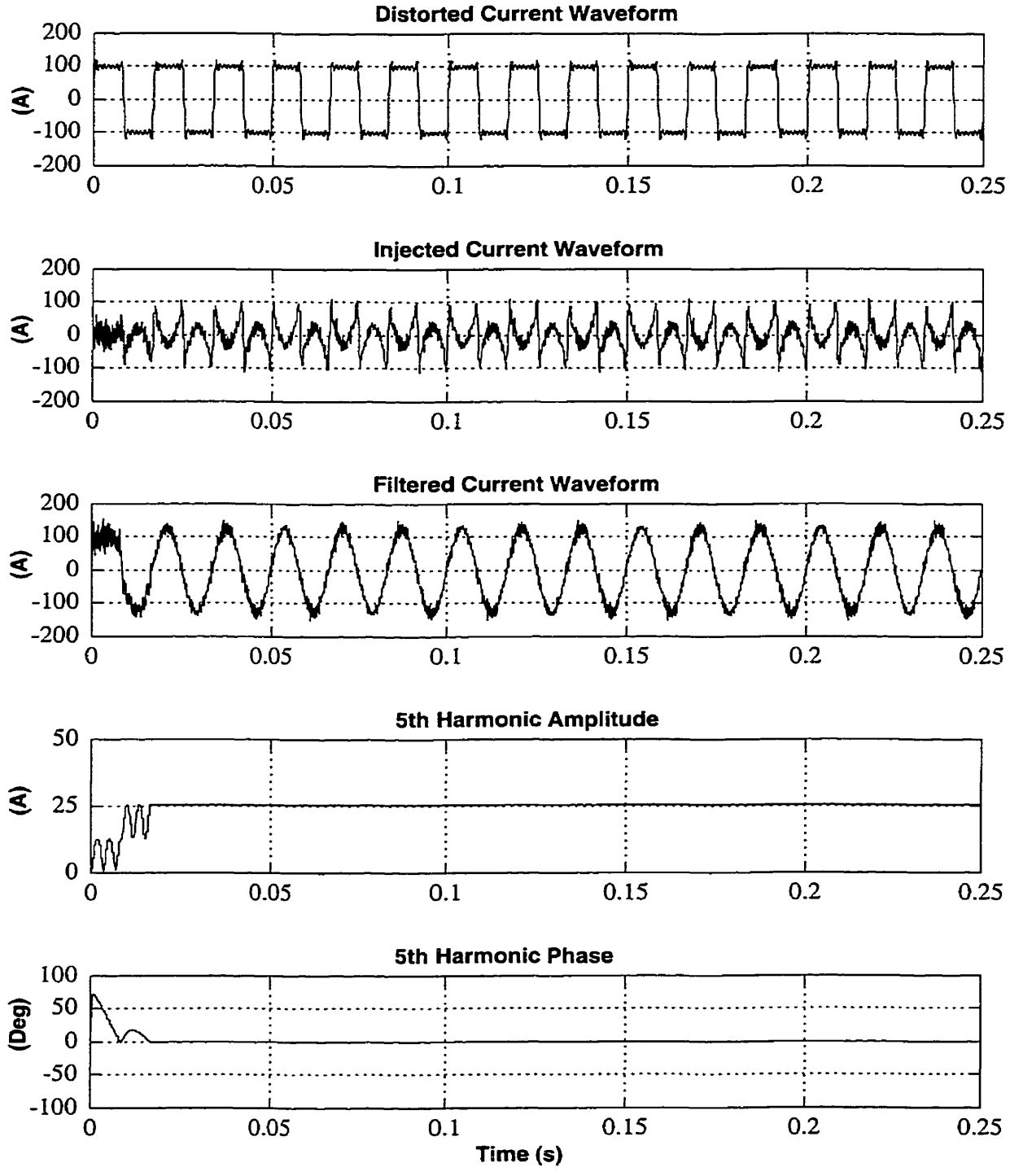


Fig. 5.10: Steady state simulation results of the proposed modular active filter

- Diode bridge rectifier (DBR)=40%,
- Phase angle voltage controller (PAVC) = 20%,
- Compact fluorescent lamp (CFL) =20%,
- Three-phase star-connected linear loads =20% (pf=0.9 lag)

The supply impedance that is equal to the secondary distribution transformer impedance plus the impedance of the line connecting the transformer to the distribution panel was equal to 0.032+j0.1169 $\Omega$, with the X/R ratio equal to 3.65. The THD of the distribution system load current was 30.18% and its dominant harmonic components are the 3$^{rd}$ and the 5$^{th}$.

Two filter modules of the proposed modular active conditioner were designed for the 3$^{rd}$ and 5$^{th}$ harmonics. Inserting the modular active filter in parallel at the point of common coupling (PCC) and injecting the appropriate 3$^{rd}$ and 5$^{th}$ harmonic components succeeded in reducing the current THD from 30.18% to 3.06%. The injected current ($i_{inj}$) from the proposed modular active filter as well as the filtered current ($i_s$) and the distorted load current ($i_L$) are shown in Fig. 5.12.

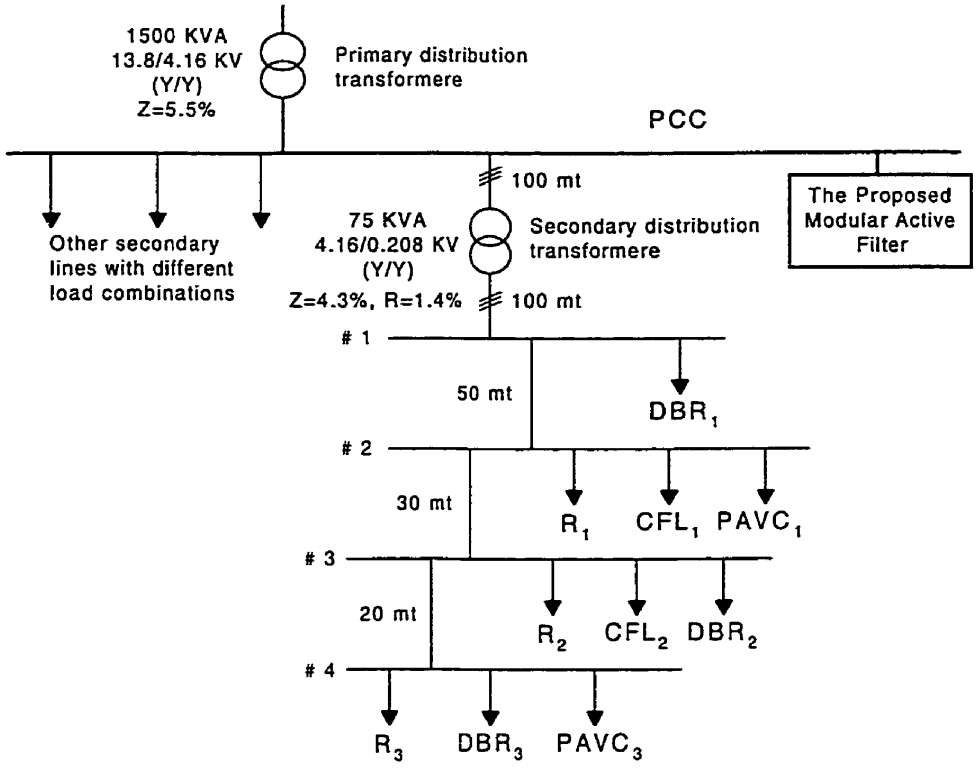


Fig. 5.11: Test secondary distribution system

Table (5.1): Secondary distribution feeder data

| Sec. # | Section Type | Length (m) | Cross sec. ($mm^2$) | R (Ω/Km) | X (Ω/Km) |
|---|---|---|---|---|---|
| 1 | 3-phase | 100.0 | 16.0 | 1.42 | 0.106 |
| 2 | 3-phase | 100.0 | 95.0 | 0.239 | 0.081 |
| 3 | 1-core, PVC | 50.0 | 50.0 | 0.464 | 0.112 |
| 4 | 2-core, PVC | 30.0 | 16.0 | 1.38 | 0.08 |
| 5 | 2-core, PVC | 20.0 | 16.0 | 1.38 | 0.08 |

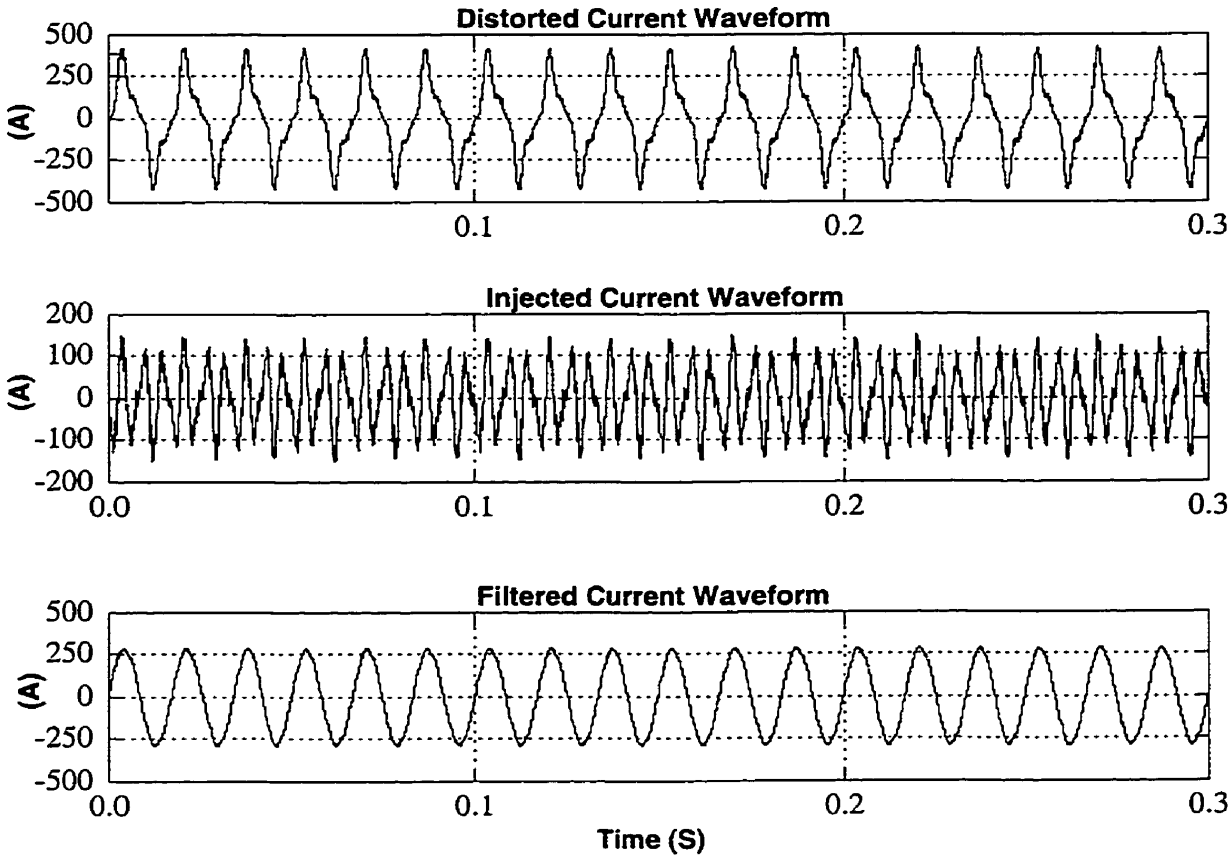


Fig. 5.12: Steady state simulation results of using two modules of the proposed modular active filter for the 3rd and 5th harmonic modules.

### 5.10.2.2 Transient Performance

This section illustrates the ability and evaluates the performance of the proposed modular active filter system in response to step changes in the magnitude and phase of the harmonic currents. A simple example system consisting of one module of the

proposed filter dedicated to the 5th harmonic with a non-linear load drawing 5th harmonic current of variable magnitude and phase angle is simulated using the EMTDC simulation package.

Fig. 5.13 displays the dc-side current ($I_{dc}$), the ADALINE output (5th harmonic component), the distorted current ($i_L$), and the filtered current ($i_s$) for step changes of +66% at t = 0 sec., +33% at t = 0.16 sec. and –55% at t = 0.33 sec. in the magnitude of the nonlinear load current. From the plots on Fig. 5.13, it is obvious that the controller of the proposed active filter is responding quickly and accurately to the sudden increase or decrease in the nonlinear load in an adaptive way. It also shows that the filtered current waveform ($i_s$) settles to the steady state value within one cycle, demonstrating the excellent transient response of the proposed active filter system.

Moreover, it shows that the value of the dc-side current ($I_{dc}$) follows the present peak value of the 5th harmonic magnitude adaptively and very quickly. This results in lower losses and higher efficiency since the conduction and switching losses are proportional to the dc-side current. For harmonics of low magnitudes, a single CSC can be assigned to filter 2 or more harmonics. Also, a CSC which is not being used to its full capacity, can be assigned the responsibility of reactive power control, i.e., behaving as a static VAR compensator (SVC) while performing the filtering job.

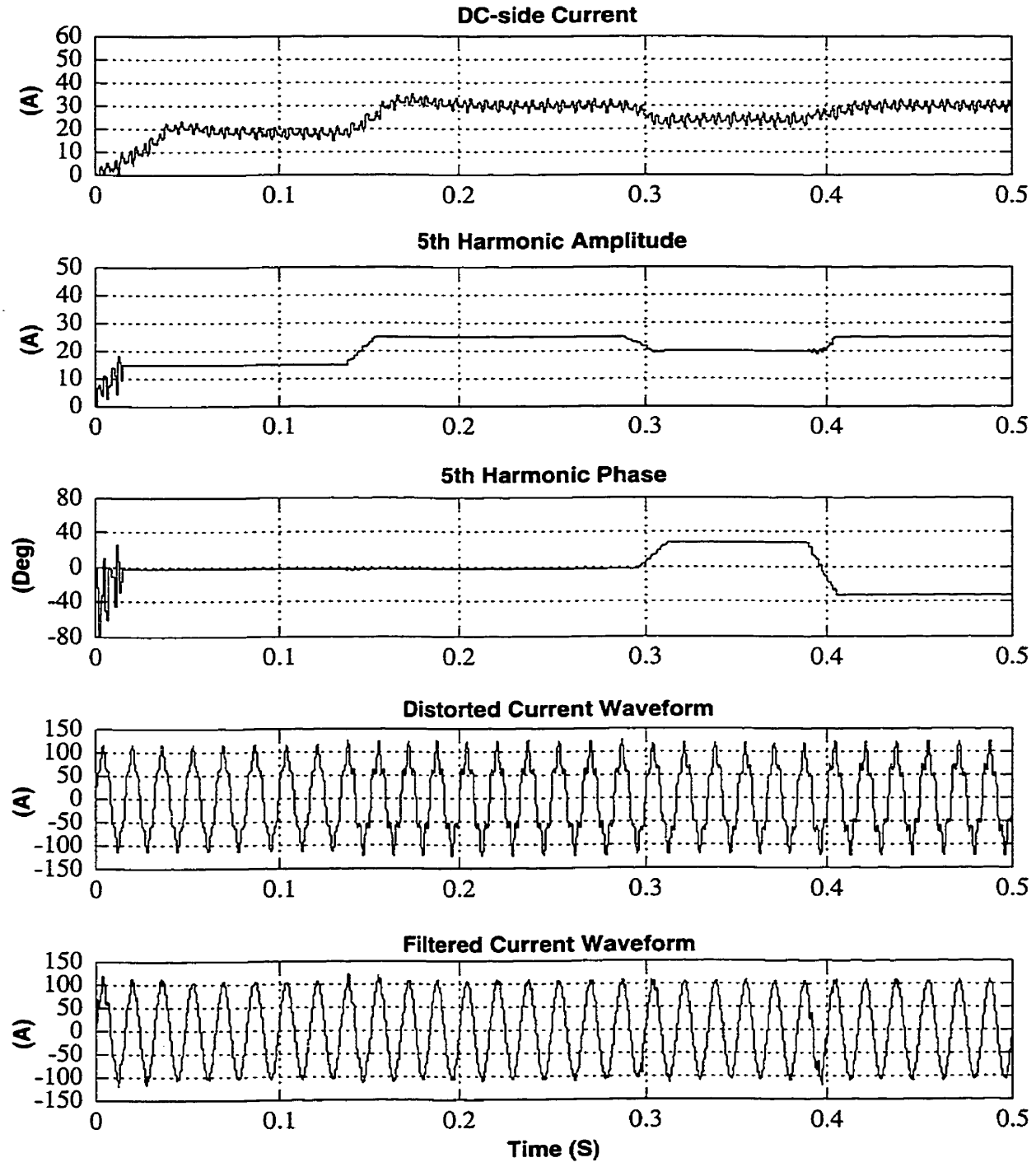


Fig. 5.13: Transient simulation results of the proposed modular active filter.

To test the transient response of the proposed active power filter system to large sudden changes, the filter was subjected to step load changes from no-load to full-load at t = 0 sec. and back to no-load at t = 0.4 sec. As illustrated in Fig. 5.15, the system shows an excellent transient performance under large and sudden load changes.

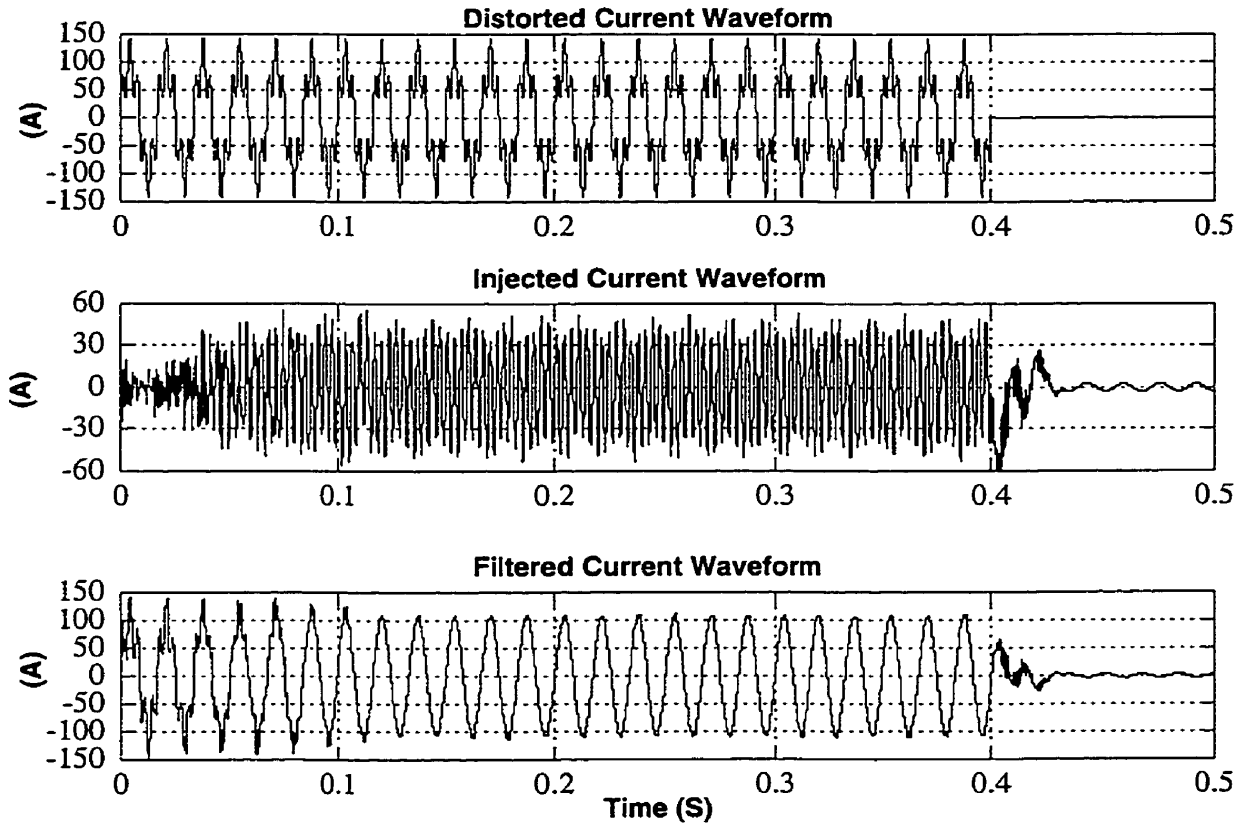


Fig. 5.15: Transient simulation results of the proposed modular active filter subjected to sudden full -load operation and full-load rejection

### 5.10.3 Performance of Three-Phase Modular Active Power Filter

**Case 1:**

The performance of the proposed 3-phase modular active filter was tested by simulating the distribution system of Fig. 5.7. The nonlinear load in the test system is an unbalanced 3-phase delta connected load. The 3-phase harmonic currents are estimated from the line currents using the 3-phase Current ADALINE. The objective here is to mitigate the first 3 dominant harmonic currents ($3^{rd}$, $5^{th}$ and $7^{th}$ harmonics) and to balance the unbalanced currents. Therefore, 3 CSC filter modules are used, each one is dedicated to suppress one harmonic current, and one module is used to correct the current imbalance. The negative sequence and $3^{rd}$, $5^{th}$ and $7^{th}$ harmonics control signals are obtained and used to generate the tri-Logic PWM switching pattern for CSC modules.

Fig.5.16 shows the waveforms of the 3-phase distorted currents, the total 3-phase injected currents into the line by the active filter modules, and the 3-phase compensated currents at the interface of the ac system. The waveforms illustrate the successful elimination of the selected harmonics from the line currents and the balancing of the line currents. The total harmonic distortion (THD, up to 3 kHz) of the 3-phase supply currents are reduced from 39.7%, 16.7% and 42.3% to 11.6%, 8.3% and 10.9% for phase a, b and c, respectively.

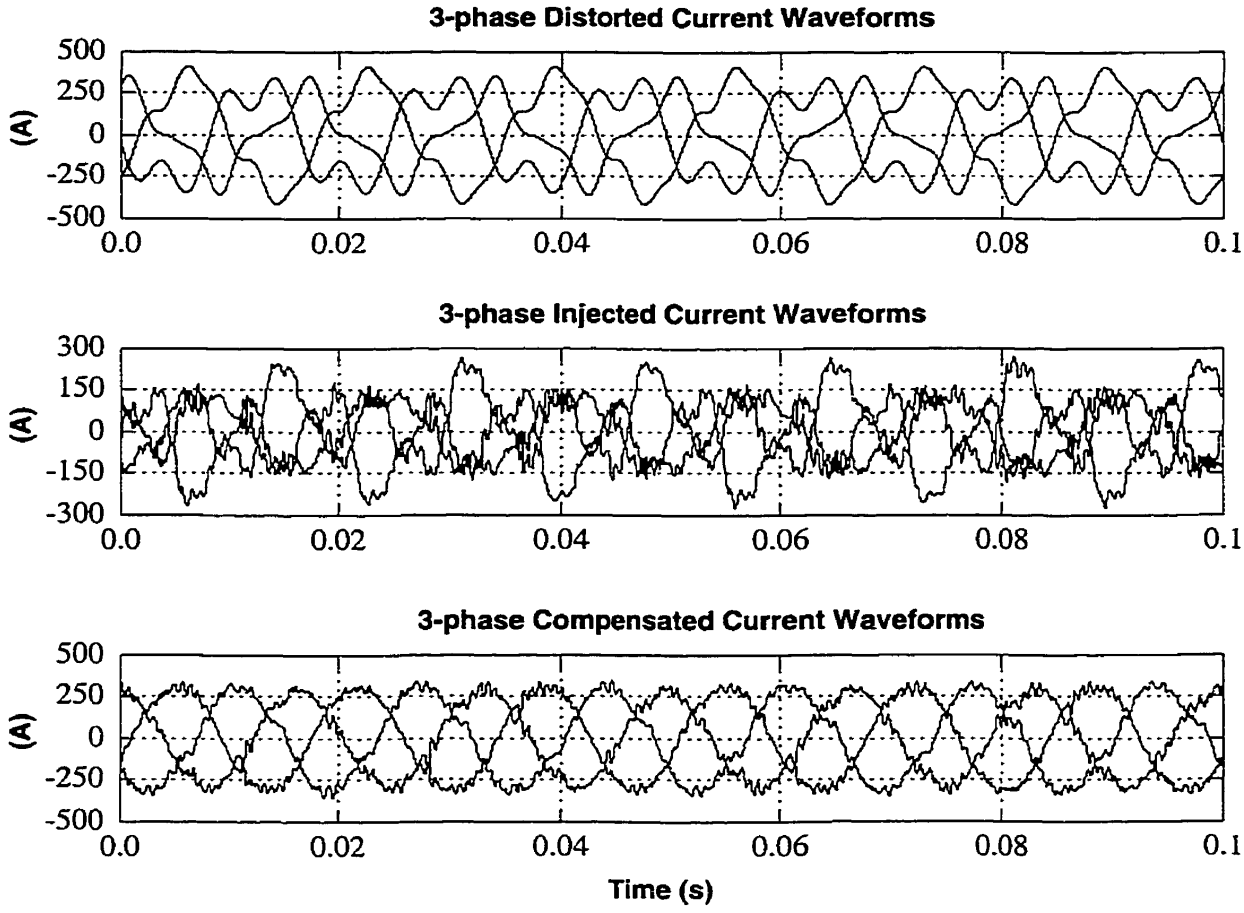


Fig. 5.16: Steady state simulation results of the proposed 3-phase modular active filter

**Case 2:**

In this section, a realistic example of a three-phase distribution system was used to demonstrate the effectiveness of the proposed 3-phase modular active conditioner. This example, shown in Fig. 5.17, is composed of a mixture of non-linear and linear

unbalanced loads and was loaded up to its rated capacity. The distribution of the nonlinear loads on the three phases is shown in Table 5.2.

Table (5.2): The distribution of the nonlinear loads on the three phases

| Phases | Percentage of Non Linear Loads | | |
|---|---|---|---|
| | Diode bridge rectifier (DBR) | Phase angle voltage controller (PAVC) | Compact fluorescent lamp (CFL) |
| Phase (a) | 60 % | 40% | 0% |
| Phase (b) | 50% | 33% | 17% |
| Phase (c) | 40% | 40% | 20% |

Three filter modules of the proposed 3-phase modular active conditioner were designed for the 3rd , 5th harmonics and current imbalance. Inserting the modular active filter in parallel at the point of common coupling (PCC) and injecting the appropriate 3rd and 5th harmonic components succeeded in reducing the current THD from 9.15% to 4.19% and successfully balancing the line unbalanced currents. The injected current ($i_{inj}$) from the proposed 3-phase modular active filter as well as the filtered current ($i_s$) and the distorted load current ($i_L$) are shown in Fig. 5.18.

Note that since the 3rd filter module is switched at low frequency, it could be used for both eliminating the third harmonic and balancing the line currents provided that its rating can accommodate the two jobs.

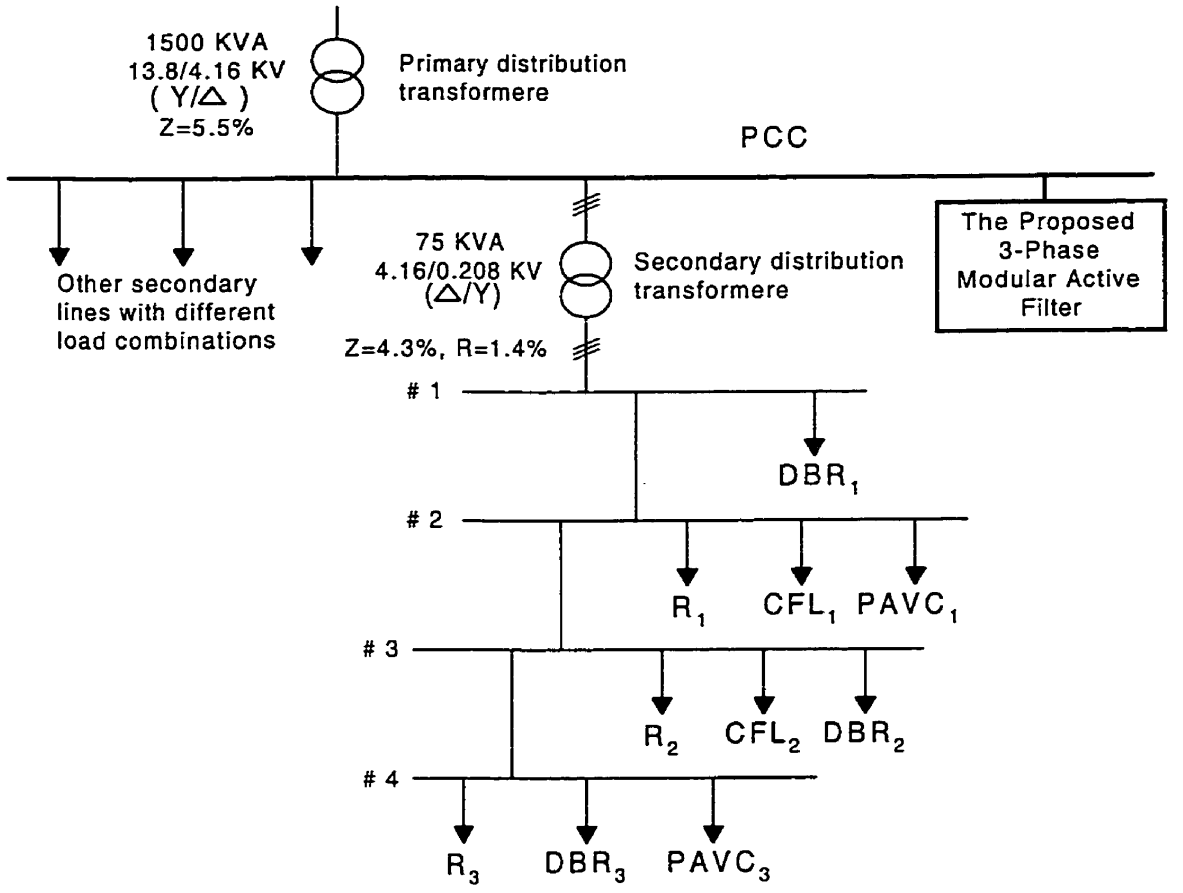


Fig. 5.17: 3-phase imbalance distribution system

Again, a single CSC filter module can be assigned to filter 2 or more low magnitude harmonic currents. Also, a CSC which is not being used to its full capacity, can be assigned the responsibility of reactive power control, i.e., behaving as a static VAR compensator (SVC) while performing the filtering job.

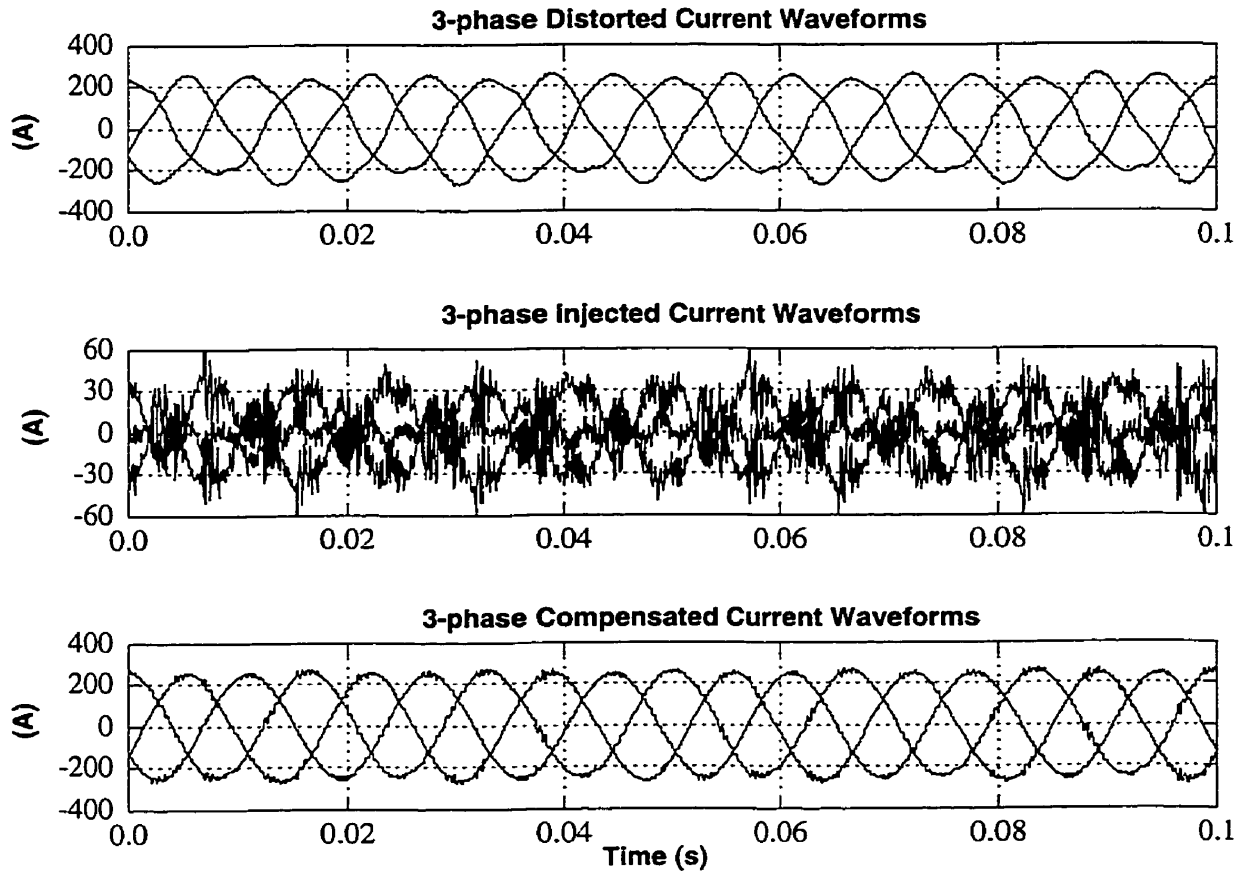


Fig. 5.18: Steady state simulation results of the proposed 3-phase modular active filter with the distribution system shown in Fig. 5.17.

## 5.11 Summary

In this chapter, a novel modular single-phase active power filter system, based on current-source converter (CSC) modules is proposed which is capable of performing the harmonic filtering in 3-phase 4-wire distribution system. A topology which is suitable for balancing or/and harmonic mitigation in 3-phase 3-wire distribution systems is also

introduced. The improved ADALINE is equipped with frequency tracking capabilities which have the ability to estimate simultaneously the time-varying fundamental frequency and harmonic components within one cycle of the fundamental frequency.

The proposed active filter system includes the extraction, computation and mitigation stages and offers the following advantageous features:

- High efficiency due to low conduction and switching losses.
- High reliability due to parallel connection of CSC modules and single harmonic treatment.
- Fast and accurate tracking of harmonic components and system frequency due to ADALINE-based control.
- Adaptation of dc-side current of the converter modules to the changes in the magnitude of the harmonics, resulting in optimum $I_{dc}$ value and minimal converter losses.
- Additional savings in the running costs compared to the conventional one-converter approach
- Flexibility of selecting the harmonic order to be eliminated due to the availability of information on the individual harmonic components.

- The ability to extract the fundamental system voltage (the voltage at the common point of coupling) in case the line voltage is harmonic polluted.

The proposed active filter system has the ability to extract information rather than data from the power system. This information on individual harmonic components allows us not only to reduce the THD but also to suppress each harmonic component to meet the strike requirements of the IEEE 519 standard which emphasizes that each harmonic component be below a certain level. The information available on the magnitude of each harmonic component allows us to select the active filter bandwidth (i.e., the highest harmonic to be suppressed). This increases the efficiency and improves the performance of the proposed active filter system.

The analytical expectation has been verified by extensive simulation results using the EMTDC simulation package.

# Chapter 6
# Power-Splitting Approach to Active Harmonic Filtering

## 6.1 Overview

The proposed modular active filter explained in Chapter 5 is based on splitting the filtering job among several active filter modules, each dedicated to take care of a specific harmonic. We will refer to this technique as Frequency Splitting.

In this chapter, an alternative approach to frequency splitting active harmonic filtering which is based on splitting the filtering load equally among identical modules (Power-Splitting) is proposed. In this approach, the filtering job is distributed equally among CSC filter modules of identical power circuit and control circuit design. The power rating and switching frequency of each CSC module is equal to the power rating

and switching frequency required for the filtering task, divided by the number of modules. This makes it possible to use the present gate-turn-off switch technology to realize high-power active filters for the desired performance. The control system of the power splitting approach utilizes two ADALINEs to process the signals obtained from the line. The first ADALINE (the Current ADALINE) extracts the harmonic components of the distorted line current signal, whereas the second ADALINE (the Voltage ADALINE) estimates the fundamental component of the line voltage signal. The outputs of both ADALINEs are used to construct the modulating signals of the identical CSC filter modules.

In the following sections, the system configuration is presented, followed by a description of the system performance and control scheme of the proposed power splitting modular active filter. Some digital simulation results from EMTDC simulation package are presented at the end of this chapter to verify the theoretical expectations.

## 6.2 System Configuration and Control Scheme

The power splitting modular active power filter is illustrated in the block diagram of Fig. 6.1. The filtering job has been split among N identical active filter modules connected in parallel. Each filter module is a single-phase PWM- CSC comprised of a dc reactor (for dc-energy storage), a small capacitor (for filtering of switching harmonics) and four controllable (gate-turn-off) semiconductor switches.

If the total power rating of $S$ *(VA)* and switching frequency of $f_{sw}$ are required for successful performance, the power rating and switching frequency (bandwidth) of each module will be *S/M* and $f_{sw}/M$, respectively.

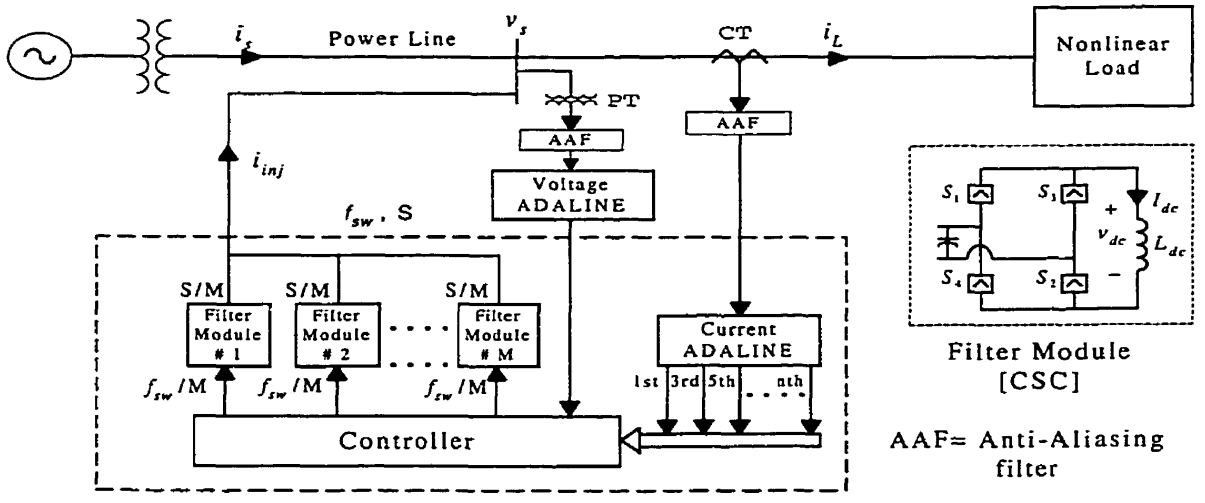


Fig. 6.1: Block diagram of power splitting scheme

For each phase, the line current signal ($i_L$) is obtained through a current transformer (CT) and fed to the current ADALINE which adaptively and continuously estimates the fundamental and harmonic components of the line current signal. The phase voltage signal is obtained by a potential transformer (PT) and processed by another ADALINE (voltage ADALINE) to extract the fundamental component of the phase voltage waveform. The output of the current ADALINE is used to generate the PWM switching

signals for the CSC units which inject the corresponding distortion in order to suppress the harmonic components in the line current ($i_L$). The output of the second ADALINE is used as a synchronization signal in the control loop that maintains the dc-side current ($I_{dc}$) of each CSC module at a desired value. The output currents of all the CSCs are added at a junction point and injected into the power line. The total injected current, $i_{inj}$, is equal, but opposite to the sum of the harmonic components to be eliminated ($\sum i_h$).

Fig. 6.2 shows the proposed control scheme for one CSC module of the proposed power splitting active filter. In this controller, the signal representing the sum of the current harmonics to be filtered ($\sum i_h$) is reconstructed from the output of the current ADALINE and divided first by the number of modules (M) and then by the gain of each CSC module. Note that a CSC under the PWM strategy behaves as a linear amplifier. The gain of this amplifier is equal to $I_{dc}/V_{tri}$, where $I_{dc}$ is the dc-side current of the CSC and $V_{tri}$ is the peak value of the triangular waveform to which the modulating signal of each CSC module is compared to generate the PWM switching signals. The carrier frequencies of the active filter modules are the same and equal to the switching frequency required for successful performance, $f_{sw}$, divided by the number of modules (M). The carrier signals of the modules are phase-shifted with respect to one another by *1/M* multiplied by the switching period. This results in the elimination of switching frequency harmonics in the total injected current.

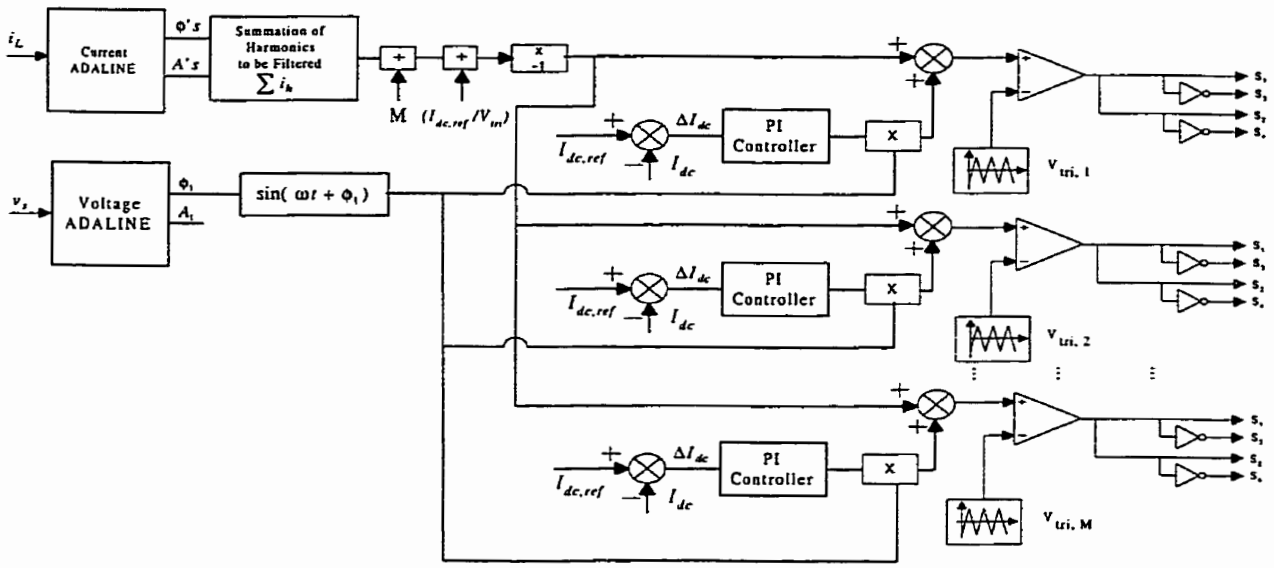


Fig. 6.2 The Control Scheme of the proposed power splitting active filter (The Controller in Fig. 6.1)

To achieve a linear amplification, and to withstand the system disturbance and to compensate for the system losses, the dc-side current ( $I_{dc}$ ) of each filter module should always be active and has a constant value. This can be accomplished by regulating the $I_{dc}$ of each CSC by means of a feedback control loop. In this feedback loop, the modulating signal for charging the dc-side inductor is synchronized with the system voltage ( $v_s$ ) obtained from the voltage ADALINE. This results in a small current at fundamental frequency contributing only to active power required for the regulation of $I_{dc}$.

# 6.3 Simulation Results

## 6.3.1 Steady-State Performance

The steady-state performance of the proposed power splitting modular active filter has been verified and tested using the same test system given in Chapter 5 Section 5.10.2.1. The test system with the filter configuration shown in Fig. 6.1 was simulated using EMTDC simulation package. In this case, the number of active filter modules is chosen to be 4 so that the power splitting scheme has almost the same installation cost as the single converter scheme for doing the same job [70]. In this example, the active filter modules are used to eliminate up to the $13^{th}$ current harmonic. From the summation of the harmonics (the $3^{rd}$, $5^{th}$, $7^{th}$, $9^{th}$, $11^{th}$, and $13^{th}$), a control signal is obtained which is used to generate the PWM switching pattern for each CSC module. Fig. 6.3 shows the waveforms of a distorted current, $i_L$, the total injected current into the line by the active filter modules, $i_{inj}$, and the supply current, $i_s$ of the phase-a.

The waveforms clearly illustrate the successful elimination of the selected harmonics from the line. The results prove the capabilities of the proposed power splitting active filter system in eliminating the selected harmonics from the line current. The total harmonic distortion (THD, up to 3 kHz) of the line current is reduced from 44.5% to 6.9%.

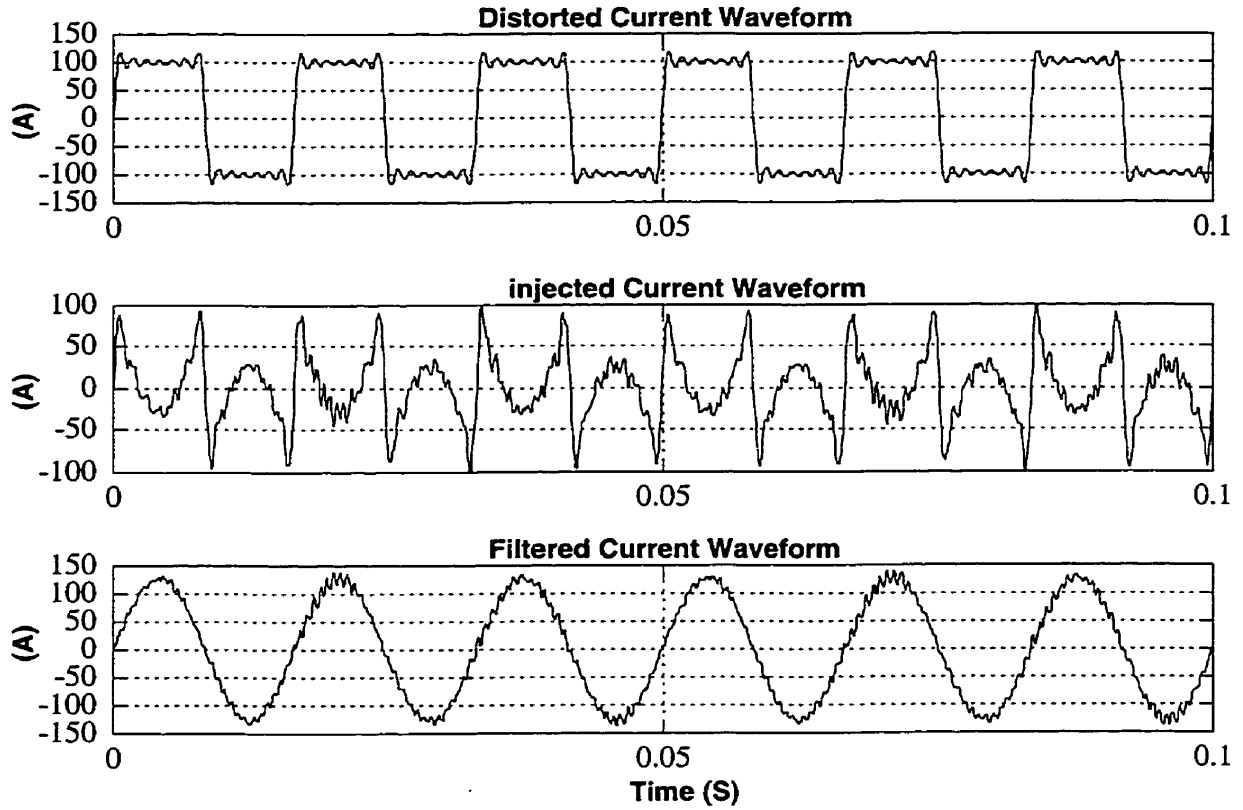


Fig. 6.3: Steady state simulation results of the proposed power splitting modular active power filter.

The proposed power splitting active power filter system is quite capable of dealing with unbalanced nonlinear load conditions, as it is based on the per-phase treatment of the line current harmonics. In a 3-phase 4-wire distribution system, three times as many CSC modules as necessary for each phase will be used.

### 6.3.2 Transient Performance

The objective of this section is to test and evaluate the transient response of the power splitting modular active filter system to sudden variations in the magnitude and phase of the harmonic currents. A simple example system consisting of two filter modules of the proposed filter with a non-linear load having variable magnitude and phase angle of the $5^{th}$ harmonic is simulated using the EMTDC simulation package. Again, the Current ADALINE input is ($i_L$) and its output is the fundamental and the $5^{th}$ harmonic. The modulating signal, $\sum i_h$ (in this case the $5^{th}$ harmonic signal), is used to control the CSC modules, and the peak value of $\sum i_h$ is used to produce the reference signal to regulate the dc-side current ($I_{dc}$) of each filter module. The input to the Voltage ADALINE is the system phase voltage. The output of the Voltage ADALINE is used to construct a sinusoidal control signal, which is in phase with the phase voltage. This signal will be used as a synchronization signal in the closed-loop control system for $I_{dc}$ regulation. Note that in order to keep $I_{dc}$ regulated, both the control signal and phase voltage should have the same frequency. This is taken care of by the voltage ADALINE which is equipped with line frequency tracker.

Fig. 6.4 displays the dc-side current ($I_{dc}$) of one of the CSC modules, the ADALINE output ($5^{th}$ harmonic magnitude and phase), the distorted current ($i_L$), and

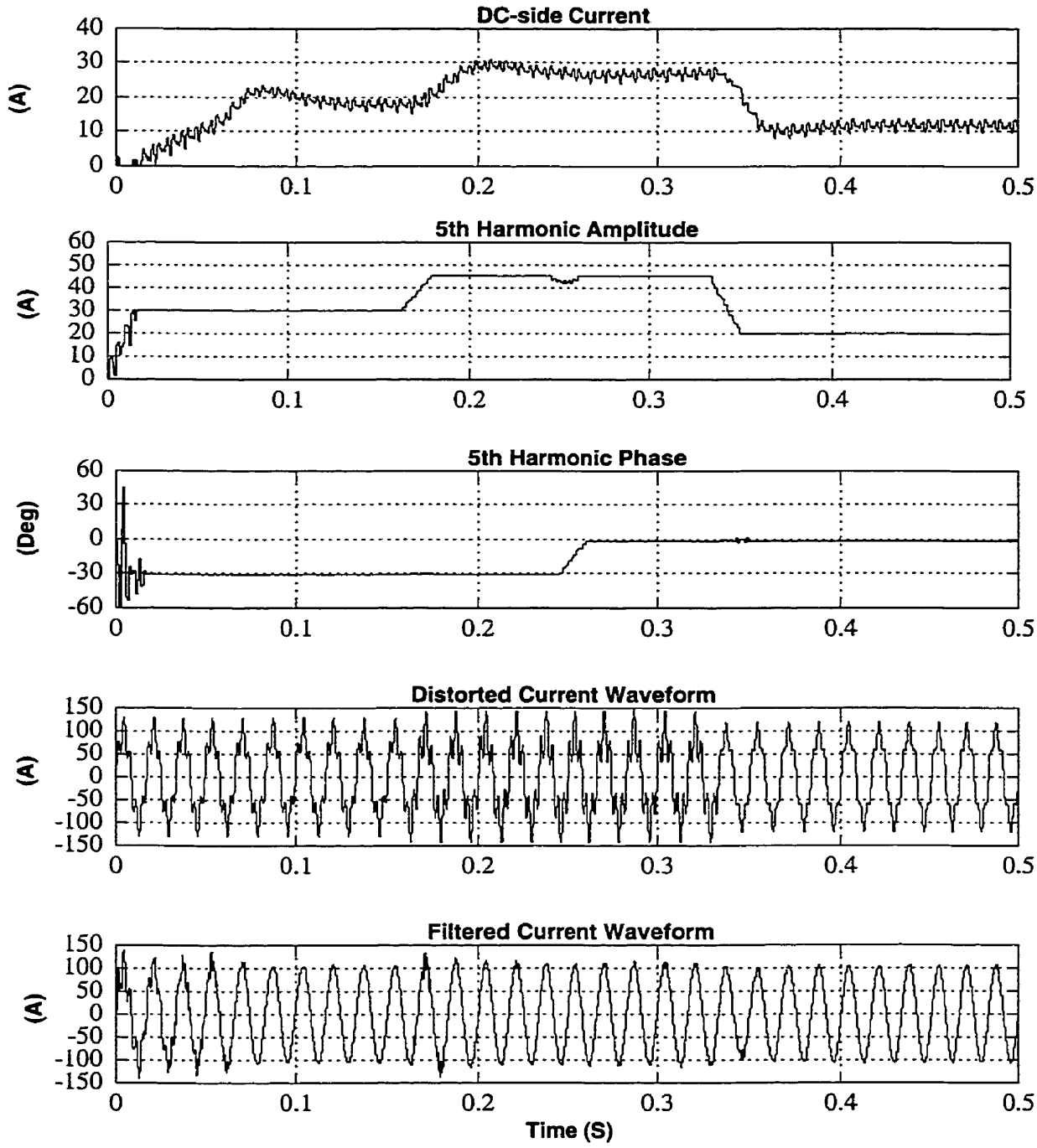


Fig. 6.4: Transient simulation results of the proposed power splitting modular active power filter.

the filtered current ($i_s$) for sudden changes in the nonlinear load current. From Fig. 7.4, it is obvious that the controller of the proposed active filter is responding quickly and accurately to the sudden increase or decrease in the nonlinear load in an adaptive way. It also shows that the filtered current waveform ($i_s$) settles to steady state within one cycle, and demonstrates the excellent response of the proposed active filter. The adaptation of $I_{dc}$ to load changes is an outstanding feature of the controller used which results in optimum $I_{dc}$ value and minimal converter losses.

## 6.4 Summary

The proposed modular active filter offers the following advantage: 1) high efficiency due to low conduction and switching losses; 2) high reliability and 3) high serviceability. The proposed active power-line filter treats the ac system on a per-phase basis, has fast response and adapts to the load variations. Theoretical expectations are verified by digital simulation using EMTDC simulation package.

# Chapter 7
# Power and Control Circuits Design

## 7.1 Overview

The purpose of this chapter is to provide a detailed power and control circuits design of the proposed modular active power filter which is given in Chapter 5. Due to their similarity, the design and control aspect of only one single-phase CSC filter module is considered.

The design of the active filter module is given in Section 7.2. In this section, the design of the power circuit, the energy storage element and the output filter capacitor are discussed. Section 7.3 gives a design example of one of the CSC filter modules. The

control aspect of the proposed filter with an emphasis on a detail design of the closed loop control system of the single-phase CSC module is discussed in Section 7.4.

# 7.2 Design of Active Filter Module

## 7.2.1 Power Circuit

The power circuit of each filter module is a standard single-phase PWM- CSC bridge. It consists of a dc reactor (for dc-energy storage), a small capacitor (for filtering of switching harmonics on the ac-side) and four controllable (gate-turn-off) semiconductor switches. The current which must be supported by each switch is the maximum dc-side current $I_{dc}$, that is the peak value of the corresponding harmonic current. The voltage, which must be supported by each switch, is the peak value of the system phase voltage.

## 7.2.2 Energy Storage Element

The energy element used in each CSC module is a dc reactor ($L_{dc}$). The size of $L_{dc}$ affects the peak-to-peak ripple of the dc-side current of the CSC module.

The dc-side inductor $L_{dc}$ of the CSC module is designed to limit the dc current ripple to a specified value, typically between 3% and 5%. The procedure to design the inductor is as follows:

The dc-side voltage of the CSC, which is placed across $L_{dc}$, is a pulse-width-modulated signal as shown in Fig. 7.1a. To consider the worse case condition for the peak-to-peak ripple in the dc-side current ($I_{ripple,p-p}$), one can assume that the supply voltage ($v_s$) is at the peak and the duty cycle is equal to 0.5. With the help of Fig. 7.1b, which shows the ripple component of the dc-side current, one can find

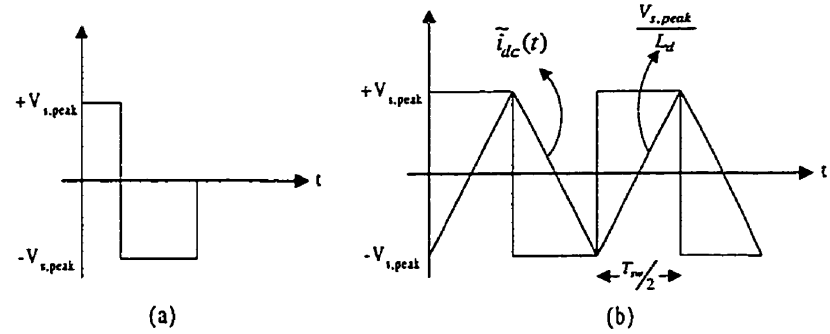


Fig. 7.1: (a) The dc-side voltage of the CSC. (b) The dc-side current ripple.

$$I_{ripple,p-p} = \frac{V_{s,peak}}{L_{dc}} \times \frac{T_{sw}}{2} = \frac{V_{s,peak}}{2 f_{sw} L_{dc}} \tag{7.1}$$

or,

$$I_{ripple,p-p}\% = \frac{I_{ripple,p-p}}{I_{dc}} \times 100\% = \frac{V_{s,peak}}{2 f_{sw} L_{dc} I_{dc}} \times 100\% \tag{7.2}$$

The minimum size of $L_{dc}$ can be calculated from

$$L_{dc,min} = = \frac{V_{s,peak} \times 100}{2 f_{sw} I_{dc} I_{ripple,p-p}\%} \tag{7.3}$$

From the above equation, as the switching frequency increases, the size of the inductor that can limit the current ripple to a specified value decreases. But, increasing the switching frequency will increase the power loss in the switches. Therefore a

compromise between the switching frequency and the inductor size should be considered.

### 7.2.3 Output Filter Capacitor

The ac-side filter capacitor is required to filter out the switching harmonics of the compensating current generated by the active filter modules. The filter capacitor and the line inductance form a second order low pass filter which may amplify low-order harmonics. Therefore, the size of the output capacitor must be selected carefully to make sure that no low-order harmonics are close to the resonant frequency of the LC tank circuit. The higher the switching frequency, the larger the resonant frequency, and the smaller the filter capacitor.

## 7.3 Design Example

The design of the proposed active filter will be performed through a realistic numerical example. Assume a single-phase diode bridge rectifier is fed by a distribution feeder. It is intended to filter up to the $7^{th}$ current harmonics. The magnitudes of the fundamental, $3^{rd}$ , $5^{th}$ and $7^{th}$ harmonic currents are as follows:

$I_{1,peak} = 1$ p.u.

$I_{3,peak} = 0.33$ p.u.

$I_{5,peak} = 0.2$ p.u.

$I_{7,peak} = 0.14$ p.u.

The switching frequency is chosen to be $21 \times$ highest harmonic order to be filtered$\times f_1$. The number of the proposed active filter modules is chosen to be 3 each is dedicated to filter one harmonic. Each module consists of 4 switches and 1 dc reactor.

Therefore, for 3rd harmonic active filter module,

- the maximum value of the dc-side current $I_{dc} = 0.33$ *p.u.*;
- the supply voltage peak value $V_{s,peak} = 1$ *p.u.*;
- the switching frequency = $f_{sw} = 21 \times 3 \times 60 = 3780 H_z$;

the dc-side reactor $L_{dc}$ is designed to limit ripple current to 5%.

From eqn. (7.3), one can easily find the dc-side reactor $L_{dc}$, to be equal to 0.08 p.u.

## 7.4 Modular Active Power Filter Control

The control scheme for the $l^{th}$ CSC module of the proposed modular active filter is shown in Fig.7.2. The controller of each CSC module consists of an open-loop control

and a closed-loop control. In the open loop system, the $l^{th}$- harmonic signal $A_l \sin(l\omega t + \varphi_l)$ is reconstructed from the output of the current ADALINE is divided by the gain $I_{dc}/V_{tri}$ of the filter module (the amplifier) and then compared to a triangular waveform to create the PWM switching pattern for the switches of the CSC module dedicated to that particular harmonic.

The converter losses and system disturbances, such as sudden load fluctuations, affect the dc-side currents of the CSC modules. For successful operation of CSCs as linear power amplifiers, $I_{dc}$ of each module must be regulated by means of closed-loop control. The control loop adjusts the amplitude of a sinusoidal template, synchronized with the system voltage ($v_s$) obtained from the voltage ADALINE. The above signal will be used as a part of the modulating signal of the CSCs, as shown in Fig.7.2. It results in drawing a small current component at fundamental frequency in phase with the system voltage (for charging up the $L_{dc}$ or increasing $I_{dc}$) or out of phase by 180° with respect to the system voltage (for discharging the $L_{dc}$ or decreasing $I_{dc}$). This action involves only real power transfer between the system and CSC modules whereas harmonic current injection involves only reactive power transfer.

The energy stored in $L_{dc}$ is given by:

$$\Delta W = \frac{1}{2} L_{dc} \Delta I_{dc}^2 \tag{7.4}$$

Charging $L_{dc}$ from $I_{dc1}$ to $I_{dc2}$ in a period of $\Delta t$ is associated with a change in the stored energy:

$$\Delta W = \frac{1}{2} L_{dc} ( I_{dc2}^2 - I_{dc1}^2 ) = ( P_{CSC} - P_{loss} ) \Delta t \tag{7.5}$$

where $P_{CSC}$ and $P_{loss}$ are the real power drawn from the system by one of the CSC modules and the power losses in that module, respectively. $P_{CSC}$ can be written as:

$$P_{CSI} = \pm V_s \cdot I_{CSC} \tag{7.6}$$

where the positive and negative signs correspond to the cases where real power flow from the system to the CSC and from the CSC to the system, respectively.

Substituting (7.6) in (7.5) yields

$$\frac{1}{2} L_{dc} ( I_{dc2}^2 - I_{dc1}^2 ) = ( \pm V_s I_{CSC} - P_{loss} ) \Delta t \tag{7.7}$$

or:

$$( I_{dc2}^2 - I_{dc1}^2 ) = \frac{2}{L_{dc}} ( \pm V_s I_{CSC} - P_{loss} ) \Delta t \tag{7.8}$$

The above relation clearly state that in order to increase $I_{dc}$,

$$( \pm V_s I_{CSC} - P_{loss} ) > 0 \tag{7.9}$$

i.e., $i_{CSC}$ must be in phase with $v_s$ (i.e., positive sign in(7.8)) and the following must hold:

$$I_{CSC} > \frac{P_{loss}}{V_s} \tag{7.10}$$

On the other hand, in order to decrease $I_{dc}$,

$$(\pm V_s I_{CSC} - P_{loss}) < 0 \tag{7.11}$$

i.e., $I_{CSC} < \frac{P_{loss}}{V_s}$ for $i_{CSC}$ in phase with $v_s$, or $I_{CSC} > -\frac{P_{loss}}{V_s}$ for $i_{CSC}$ out of phase by 180° with respect to $v_s$.

A shown in Fig. 7.2, the control loop adjusts the magnitude and the phase of $i_{CSC}$ based on the magnitude and the sign of the error between the $I_{dc,ref}$ and $I_{dc}$. Each CSC has an independent control loop for $I_{dc}$ regulation. This adds to the reliability of the system. Note that the value of the dc-side current is regulated based on the present peak value of the harmonic current available from the Current ADALINE. In other words, $I_{dc,ref}$ of each CSC is set to be equal to the amplitude of the corresponding harmonic to be filtered by the CSC module. This will reduce the conduction and switching losses, which are proportional to the dc-side current, and enhance the system performance thanks to the adaptive nature of the ADALINE.

For successful regulation of the CSC dc-side current, one should provide the appropriate compensation in the feedback loop for certain steady-state and transient response requirements using one of the conventional frequency-domain design methods

such as Bode plot. To design a proper controller, a linear mathematical model for each CSC, particularly the power stage, should be developed. The model is derived based on the state-space averaging technique.

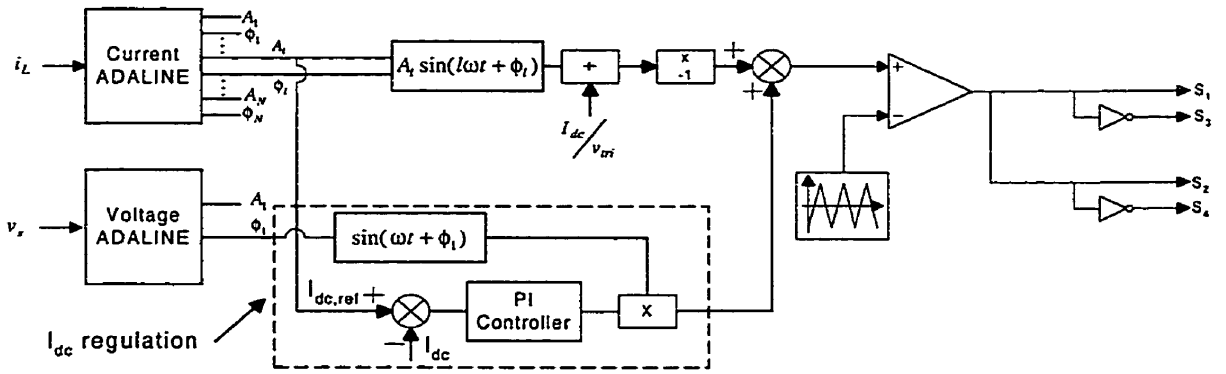


Fig. 7.2: Control Scheme of the $l^{th}$ CSC module of the proposed active filter

## 7.4.1 The System Equations

A state space model is used to represent one of the CSC modules of the modular active power filter (the plant) which is shown in Fig. 7.3. The state variables have been chosen to be the voltage across the capacitor and the currents through inductors. According to the conventions of voltage polarities and current direction chosen in Fig. 7.3, the differential equations that govern the CSC operation can be found as:

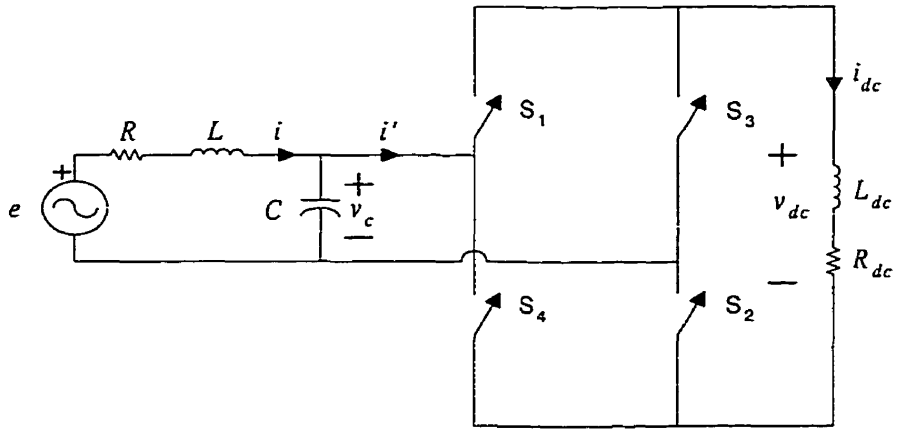


Fig. 7.3: Single-Phase Current Source Converter

$$v_c = e - Ri - L\frac{di}{dt} \tag{7.12-a}$$

$$i = C\frac{dv_c}{dt} + i' \tag{7.12-b}$$

$$v_{dc} = R_{dc}i_{dc} + L_{dc}\frac{di_{dc}}{dt} \tag{7.12-c}$$

The input current $i'$ and the output dc-voltage $v_{dc}$ of the CSC in equation (7.12) are giving by

$$\begin{aligned} i' &= Si_{dc} \\ v_{dc} &= Sv_c \end{aligned} \tag{7.13}$$

where $S$ represents the switching function that controls the converter switches in the CSC module, based on bipolar PWM. The CSC circuit, shown in Fig. 7.3, can be represented by the equivalent circuit shown in Fig. 7.4.

To find the mathematical model of the PWM-CSC module based on the state-space averaging technique, the switching function $s$ has been replaced by its low-frequency content, i.e., the local average or instantaneous average which is the fundamental component. The high frequency components in the output current are eliminated because of the low-pass filter at the output of the converter. The switching function $s$ can be replaced by the modulating signal ($m$) which is used to control the switches in the CSC module.

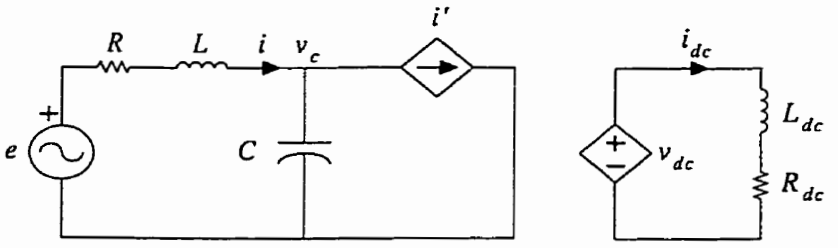


Fig. 7.4: Equivalent circuit for CSC module given in Fig. 7.3

Now, substitute equation (7.13) in (7.12) and use the modulating signal ($m$), equation (7.12) can be written as:

$$v_c = e - Ri - L\frac{di}{dt} \tag{7.14-a}$$

$$i = C\frac{dv_c}{dt} + mi_{dc} \tag{7.14-b}$$

$$v_{dc} = mv_c = R_{dc}i_{dc} + L_{dc}\frac{di_{dc}}{dt} \tag{7.14-c}$$

or,

$$\frac{di}{dt} = -\frac{R}{L}i - \frac{1}{L}v_c + \frac{1}{L}e \tag{7.15-a}$$

$$\frac{dv_c}{dt} = \frac{1}{C}i - \frac{m}{C}i_{dc} \tag{7.15-b}$$

$$\frac{di_{dc}}{dt} = \frac{m}{L_{dc}}v_c - \frac{R_{dc}}{L_{dc}}i_{dc} \tag{7.15-c}$$

Let's assume that:

$e = E_m \cos\omega t$ , $i = I_m \cos(\omega t + \varphi)$ , $v_c = V_m \cos(\omega t + \gamma)$ and $m = M \cos(\omega t + \theta)$

Then,

$i = (I_m, \varphi)$ , $v_c = (V_m, \gamma)$ and $i_{dc}$ are the state variables, $m = (M, \theta)$ is the input and $i_{dc}$ is the output.

Substituting for $e, i, v_c$ and $m$ in equation set (7.15), expanding and equating the coefficients of $\cos\omega t$ and $\sin\omega t$ terms on both sides of each equation, the following set of 1st-order non-linear differential equations will be obtained:

$$\frac{dV_m}{dt} = \frac{1}{C}\left[I_m \cos(\varphi - \gamma) - Mi_{dc} \cos(\theta - \gamma)\right] - \omega \tag{7.16-a}$$

$$\frac{d\gamma}{dt} = \frac{1}{CV_m}\left[I_m \sin(\varphi - \gamma) - Mi_{dc} \sin(\theta - \gamma)\right] - \omega \tag{7.16-b}$$

$$\frac{dI_m}{dt} = \frac{1}{L}\left[E_m \cos\varphi - RI_m - V_m \cos(\varphi - \gamma)\right] \tag{7.16-c}$$

$$\frac{d\varphi}{dt} = \frac{1}{LI_m}\left[V_m \sin(\varphi - \gamma) - E_m \sin\varphi\right] \tag{7.16-d}$$

$$\frac{di_{dc}}{dt} = \frac{1}{L_{dc}}\left[\tfrac{1}{2} MV_m \cos(\theta - \gamma) - R_L i_{dc}\right] \tag{7.16-e}$$

The equation set (7.16) can be written in the general form as:

$$\dot{\mathbf{x}} = \mathbf{f}(\mathbf{x}, \mathbf{u}) \tag{7.17}$$

where

$$\mathbf{x} = \begin{bmatrix} x_1 \\ x_2 \\ x_3 \\ x_4 \\ x_5 \end{bmatrix} = \begin{bmatrix} V_m \\ \gamma \\ I_m \\ \varphi \\ I_{dc} \end{bmatrix} \text{ and } \mathbf{u} = \begin{bmatrix} u_1 \\ u_2 \end{bmatrix} = \begin{bmatrix} M \\ \theta \end{bmatrix}$$

The above system can be linearized around a certain steady-state operating point and the linearized system can be expressed as:

$$\Delta\dot{\mathbf{x}} = \frac{\partial \mathbf{f}}{\partial \mathbf{x}}\Big|_* \Delta\mathbf{x} + \frac{\partial \mathbf{f}}{\partial \mathbf{u}}\Big|_* \Delta\mathbf{u} \tag{7.18}$$

where $\frac{\partial \mathbf{f}}{\partial \mathbf{x}}|_*$ and $\frac{\partial \mathbf{f}}{\partial \mathbf{u}}|_*$ are the Jacobian matrices, evaluated at the steady state operating points.

Thus, the general linearized system can be represented by:

$$\dot{\mathbf{x}} = \mathbf{A}\mathbf{x} + \mathbf{B}\mathbf{u} \tag{7.19-a}$$

$$\mathbf{y} = \mathbf{C}\mathbf{x} + \mathbf{D}\mathbf{u} \tag{7.19-b}$$

where,

$$\mathbf{x} = \begin{bmatrix} \Delta V_m \\ \Delta\gamma \\ \Delta I_m \\ \Delta\varphi \\ \Delta I_{dc} \end{bmatrix}, \quad \mathbf{A} = \begin{bmatrix} \frac{\partial f_1}{\partial x_1}\Big|_* & \frac{\partial f_1}{\partial x_2}\Big|_* & \frac{\partial f_1}{\partial x_3}\Big|_* & \frac{\partial f_1}{\partial x_4}\Big|_* & \frac{\partial f_1}{\partial x_5}\Big|_* \\ \frac{\partial f_2}{\partial x_1}\Big|_* & \frac{\partial f_2}{\partial x_2}\Big|_* & \frac{\partial f_2}{\partial x_3}\Big|_* & \frac{\partial f_2}{\partial x_4}\Big|_* & \frac{\partial f_2}{\partial x_5}\Big|_* \\ \frac{\partial f_3}{\partial x_1}\Big|_* & \frac{\partial f_3}{\partial x_2}\Big|_* & \frac{\partial f_3}{\partial x_3}\Big|_* & \frac{\partial f_3}{\partial x_4}\Big|_* & \frac{\partial f_3}{\partial x_5}\Big|_* \\ \frac{\partial f_4}{\partial x_1}\Big|_* & \frac{\partial f_4}{\partial x_2}\Big|_* & \frac{\partial f_4}{\partial x_3}\Big|_* & \frac{\partial f_4}{\partial x_4}\Big|_* & \frac{\partial f_4}{\partial x_5}\Big|_* \\ \frac{\partial f_5}{\partial x_1}\Big|_* & \frac{\partial f_5}{\partial x_2}\Big|_* & \frac{\partial f_5}{\partial x_3}\Big|_* & \frac{\partial f_5}{\partial x_4}\Big|_* & \frac{\partial f_5}{\partial x_5}\Big|_* \end{bmatrix},$$

$$\mathbf{B} = \begin{bmatrix} \frac{\partial f_1}{\partial u_1}\Big|_* & \frac{\partial f_1}{\partial u_2}\Big|_* \\ \frac{\partial f_2}{\partial u_1}\Big|_* & \frac{\partial f_2}{\partial u_2}\Big|_* \\ \frac{\partial f_3}{\partial u_1}\Big|_* & \frac{\partial f_3}{\partial u_2}\Big|_* \\ \frac{\partial f_4}{\partial u_1}\Big|_* & \frac{\partial f_4}{\partial u_2}\Big|_* \\ \frac{\partial f_5}{\partial u_1}\Big|_* & \frac{\partial f_5}{\partial u_2}\Big|_* \end{bmatrix}, \quad \mathbf{u} = \begin{bmatrix} \Delta M \\ \Delta\theta \end{bmatrix}$$

$$\mathbf{C} = \begin{bmatrix} 0 & 0 & 0 & 0 & 1 \end{bmatrix}, \text{ and } \mathbf{D} = \begin{bmatrix} 0 \end{bmatrix}$$

In order to find the steady state operating point, the right hand sides in equation set (7.16) are equated to zero (all the derivatives are equal to zero). Therefore,

$$0 = \frac{1}{C}\left[ I_m^* \cos(\varphi^* - \gamma^*) - M^* i_{dc}^* \cos(\theta^* - \gamma^*) \right] - \omega \tag{7.20-a}$$

$$0 = \frac{1}{CV_m^*}\left[ I_m^* \sin(\varphi^* - \gamma^*) - M^* i_{dc}^* \sin(\theta^* - \gamma^*) \right] - \omega \tag{7.20-b}$$

$$0 = \frac{1}{L}\left[ E_m \cos\varphi^* - RI_m^* - V_m^* \cos(\varphi^* - \gamma^*) \right] \tag{7.20-c}$$

$$0 = \frac{1}{LI_m^*}\left[ V_m^* \sin(\varphi^* - \gamma^*) - E_m \sin\varphi^* \right] \tag{7.20-d}$$

$$0 = \frac{1}{L_{dc}}\left[ \tfrac{1}{2} M^* V_m^* \cos(\theta^* - \gamma^*) - R_L i_{dc}^* \right] \tag{7.20-e}$$

Given the system parameters, *i.e.*, $R, L, C, R_{dc}, L_{dc}$ and $E_m$, as well as $\varphi^*$ and $I_{dc}^*$, one can solve for the $I_m^*, V_m^*, \gamma^*, M^*$ and $\theta^*$ from the above equations. Thus,

$$I_m^* = \frac{E_m \pm \sqrt{E_m^2 - 8RR_{dc}I_{dc}^2}}{2R} \tag{7.21-a}$$

$$V_m^* = \sqrt{(E_m - RI_m^*)^2 + (\omega LI_m^*)} \tag{7.21-b}$$

$$\gamma^* = \sin^{-1}\left\{ \frac{-\omega LI_m^*}{V_m^*} \right\} \tag{7.21-c}$$

$$M^* = \frac{\sqrt{(I_m^* \cos\gamma^*)^2 + (I_m^* \sin\gamma^* + \omega CV_m^*)^2}}{I_{dc}^*} \tag{7.21-d}$$

$$\theta^* = \sin^{-1}\left\{ \frac{-I_m^* \sin\gamma^* - \omega CV_m^*}{M^* I_{dc}^*} \right\} + \gamma^* \tag{7.21-e}$$

The CSC closed loop control system for charging the dc-side current will be as shown in Fig. 7.5.

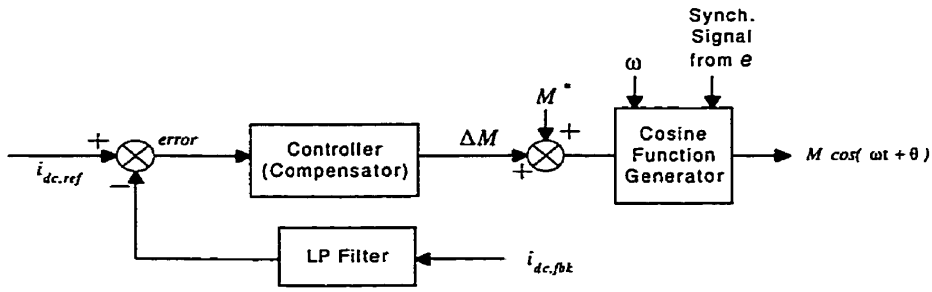


Fig. 7.5: Active power control loop for charging the dc-side current

## 7.4.2 Controller Design

The performance and stability of the feedback control system for regulating the dc-side current of the CSC, shown in Fig. 7.2, can be determined from the open-loop characteristics. Let us assume that the overall open loop transfer function is

$$G_{OL}(s) = G_C(s)GH(s)$$

where $G(s)$ is the CSC transfer function between $\Delta I_{dc}$ and $\Delta M$ obtained from state-space model, $H(s)$ is the transfer function of the low-pass filter ( see Appendix (C)). $G_C(s)$ is the transfer function of the compensator.

The parameters of $G_C(s)$ should be designed such that $G_{OL}(s)$ meets the following performance and desired characteristics:

1. The low frequency gain should be large so that the steady state error between the actual dc-current and the reference signal is small.
2. The gain at converter's switching frequency should be small.
3. The cross over frequency (the frequency at which the open loop gain is unity) should be as high as possible but below the switching frequency for a fast transient response such as a sudden change of the load.
4. The open loop phase at the cross over frequency (phase margin) should be at least $45^0$.

Fig. 7.6 shows the Bode plot for the transfer function $GH(s)$ using the numerical values given in the Appendix (C). It clearly shows that the transfer function has a fixed gain and minimal phase at low frequency. Beyond the resonant frequency $\omega_0 = \frac{1}{\sqrt{LC}}$, the gain began to fall with slope of –40dB/decade and the phase tends toward $-180^0$.

The additional phase-lag should be considered in designing the compensation of such a system to provide enough gain and phase margins. To meet the above requirements simultaneously, a phase-lag compensator of the form $G_C(s) = K\frac{(1+\tau s)}{(1+\alpha\tau s)}$ is used.

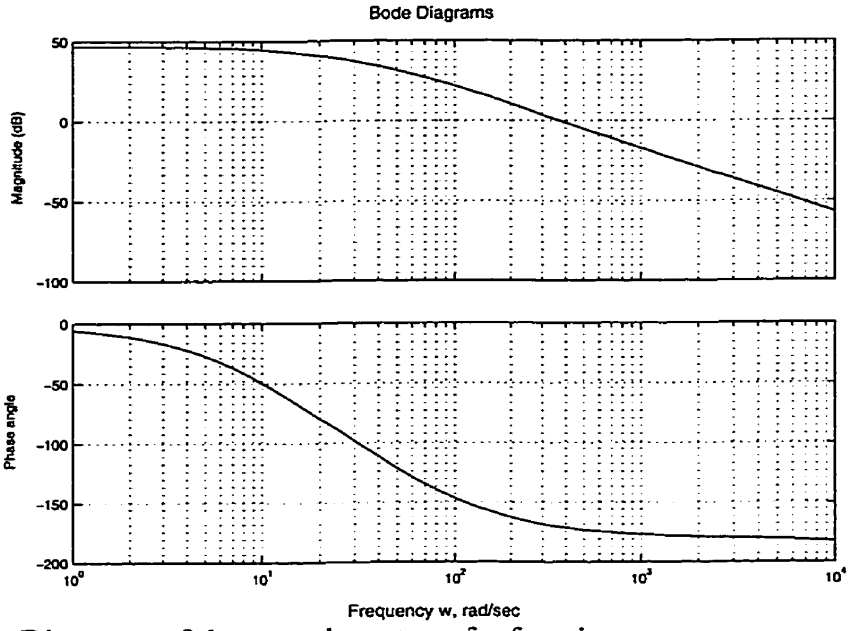


Fig. 7.6: Bode Diagrams of the open loop transfer function

The parameters of the compensator $G_C(s)$ can be determined using the Bode plot technique. The design criteria and procedures are outlined in the Appendix (C). The controller parameters are derived to be:

$K = 0.087$

$\tau = 0.2$

$\alpha = 2.82$

The bode plots of the open loop transfer function including the controller are shown in Fig. 7.7. As seen, the gain margin of $55^0$ has been achieved.

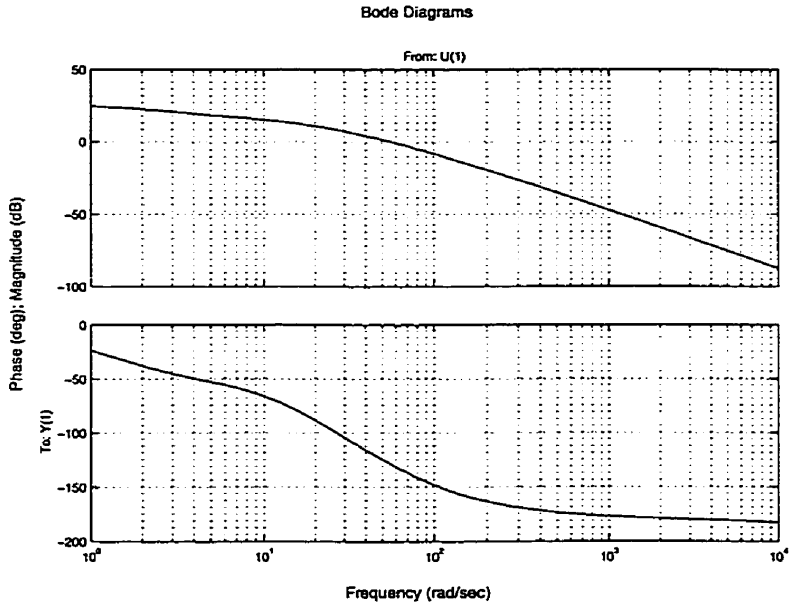


Fig. 7.7: Bode Diagrams of the open loop transfer function including the controller

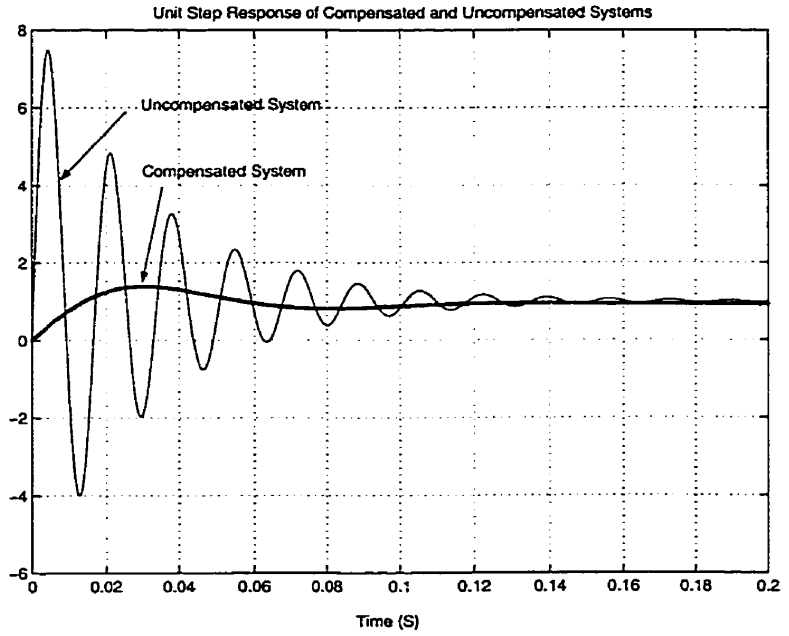


Fig. 7.8: Unit step response curves for the compensated and uncompensated systems

The step response of the system is shown in Fig. 7.8 and shows that the steady- state error of less than 5% has been achieved.

## 7.5 Summary

This chapter discussed the control system of the proposed modular active power filter and provided simplified design procedures of the CSC filter components. A design example was introduced to illustrate the design procedures. The filter control scheme is clearly described. A detailed mathematical model of the CSC filter module which is used in controller design is given. The design of the closed loop control system is also discussed.

# Chapter 8
# Evaluation Of The Proposed Modular Approach

## 8.1 Overview

The objective of the chapter is to evaluate and compare the proposed modular active filtering approach (Frequency Splitting approach) against the conventional one-converter and power-splitting approaches from the installation and operating costs, as well as performance points view. We will also draw some conclusions as to when and where each modular scheme should be used.

Section 8.2 provides a comparison between the proposed modular active (frequency splitting) and the conventional 1-converter schemes. The comparative evaluation of the

two modular active filtering approaches from different points of view is discussed in Section 8.3. Finally, the summary of this chapter is given in Section 8.4.

## 8.2 Frequency Splitting Versus Single Converter

In this section, the proposed modular active filtering (frequency splitting) approach will be compared to the conventional 1-converter approach from the economical, reliability, and flexibility points of view. Fig. 8.2 shows the block diagrams of the 2 schemes.

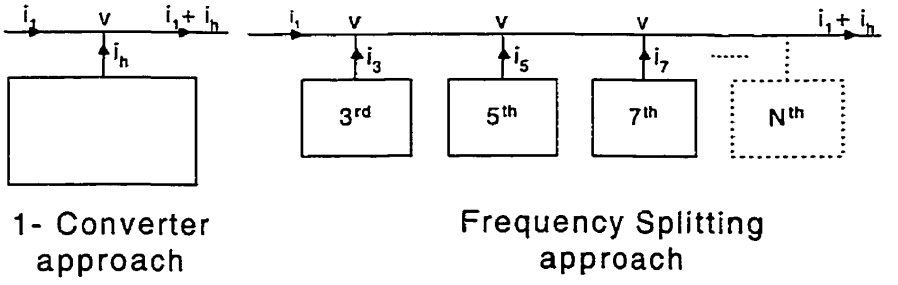


Fig. 8.2: Block diagram of the frequency splitting and 1-converter schemes.

### 8.2.1 Economical Comparison

The installation cost of the modular scheme will be higher than that of the 1-converter approach, but the operating cost will be lower. Therefore, as the operating time increases, there will be a break-even point at which the total costs of the two schemes

become equal. Beyond the break-even point, the modular approach offers more savings. This is illustrated in Fig. 8.3.

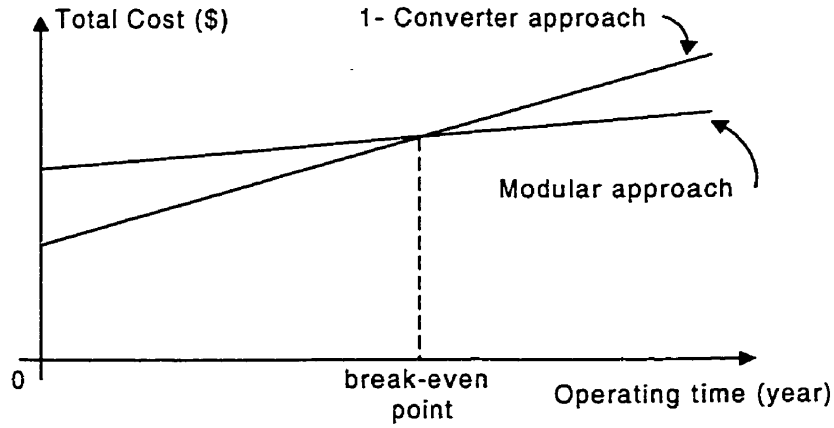


Fig. 8.3: Total cost comparison between the 1-converter scheme and frequency splitting converter scheme.

The economic comparison will be performed through a realistic numerical example. Assume a single-phase diode bridge rectifier is fed by a 400 V feeder. It is intended to filter the 3rd, 5th, and 7th current harmonics. The magnitudes of the fundamental, 3rd , 5th and 7th harmonic currents, and the total distorted current ($i_{dis}$) are as follows:

$I_1$ = 247.5 A, rms (350 A, peak)

$I_n = (1/n)\, I_1$; $I_3$ = 117 A, peak; $I_5$ = 70 A, peak; $I_7$ = 50 A, peak; $I_{dis}$ = 205 A, peak.

The switching frequency is chosen to be 21 × highest frequency to be filtered. Each CSC has 4 switches and 1 dc reactor. The cost of electricity is calculated based on the Canadian rates (see Appendix D).

To simplify the problem, the installation cost includes the cost of the components and the operating cost includes the cost of the conduction and switching losses. The costs are given in Canadian dollars. Table (8.1) and Table (8.2), summarize the installation cost and the operating losses of both schemes, respectively.

Table (8.1): Installation costs of 1-converter and frequency splitting schemes

| | | 1 Converter | Modular Converter |
|---|---|---|---|
| Installation Cost | **Switches*** | **$ 897▲** | **$ 897▲** |
| | **Reactors**** | **$1705▲** | **$2018▲** |
| Total Cost | | **$2602** | **$2915** |

- * Based on the Fuji dual NPT IGBT modules, 600 V
- ** Based on the Hammond 5 mH dc reactors
- ▲ See Appendix E

Table (8.2): Operating losses and cost per month of 1-converter and frequency splitting schemes

| | 1 Converter | Modular Converter |
|---|---|---|
| Conduction* Losses | **898 kWh/month** | **1038 kWh/month** |
| Switching* Losses | **1426 kWh/month** | **1044 kWh/month** |
| Total Losses | **2324 kWh/month** | **2082 kWh/month** |
| Cost of Total Losses | **191.4 $/month** | **172.6 $/month** |

- * See Appendix D

The yearly net saving in the operating losses using the modular scheme is $ 226 (based on the Canadian tariff, see Appendix D). This means that the difference between the installation costs of the 1-converter and the proposed frequency splitting approaches ($313) will be compensated in less than $1\frac{1}{2}$ years of operation. Since the dc-side current of each CSC module in the proposed modular filter is regulated at the present peak value of the corresponding harmonic, it is expected that the total losses will be less and hence the savings will be more. Also, on a larger scale, the savings will be greater.

### 8.2.2 Reliability

Since the power converter units of the proposed frequency splitting active power filter are acting as standalone devices, a partial harmonic cancellation of a distorted waveform is expected even if one or more power converters fail to operate. This will still result in a better line current spectrum than in the uncompensated case. Note that, in the one converter scheme, the converter failure means no harmonic elimination at all.

### 8.2.3 Flexibility

Since each converter is independently connected to the AC system, selective harmonic elimination based on the dominant harmonic component is possible. Also, simultaneous multi-function strategies to take care of other disturbances, such as voltage or current

imbalance and voltage fluctuations are feasible. This will result in great flexibility and enhancement of the overall performance of the proposed active filter.

## 8.3 Frequency-Splitting Approach Verses Power-Splitting Approach

In this section, the two modular active filtering approaches are compared.

### 8.3.1 Power rating

The total power rating in power splitting approach is determined by the peak of the total distortion, i.e., $(\sum i_h)_{peak}$, $h$ being the harmonic order. In the frequency splitting scheme, the total power rating is determined by the sum of the peaks of the individual harmonics to be filtered, i.e., $\sum i_{h,peak}$. Due to the diversity effect of harmonics, $(\sum i_h)_{peak} < \sum i_{h,peak}$. This implies that for the same filtering job, the installed VA is higher in frequency splitting approach than in power splitting scheme. This naturally results in higher initial (installation) cost for frequency splitting technique.

### 8.3.2 DC term: $I_{dc}$

In power splitting, the dc term ($I_{dc}$) of each converter is equal to $(\sum i_h)_{peak}/N$, i.e., the peak of the sum of the harmonics to be filtered divided by the number of filter modules

in parallel. The information on $(\sum i_h)_{peak}$ is necessary for sizing the individual converter modules and the regulation of $I_{dc}$ of each module. The dc term ($I_{dc}$) of each converter in frequency splitting is equal to $i_{h.peak}$. This information is readily available in frequency splitting modular active filter. The information on the peak values of the individual harmonics allows for dynamic adjustment of $I_{dc}$ of converter modules according to the present magnitude of the corresponding harmonic components. This feature can result in a reduction of conduction and switching losses through avoiding unnecessary high $I_{dc}$ values.

### 8.3.3 Identical modules

In the power splitting approach, the converter modules are identical. This offers an advantage in terms of maintenance and serviceability. The operator of the equipment has to keep only one type of module in stock. In frequency splitting, converter modules are different and can be replaced only by a similar module.

### 8.3.4 Conduction losses

In the power splitting approach, the total conduction loss is proportional to the peak of the sum of harmonics to be filtered, $(\sum i_h)_{peak}$. The total conduction losses in the frequency splitting approach is proportional to the sum of the peaks of the harmonics to

be filtered, $\sum i_{h,peak}$. Since $(\sum i_h)_{peak} < \sum i_{h,peak}$, the total conduction losses in the power splitting approach is less than those in the frequency splitting scheme.

## 8.3.5 Switching losses

In the power splitting approach, the switching losses in each converter module are proportional to $((\sum i_h)_{peak}/N)(f_{sw}/N)$. The total switching loss of $N$ converter modules will be proportional to $((\sum i_h)_{peak} \times f_{sw}/N)$. $f_{sw}$ is conventionally taken to be equal to $21 \times$ highest order of harmonic to be filtered $\times$ fundamental frequency ($f_1$) [4]. In the frequency splitting scheme, the switching frequency of a converter module is proportional to $(i_{h,peak}) \times (f_{sw,h})$. Here, $f_{sw,h}$ is assumed to be $21 \times h \times f_1$. As $h$ increases, $i_{h,peak}$ decreases and $f_{sw,h}$ increases. In typical non-linear loads such as diode rectifiers of a constant dc-side current, $i_{h,peak} \propto \frac{1}{h}$, and $f_h \propto h$. Since $f_{sw,h} \propto f_h$, therefore $f_{sw,h} \propto h$. As a result, the switching loss of a converter module is proportional to $\frac{1}{h} \times h$ or is a constant for all converter modules. The total switching loss will be proportional to $\sum (i_{h,peak} \times f_{sw,h})$. As seen, the total switching loss of the power splitting approach decreases as $N$ (the number of modules) increases. For low $N$ values, the total switching losses of the power splitting approach can be higher than those of the frequency splitting scheme. As $N$ is increased, at a break even point, the switching losses of both schemes become equal and

for larger $N$, the switching losses of the power splitting approach will be lower than those of the frequency splitting scheme.

## 8.3.6 Economical Comparison

The economical comparison will be performed through a realistic numerical example. Assume a single-phase diode bridge rectifier is fed by a 400 V feeder. It is intended to filter the 3rd, 5th, and 7th current harmonics. Therefore, 3 modules of frequency splitting scheme will be used. The magnitudes of the fundamental, 3rd, 5th and 7th harmonic currents, and the total distortion current ($i_{dis} = \sum_{h=3,5,7} i_h$) are as follows:

$I_{1,rms} = 247.5$ A ($I_{1,peak} = 350$ A)

$I_h = (1/h) \cdot I_1$; $I_{3,peak} = 117$ A; $I_{5,peak} = 70$ A; $I_{7,peak} = 50$ A; $I_{dis,peak} = 205$ A.

The switching frequency is chosen to be 21×highest order of harmonic to be filtered× $f_1$. To simplify the problem, the installation cost includes the cost of 4 switches and 1 dc reactor per CSC module and the operating cost is the sum of the costs of the conduction and switching losses. The cost of electricity is calculated based on the rates used by Waterloo North Hydro (see Appendix D) and is given in Canadian dollars. The number of active filter modules of power splitting scheme is chosen to be 4 so that both schemes have almost the same installation cost. Table (8.3) gives the installation

costs of the two schemes and Table (8.4) lists the conduction and switching losses as well as the operating costs of both schemes.

Table (8.3): Installation costs of frequency-splitting and power-splitting schemes

| | | Power-splitting approach | Frequency-splitting approach |
|---|---|---|---|
| Installation Cost | **Switches*** | **$ 897** | **$ 897** |
| | **Reactors**** | **$2296** | **$2018** |
| Total Cost | | **$3193** | **$2915** |

- * Based on the Fuji dual NPT IGBT modules, 600 V
- ** Based on the Hammond 5 mH dc reactors

Table (8.4): Operating losses per month of frequency-splitting and power-splitting schemes

| | Power-splitting approach | Frequency-splitting approach |
|---|---|---|
| Conduction* Losses | **590 kWh/month** | **683 kWh/month** |
| Switching* Losses | **352 kWh/month** | **1030 kWh/month** |
| Total Losses | **942 kWh/month** | **1713 kWh/month** |
| Cost of Total losses | **84.2 $/month** | **144.4 $/month** |

- * See Appendix E

From the data presented in Table (8.4), it can be concluded that in the power splitting approach, the operating costs are lower and thus, this scheme is more economical than the frequency splitting approach.

The results of the operating cost comparison happen to be strongly case dependent. Under different loading conditions, the power splitting scheme might be more economical than frequency splitting approach or vice versa. As the number of filter modules in power splitting approach ($N$) is increased, the conduction losses remain the same, but the switching losses will decrease. Generally speaking, if the initial (installation) cost can be justified, the power splitting approach offers a more economical solution to modular active power filtering.

### 8.3.7 Reliability

The loss of one converter in the power splitting approach implies an increase of $(1/N)\times 100\%$ in the magnitude of each filtered harmonic component. The loss of a filter unit reduces the effective switching frequency and causes waveform distortion due to the incorrect phase shift between the carrier signals of the remaining filter modules. These effects are expected to cause an increase in the total harmonic distortion (THD) beyond $(1/N)\times 100\%$. For the example given in the previous section, the THD (up to 3 kHz) will increase from 5.9% to 48.7% if one active filter module is lost. The considerable increase in the THD beyond expectation is due to additional distortion resulting from the drop in the effective switching frequency and the incorrect phase shift superimposed on it.

In the frequency splitting scheme, the loss of one filter module adds a percentage to the THD depending on which converter is lost. If the failed filter module is the one responsible for filtering the harmonic of the largest magnitude, the effect will be the most dramatic. For the example given in the previous section, the THD (up to 3 kHz) will increase from 5.78% to 30.76% if the active filter module dedicated to the $3^{rd}$ harmonic current is lost and to 19.3% and 14.88% if the $5^{th}$ active filter module and the $7^{th}$ active filter module are lost, respectively. From the above discussion, it can be concluded that in frequency splitting scheme, even if the converter responsible for filtering the harmonic of the largest magnitude is lost, the resulting line current spectrum is better than that of losing a unit in power splitting approach.

### 8.3.8 Flexibility

In the power splitting approach, selective harmonic elimination is not accommodated. All the harmonics in the window defined by the bandwidth of the filter system will be filtered. The frequency splitting scheme allows for selective harmonic elimination thanks to the availability of information on individual harmonic components. By implementing a criterion in the control algorithm, the harmonics of magnitude higher than a specified value will be selected for elimination and the corresponding active filter modules will be activated and connected to the power line. This feature results in reduced overall losses.

## 8.3.9 Steady-State Performance

To test the performance of the two modular active filter schemes in steady state, the example given in section 8.3.6 was simulated using the EMTDC simulation package. Fig. 8.4(a) shows the distorted current ($i_L$) waveform. Fig. 8.4(b) and Fig 8.4(c) display the filtered current ($i_S$) conditioned by frequency splitting and power splitting modular

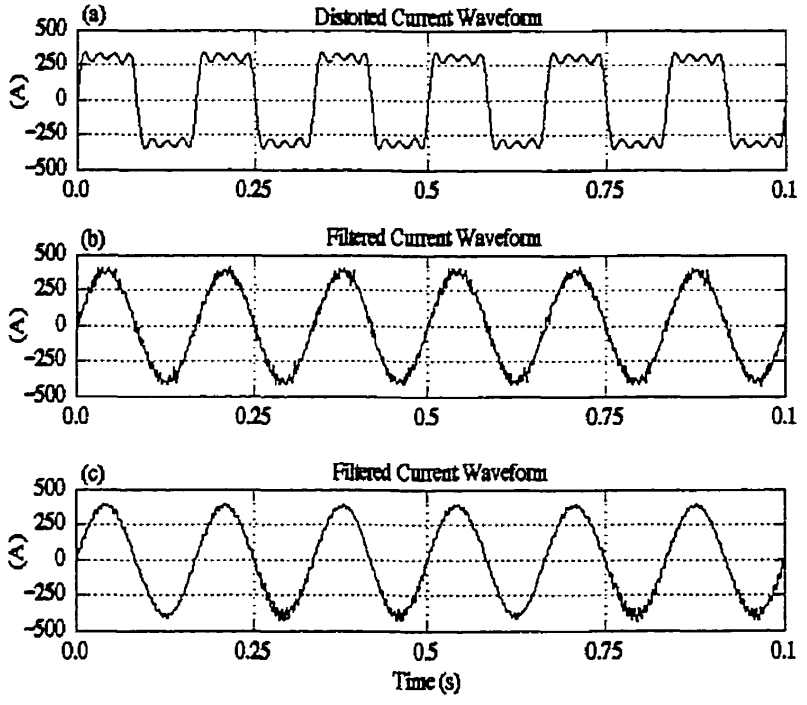


Fig 8.4: Steady state simulation results of the two modular active filter schemes
(a) Distorted current ($i_L$) waveform
(b) The filtered current for frequency splitting scheme
(c) The filtered current for power splitting scheme

active filter schemes, respectively. The waveforms clearly demonstrate the effectiveness and validity of both schemes in eliminating the selected harmonics from the line current. The THD (up to 3 kHz) of the filtered current of Fig. 8.4(b) is 5.78%, and that of Fig 8.4(c) is 5.9%, down from 37.34% in the distorted line current.

## 8.4 Summary

The comparison between the proposed modular active filter (frequency splitting approach) and the conventional 1-converter scheme shows that the proposed filter is more economical, reliable and flexible.

The comparative evaluation of the power splitting and frequency splitting approaches for active power filtering shows that when the initial (installation) cost is not a limiting factor for the number of filter modules, the power splitting approach offers a more economical solution to modular active power filtering. In the power splitting scheme, the diversity effect of harmonics results in the reduction of the installed VA and operating costs. The frequency splitting approach, on the other hand, offers the following advantages thanks to the availability of full information on individual harmonic components: 1) reliability; 2) flexibility (selected harmonic elimination) and 3) dynamic adjustment of the dc-terms of the CSC filter modules according to the present magnitudes of the individual harmonics to be filtered (resulting in reduced losses). Moreover, for harmonic current components that have high ratings,

the concept of the power splitting can be used to compensate a particular harmonic using the frequency splitting approach.

# Chapter 9
# Conclusions and Future Work

The main objective of this research is to develop an innovative harmonic mitigating technique using a modular active power filter. In this thesis, an efficient and reliable modular active harmonic filtering approach has been taken. Rather than trying to provide active filtering for the entire spectrum of harmonic components, the proposed modular active power system targets the low-order harmonics individually.

Different active power filtering schemes and concepts have been introduced for the purpose of power quality improvement. The power converter used as an active filter is rated based on the magnitude of the injected current and is operated at the switching frequency required to perform the filtering job successfully. Almost all of the recently proposed active power filters are realized by one PWM voltage source or current source converter. If the converter's power rating and switching frequency are both high, excessive losses are expected

The proposed modular active filter system consists of a number of parallel single-phase CSC modules: each dedicated to suppress a specific low-order harmonic of choice (Frequency-Splitting Approach). The power rating of the modules will decrease and their switching frequency will increase as the order of the harmonic to be filtered is increased. As a result, the overall switching losses are considerably reduced due to a balanced "power rating"-"switching frequency" product and selected harmonic elimination.

The reliability of the existing active filters is another major concern. Most of the existing active power filters connected to distribution systems consist mainly of a single power converter with a high rating which takes care of all the harmonic components in the distorted signal. A failure in any of the active filter devices will result in no compensation at all. Also, active power filters that are based on cascade multi-converter and multi level topologies suffer from low reliability. Since the power converter units of the proposed modular active power filter are acting as standalone devices, a partial compensation of harmonic distortion is expected even if one (or more) power converters fails to operate. This will still result in a better line current spectrum than in the uncompensated case.

The proposed filter system exhibits great flexibility and superior overall performance due to the independent connection of the filter modules to the AC system and the possibility of the selected harmonic elimination based on the dominant

harmonic component. To take advantage of the diversity principle, the proposed filter system can filter a group of harmonics using one filter module or more by combining them and compensating them in groups. Also, simultaneous multi operation strategies to take care of other disturbances, such as voltage or current imbalance and voltage fluctuations are feasible.

The control methodology of the active power-line filter is the key element for enhancing its performance in mitigating the harmonic current and voltage waveforms. Active power line filtering can be performed in the time domain or in the frequency domain. The control system processes the distorted line current and the voltage signals and forces the converter to inject the proper compensating current. At the same time it regulates the dc-side current or voltage of the converter. One important factor which influences the performance of the active power filters in the frequency domain is the speed and accuracy of the detection tool for the power line harmonic currents. In this thesis, the ADALINE-based harmonic analyzer has been improved by modifying the original ADALINE algorithm to track the system frequency variations. The proposed estimation scheme is tested on simulated data and compared with the Kalman filter and FFT algorithms. The improved ADALINE scheme provides excellent accuracy and convergence speed in tracking the fundamental frequency and the harmonic components. It is highly adaptive and is capable of estimating the variations in the

fundamental frequency, amplitude and phase angle of the harmonic components. It exhibits better performance compared with the Kalman filter and FFT approaches.

Another important factor, affecting the control of the active filters, is the derivation of the synchronizing signal, which is in phase with the bus voltage and is used to regulate the dc-side current or voltage of the power converter. In this thesis, a new ADALINE-based controller scheme for the proposed modular active filter is introduced. The proposed controller utilizes another ADALINE to track the system voltage and extract the fundamental component of the source voltage which is used as a synchronize signal for the $I_{dc}$ regulation loop. This improves the filtering capability of the proposed modular active filter even if the source voltage is harmonic polluted. The controller adjusts the dc-side current $I_{dc}$ of the converter modules according to the magnitude of the harmonics to be filtered. This results in optimum dc-side current value and minimal converter losses.

The proposed controller is also responsible for invoking specific CSC filter module(s) to start the filtering job by connecting it to the electric grid. The automated connection of the corresponding filter module(s) is based on decision-making rules in such a way that the IEEE 519-1992 limits are not violated. The information available on the magnitude of each harmonic component allows us to select the active filter bandwidth (i.e., the highest harmonic to be suppressed). This will result in more efficiency and higher performance.

In this research, the comparative evaluation on practical use in industry shows that the proposed filter is more economical, reliable and flexible compared to the conventional approach of filtering all the harmonics using one converter. The comparison between the power splitting and frequency splitting approaches presented in Chapter 8 shows that the power splitting scheme offers a more economical solution to modular active power filtering when the installation cost is not a limiting factor. The frequency splitting approach, on the other hand, is more reliable, flexible and is capable of dynamic adjustment of the dc-terms of the CSC filter modules according to the present magnitudes of the individual harmonics to be filtered. This results in reduced losses. Moreover, for harmonic current components that have high ratings, the concept of power splitting can be used to compensate a particular harmonic using the frequency splitting approach.

The proposed active power filter system is quite capable of dealing with unbalanced nonlinear load conditions, as it is based on the per-phase treatment of the line current harmonics. In a three-phase 4-wire distribution system, three single-phase CSCs will be required for filtering a specific harmonic in the three lines. The frequency splitting concept is also applicable to three-phase 3-wire distribution systems. In this case, instead of using three single-phase CSC modules, only one three-phase module is required to suppress a specific harmonic of choice in the three lines.

In light of the drawbacks presented in previously proposed schemes and concepts, the active filtering topology and control scheme proposed in this thesis have been successfully demonstrated to be a valuable contribution to active power harmonic filtering. The concept and performance of the proposed filter system have been verified by extensive simulation experiments using the EMTDC and the MATLAB simulation packages.

The followings are some specific conclusions which reflect the bold features of the proposed modular active filter system:

1. The proposed frequency splitting modular design which is based on filtering specific harmonics results in high efficiency due to low conduction and switching losses. This results in more savings in the running costs compared to the conventional approach.
2. The proposed filter exhibits high reliability due to the parallel connection of CSC modules and single harmonic treatment.
3. The ADALINE based-harmonic analyzer has been utilized for the first time as a part of active power filtering. This enhances the performance response of the proposed filter due to the adaptability and the ADALINE's speed in tracking the harmonic components.

4. The ADALINE-based measurement scheme has been enhanced by modifying the original algorithm to track the fundamental frequency variations. This is important for successful charging of the dc-side current of the CSCs and hence successful harmonic filtering.

5. The controller of the proposed active filter has been improved by utilizing another ADALINE to track the system voltage to extract the fundamental component of the source voltage which is used as a synchronize signal for the $I_{dc}$ regulation loop. This improves the filtering capability of the proposed modular active filter even if the source voltage is harmonic polluted.

6. The controller is further enhanced by dynamically adjusting the dc-side current $I_{dc}$ of the CSC filter modules according to the present magnitudes of the individual harmonics to be filtered. This results in optimum dc-side current value and minimal converter losses.

7. The CSC topology has been chosen for its superior performance compared with VSC topology, in terms of direct control of the injected current (resulting in faster response in time-varying load environment) and lower dc-energy storage requirement (resulting in lower reactive element rating and reduced losses).

8. The proposed filter has the capability to select harmonic elimination due to the availability of information on the individual harmonic components. Also, a

single CSC filter module can be assigned to filter two or more harmonics that have low magnitudes.

# Suggestions for Future Work

During the course of this research, the following issues have been detected and are listed here as possibly topics for future work in this area.

1. The application of the proposed active filter system to mitigate other power quality problems such as sags and swells.
2. This work can be extended to investigate the possibility of balancing the unbalanced currents in 3-phase 4-wire distribution systems.
3. The focus of this research is on the fundamental theoretical problems rather than the hardware implementation. The proposed active filter could be experimentally verified and compared to the theoretical work done in this thesis.
4. Quantitive study on the savings due to dynamically adjusting the dc-side current $I_{dc}$ of the CSC could be conducted.
5. Similar topology with higher voltage and current ratings may be designed to be used for other application such as AC and DC active harmonic filtering of HVDC systems.

# List of Publications

## I. Journal Papers

[1] R. El Shatshat, M. Kazerani, and M.M.A. Salama, " Multi Converter Approach to Active Power Filtering Using Current Source Converters," IEEE trans. on Power Delivery, Vol. 16, No. 1, pp. 38-45, Jan. 2001.

[2] E. F. El-Saadany, R. El Shatshat, M.M.A. Salama, M. Kazerani, and A. Y. Chikhani, "Reactance One-Port Compensator and Modular Active Filter for Voltage and Current Harmonic Reduction in Non-Linear Distribution Systems: A Comparative Study," Electric Power Systems Research (52), 1999, pp. 197-209.

[3] R. El Shatshat, M. Kazerani, and M.M.A. Salama, " Modular Active Power-Line Conditioner," Accepted for publication in IEEE Transactions on Power Dilevery.

[4] R. El Shatshat, M. Kazerani, and M.M.A. Salama, " Estimation and Mitigation of Power System Harmonics Using Artificial Neural Networks (ANN) Algorithm," Submitted to Electric Power Systems Research Journal (Under review).

[5] R. El Shatshat, M. Kazerani, and M.M.A. Salama, "Power Quality Improvement in 3-Phase 3-Wire Distribution Systems Using Modular Active Power Filter Algorithm," Submitted to Electric Power Systems Research Journal (Under review).

[6] R. El Shatshat, M. Kazerani, and M.M.A. Salama, "Artificial Intelligent Controller for CSI-Based Modular Active Power Filters," (Under preparation).

## II. Refereed Conference Papers

[7] R. El Shatshat, M. Kazerani, and M.M.A. Salama, "ADALINE-Based Controller for Active Power-Line Conditioners," Proceedings of IEEE Transmission and Distribution Conference (99), New Orleans, Louisiana USA, vol.2, pp.566-571, 1999.

[8] R. El Shatshat, M. Kazerani, and M.M.A. Salama , "Modular Active Power Filtering Approaches: Power Splitting verses Frequency Splitting," Proceedings of Canadian Conference in electrical and computer Engineering (CCECE'99), Edmonton, Canada, 1999, pp. 1304-1308.

[9] R. El Shatshat, M. Kazerani, and M.M.A. Salama, "Modular Approach to Active Power-Line Harmonic Filtering," Proceedings of IEEE Power Electronics Specialists Conference (PESC 98), Japan, pp. 223-228, 1998.

[10] R. El Shatshat, M. Kazerani, and M.M.A. Salama, "Rule-Based Controller for Modular Active Power Filters," (Under preparation).

# APPENDIX (A)

## Discrete Fourier Transform (DFT)

The frequency content of a periodic stationary discrete time signal $x(n)$ with M samples can be expressed using the discrete Fourier transform as:

$$X(f_k) = \frac{1}{M}\sum_{n=1}^{M} x(t_n)e^{-jk\Omega n} \tag{A.1}$$

where $\Omega = 2\pi/M$

the inverse Fourier transform is

$$x(t_n) = \sum_{k=1}^{M} X(f_k)e^{jk\Omega n} \tag{A.2}$$

Both the time domain and the frequency domain are assumed periodic with a total of M samples per period. The direct and quadrature components of the $n^{th}$ harmonic of a distorted waveform V can be expressed as

$$X_n = \frac{2}{M}\sum_{k-1}^{M} V_k \sin n\omega_o t_k \tag{A.3}$$

$$y_n = \frac{2}{M}\sum_{k=1}^{M} V_k \cos n\omega_o t_k \qquad \text{(A.4)}$$

where $V_k$ is the sample of the distorted waveform at time $t_k$; $k = 1,2,...,M$ .

From equations (A.3 and A.4), one can calculate the amplitude and the phase angle of the n$^{th}$ harmonic using:

$$V_n = \sqrt{x_n^2 + y_n^2} \qquad \text{(A.5)}$$

$$\phi_n = \tan^{-1}(y_n / x_n) \qquad \text{(A.6)}$$

## References

[A.1] J. Arrillaga, D. A. Bradley and P. S. Bodger, Power System Harmonics, John Wiley & Sons, July 1985.

[A.2] G. D. Breuer *et. al.*, "HVDC-AC Harmonic interaction, Part I: Development of a Harmonic Measurement System, Hardware and Software," IEEE Trans., Vol. PAS-101, pp. 709-718, 1982

# APPENDIX (B)

## Artificial Neural Network

An artificial neural network (ANN) is a connection of many neurons that mimic the biological system with the help of electronic computational circuits or computer software. It is also defined as neuro-computer or connectionist system in the literature.

An artificial neuron, called neuron or processing element (PE), is a concept of simulating the biological neuron. Fig. B.1 shows the structure of an artificial neuron. The input signals $X_1$, $X_2$, $X_3$,....., $X_n$ are normally continuos variables, but can also be discrete values. Each input signal flows through a gain called weight or connection strength. The summing node accumulates all the input weighted signals (activation signal) and then passes it to the output through the transfer function. The transfer function can be step or threshold function (passes logical 1 if the input exceeds a threshold, else 0), signum function (output is +1 if the input exceeds a threshold, else – 1), or linear threshold (with output clamped at +1). The transfer function can also be a nonlinear continuos type, such as sigmoid or hyperbolic tan. The most commonly used function is the sigmoid function and is given by

$$g(u) = \frac{1}{1+e^{-\alpha u}}$$

where $\alpha$ is the coefficient that determines the slope of the function that changes between the two asymptotic values (0 and +1). These transfer functions are also known as squashing functions, because they squash or limit the output between the two asymptotes.

Neural networks can be classified as feedforward (or layered) and feedback (or recurrent) types, depending on the interconnections of neurons. A network can also be defined as static or dynamic, depending on whether it is simulating static or dynamical systems. Fig. B.2 shows the structure of a feedforward multilayer network with n-input and n output signals (the number of input and output signals may be different). In this network, one layer of neurons forms the input layer and a second forms the output layer, with one intermediate or hidden layers existing between them. It is assumed that no connections exist between the neurons in a particular layer.

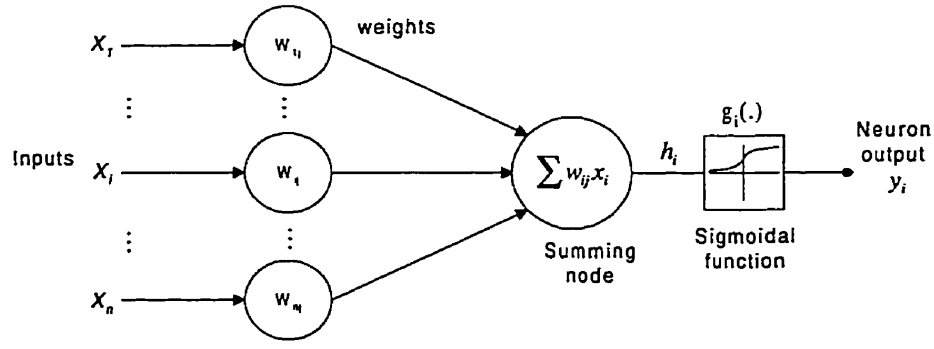


Fig. B.1 Basic artificial neuron model

The input and output layers have neurons equal to the respective number of signals. The input layer neurons do not have transfer functions, but there is a scale factor in each input to normalize the input signals. The number of hidden layers and the number of neurons in each hidden layer depend on the complexity of the problem being solved. The input layer transmits the computed signals to the first hidden layer, and subsequently the outputs from the first hidden layer are fed, as weighted inputs, to the second hidden layer. This construction process continues until the output layer is reached. Network input and output signals may be logical (0, 1), discrete bi-directional ($\pm 1$) or continuos variables. The sigmoid output signal can be clamped to convert to logical variables. It is obvious that such structure (parallel input parallel output) makes the neural network a multidimensional computing system where computation is done in a distributed manner.

For a feedforward neural network described earlier, weight learning is most commonly carried out by the method of backpropagation. Backpropagation learning rule alters the weight matrices between the output-hidden-input layers in a backward fashion. It carries out a minimization of the mean square error between the network outputs and a set of desired values for those outputs namely $d_i (i = 1, \cdots, n)$.

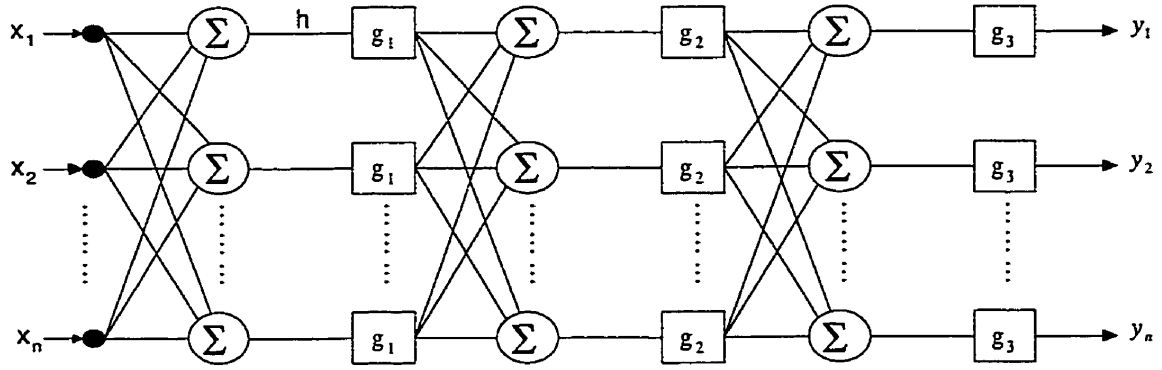


Fig. B.2 Structure of feedforward neural network

An appropriate error function is give by:

$$E(W) = \frac{1}{2}\sum_{i=1}^{n}(d_i - y_i)^T(d_i - y_i)$$

and this error, on the output must first be minimized by a best selection of output layer weights. Once the output layer weights have been selected the weights in the hidden layer next to the output can be adjusted by employing a linear backpropagation of the error term from the output layer. This procedure is followed until the weights in the input layer are adjusted.

Backpropagation rule uses out steepest descent corrections on the given weight matrices and its step-by-step procedure can be summarized as [B.1]:

Consider a network with M layers ($m = 1, 2, \ldots, M$) and use $y_i^m$ for the output of the $i^{th}$ unit in the *mth* layer. $y_i^0$ will be synonym for $x_i$, the *ith* input. Let $w_{ij}^m$ mean the connection from $y_i^{m-1}$ to $y_i^m$. Then the backpropagation procedure is:

1) Initialize the weights to small random values.

2) Choose an input pattern $x_i$ and apply it to the input layer (m=0) so that

$y_i^0 = x_i$ for all n

3) Propagate the signal forwards through the network using

$$y_i^m = g(h_i^m) = g(\sum_j w_{ij}^m y_i^{m-1})$$

for each $i$ and $m$ until the final outputs $y_i^M$ have been calculated.

4) Compute the deltas for the output layer

$$\delta_i^M = g'(h_i^M)[d_i - y_i^M]$$

by comparing the actual outputs with the desired ones $d_i$ for the corresponding input pattern.

5) Compute the deltas for the proceeding layers by propagating the errors backwards

$$\delta_i^M = g'(h_i^M)[d_i - y_i^M]$$

for $m = M, M-1, \ldots, 2$ until a delta has been calculated for every unit.

6) Use

$$\Delta w_{ij}^m = \eta \delta_i^m y_i^{m-1}$$

($\eta$ = learning rate parameter) to update the connections according to $w_{ij}^{new} = w_{ij}^{old} + \Delta w_{ij}$

7) Go back to step 2 and repeat for the next pattern.

## References

[B.1] J. Hertz, A. krogh and G. P. Richard, "Introduction to the theory of neural computation," *Addison-Wesley Publication Company, 1991.*

# APPENDIX (C)

## System Parameter and Controller Design Procedure

Supply Voltage $E_m$ =170 V
Line inductance =0.72 mH,
Line resistance = 0.272 $\Omega$
Output Capacitor = 2.65 $\mu$ F.
dc-side inductance=30 mH.
dc-side resistance=0.38 $\Omega$
Fundamental frequency = 60 Hz.
dc-side current $(I_{dc}^{*})=15A$,
$\varphi^{*}=0.0$,
Using the above system parameters and equation set (7.19), the matrices A, B, C and D can be determined as:

$$\mathbf{A}=\begin{bmatrix} 0 & 63986.7 & 377360 & -612.6 & -25346 \\ -2.22 & 0 & 3.58 & 2240 & 24.89 \\ -1388.9 & -379.83 & -377.78 & 379.83 & 0 \\ 2.22 & -233974 & -374.2 & -377.78 & 0 \\ 1.12 & -31.67 & 0 & 0 & -12.67 \end{bmatrix}$$

$$\mathbf{B}=\begin{bmatrix} -5583340 & -63374 \\ 5483.5 & -2240 \\ 0 & 0 \\ 0 & 0 \\ 2790.3 & 31.67 \end{bmatrix}$$

$\mathbf{C}=[0 \quad 0 \quad 0 \quad 0 \quad 1]$ and $\mathbf{D}=[0]$

$$G(s)=\frac{2790s^4-4.316\times10^6 s^3+2.921\times10^{12}s^2-2.263\times10^{15}s+7.648\times10^{20}}{s^5+768.2s^4+1.049\times10^9 s^3+4.094\times10^{11}s^2+2.746\times10^{17}s+3.483\times10^{18}}$$

$$H(s)=\frac{1}{0.02s+1}$$

$$GH(s)=\frac{2790s^4-4.316\times10^6 s^3+2.921\times10^{12}s^2-2.263\times10^{15}s+7.648\times10^{20}}{0.02s^6+16.63s^5+2.097\times10^7 s^4+9.237\times10^9 s^3+5.492\times10^{15}s^2+3.442\times10^{17}s+3.483\times10^{18}}$$

The objective is to design a controller that satisfy the following specifications:

- Steady state error ($e_{ss}$) to a unit step should be less than 5%.
- Phase margin of the compensated system should be more than 50°.

Procedure:

1. Use the final value theorem to calculate the low frequency gain $k$ required to achieve $e_{ss}$ specifications. For a type 0 system and a unit step

$$e_{ss}=\frac{1}{1+k_p}, \text{where } k_p=\lim_{s\to0} kGH(s)$$

$$\therefore k_p=219.55k$$

*and*

$$e_{ss}=\frac{1}{1+219.55}\le 0.05$$

$$\Rightarrow k=0.087$$

2. Make the Bode plot of $kGH(s)$

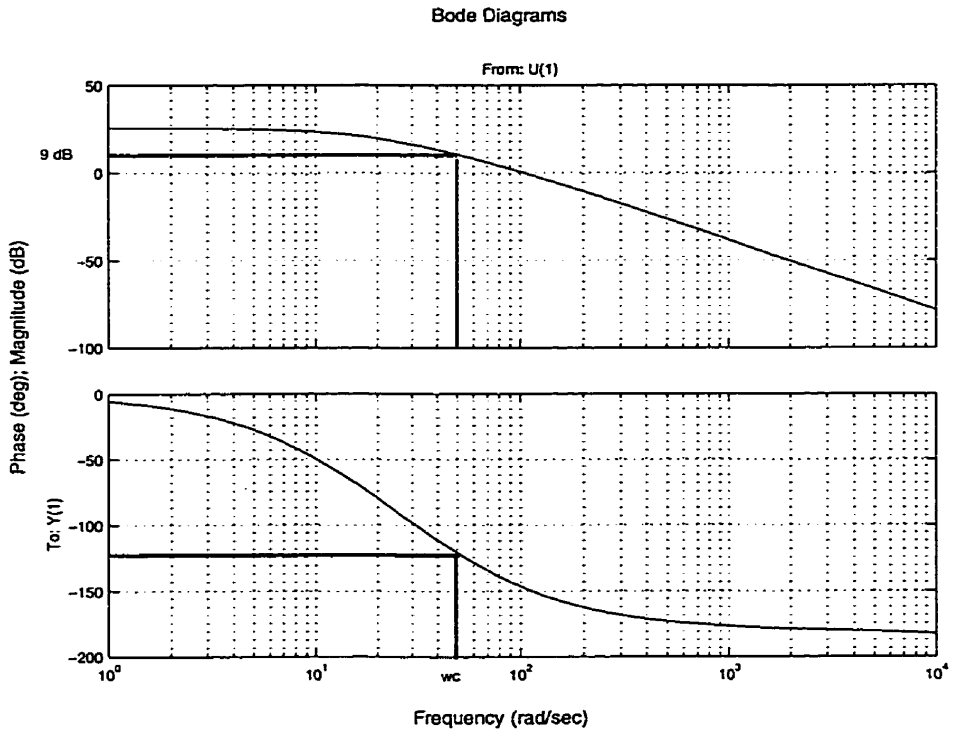


Fig. C.1: Bode diagram of $kGH(s)$ transfer function

3. find the frequency $\omega_c'$ at which the uncompensated phase margin is

$$\underline{|kGH(j\omega_c')} = -180^0 + \phi_m^* + \delta$$
$$= -180^0 + 50 + 5 = -125^0$$

Therefore, from Bode plot of $kGH(s)$, shown in Fig. C.1, $\omega_c' = 50\ rad/\sec$ and,

$|kGH(j\omega_c')| = 9\,dB$.

4. The gain reduction required to make $\omega_c'$ (the new zero crossover frequency) is equal to $9\,dB$.

$$\text{i.e. } \left|\frac{1}{\alpha}\right|_{dB} = -20\log_{10}(\alpha) = -9\,dB$$

$$\therefore \alpha = 10^{9/20} = 2.82$$

5. place the zero one decade below $\omega_c'$

$$\therefore \frac{1}{\tau} = \frac{\omega_c'}{10} = \frac{50}{10} = 5$$

$$\Rightarrow \tau = 0.2$$

$$\therefore G_c(s) = 0.087\left(\frac{1+0.2s}{1+(2.82)(0.2)s}\right) = \frac{0.0174s+0.087}{0.564s+1}$$

# APPENDIX (D)

## Cost of electricity according to waterloo North Hydro:

- The first 250 kWh/month, $0.121/kWh,
- The next 12,000 kWh/month, $0.078/kWh,
- The next 1,851,350 kWh/month, $0.057/kWh,
- Above 1,863,600 kWh/month, $0.078/kWh.

# APPENDIX (E)

## • Conduction Losses:

$P_{cond,\ loss} = 2\ (switches) \times I_{dc} \times V_f$

$V_f$ = Forward voltage drop of an IGBT.

## • Switching Losses:

$P_{switch,\ loss} = 4(switches) \times [1/2 \times V_{OFF} \times I_{ON} \times f_{sw} \times (t_{ON} + t_{OFF})]$

$V_{OFF}$ = Half-cycle average of the voltage across IGBT during OFF-period
= Half-Cycle average of line voltage

$I_{ON}$ = Current through IGBT during ON-period

# References

[1] R. C. Dugan, M. F. McGranaghan and H. W. Beaty, Electrical power systems Quality, McGraw-Hill, 1996

[2] J. Arrillaga, D. A. Bradley and P. S. Bodger, Power System Harmonics, John Wiley & Sons, July 1985.

[3] " IEEE Recommended Practices and Requirements for Harmonic Control in Power System," IEEE Std. 519-1992, IEEE, New York, 1993

[4] S. N. Govindarajan et. al., "Survey of Harmonic Levels on the Southwestern Electric power Company System," IEEE trans. on Power Delivery, Vol. 6, No. 4, pp. 1869-1873, Oct. 1991.

[5] IEEE Working Group on Power System Harmonic, "Bibliography of Power System Harmonics, Part I and II," Papers 84WM 214-3, IEEE PES Winter Meeting, January 29-February 3, 1984

[6] IEEE Working Group on Power System Harmonic, "Power System Harmonics: An Overview," IEEE trans. on Power App. Syst., PAS-102 (8), pp. 2455-2460, Aug. 1983.

[7] Greenwood, Electrical Transients in Power Systems, John Wiley & Sons, Inc. New York, 1991.

[8] M. D. Cox and A. Mirbod, "A New Static Var Compensator for an Arc furnace," IEEE Trans. on Power Systems, Vol. PWRS-1(3):110-119 August 1986.

[9] G. Manchur and C.C. Erven, "Development of a Model for Predicting Flicker from Electric Are Furnaces," IEEE Tran. On Power Delivery, Vol.7, No. 1, pp. 416-426, January 1992.

[10] R. Yacamimi and J. C. Oliveira, " Harmonics in multiple Converter System: A Generalized Approach," IEE Proceeding, Vol. 127, No. 2, pp. 98-106, March 1980

[11] R. Yacamimi and J. C. Oliveira, " Comprehensive Calculation of Converter Harmonics with System Impedances and Control Representation," IEE Proceeding, Vol. 133, No. 2, pp. 95-102, March 1986

[12] G.P. Christoforidis and A. P. Meliopoulos, " Effects of Modeling the Accuracy of Harmonic Analysis," IEEE Tran. On Power Delivery, Vol.5, No. 3, pp. 1598-1607, July 1990.

[13] D. E. Steeper and R. P. Stratford, "Reactive Compensation and Harmonic Suppression for Industrial power Systems Using Thyristor Converters," IEEE Trans. Industry Applications, IA-12 (3), pp. 232-254 May/June 1976.

[14] D. E. Rice, "Adjustable Speed Drivers and Power Rectifier Harmonics – Their effects on Power System Components," IEEE Trans. Industry Applications, IA-22 (1), pp. 161-177, Jan./Feb. 1986.

[15] Douglas, J.: "Solving problems of power quality", EPRI Journal, pp. 6-15, Dec 1993.

[16] Heydt, G. H, Electrical Power Quality, Stars in a Circle Publications, 1991.

[17] D. A. Gonzalez and J. C. McCAll, "Design of Filters to Reduce Harmonic Distortion in Industrial Power System," in IEEE/IAS Conference Proceeding, pp. 361-370, 1985.

[18] M. F. McGranaghan and D. R. Mueller, "Design Harmonic Filters for Adjustable Speed Drivers to comply with IEEE-519 Harmonic Limits," IEEE Trans. Industry Applications, IA-35 (2), pp. 312-318, March/April. 1999.

[19] B. Singh, K, Al-Haddad and A. Chandra, "A Review of Active Filters for Power Quality Improvements," IEEE Trans. on Industrial Electronics, Vol.46(5), pp.960-971, Oct. 1999.

[20] W. M. Grady, M. J. Samotyj, and A. H. Noyola, "Survey of Active Line Conditioning Methodologies," IEEE Trans. on Power Delivery, Vol. PWRD-5(3), pp.1536-1542, July 1990.

[21] H. Akagi, "Trends in Active Power Line Conditioners," IEEE Trans. on Power Electronics, Vol.9(3), pp.263-268, may 1994.

[22] H. Akagi, "New Trends in Active Filters for Power Conditioning," IEEE Trans. Industry Applications, 32(6), pp. 1312-1322, Nov./Dec 1996.

[23] A. Domijan and E. Embriz-Santander, "A Summary and Evaluation of Recent Developments on Harmonic Mitigation Techniques Useful to Adjustable Speed Drivers," IEEE Trans. energy Conversion, 7(1), pp. 64-71, March 1992

[24] H.I. Yunus and R.M. Bass, "Comparison of VSI and CSI Topologies for Single-Phase Active Power Filters", in Proceedings of IEEE Power Electronics Specialists Conference, pp. 1892-1896, 1996.

[25] H. Fugita and H. Akagi, " An Approach to Harmonic-Free Power Conversion for Large Industrial Loads: The Integration of a Series Active Filter with a Double-Series Diode Rectifier," in IEEE/IAS Conference Proceedings, 1996, pp. 1040-1047, 1996.

[26] H. Sasaki and T. Machida, " A New Method to Eliminate ac Harmonic Currents by Magnetic Flux Compensation—Consideration on Basic Design," IEEE Trans. Power App. Syst., pp. 2009-2019, Feb.1971.

[27] B. M. Bird, J. F. March, and P. R. McLellan, " Harmonic Reduction in Multiplex Converters by Triple frequency Current Injection," Proc. IEE, 116(10), pp. 1730-1734, Oct. 1969.

[28] A. Ametani, "Harmonic Reduction in ac-dc Converters by Harmonic Current Injection," Proc. IEE, 119, pp. 857-864, July 1972.

[29] A. Ametani, " Harmonic reduction in Thyristor Converters by Harmonic Current Injection," IEEE Trans. Power App. Syst., PAS-95(2), pp. 441-449, Mar./Apr. 1976.

[30] L. Gyugyi and E. C. Strycula, "Active AC Power Filters," IEEE Industrial applications Society Annual Meeting, pp. 529-535, 1976.

[31] H. Akagi, Y. Kanazawa and A. Nabae, "Instantaneous Reactive Power Compensators Comprising Switching Devices without Energy Storage Components," IEEE Trans. Industry Applications, 20(3), pp. 625-630, May/June 1984.

[32] Y. Hayashi, N. Sato and K. Takahashi, " A Novel Control of a Current-Source Active Filter for AC Power System Harmonic Compensation," IEEE Trans. Industry Applications, 20, pp. 625-630, May/June. 1984.

[33] S. H. Kim, J. K. Park, J. H. Kim, G. H. Choe and M. H. Park, "An Improved PWM Current Control Method for Harmonic Elimination Using Active Power Filter," IEEE Industrial applications Society Conf. Rec., Feb 1987.

[34] R. Fisher and R. Hoft, " Three-Phase power Line Conditioner for Harmonic Compensation and Power Factor Correction," IEEE Industrial applications Society Conf. Rec., Feb 1987.

[35] M. Shashani, " Hamonic Reduction Using Gate Turn-Off Thyristors in Static VAR Compensators (Part-I)," IEEE Industrial applications Society Conf. Rec., Feb 1987.

[36] M. Takeda, K. Ikeda and Y. Tominaga, "Harmonic Current Compensation with Active Filter," in Proc. 1987 IEEE/IAS Annual Meeting, pp. 808-815, 1987.

[37] L. T. Moran, P. D. Ziogas and G. Joos, "Analysis and Design of a Novel 3-Phase Solid State Power Factor Compensation and Harmonic Suppression System," IEEE Applied Power Electronic Conf. Rec., Feb 1988

[38] P. N. Enjeti, P.D. Ziogas, and J. F. Lindsay, "Programmed PWM Techniques to Eliminate Harmonics. A Critical Evaluations," IEEE Industrial applications Society Conf. Rec., Oct. 1988.

[39] G. Choe, A. K. Wallace and M. Park, " Control Technique of Active Power Filter for Harmonic and Reactive Power Control," IEEE Industrial applications Society Conf. Rec., Oct. 1988.

[40] S. M. Williams and R. Hoft, "Discrete Controlled Harmonic and Reactive Power Compensator," IEEE Industrial applications Society Conf. Rec., Oct. 1988.

[41] S. M. Williams and R. G. Hoft, "Implementation of Current Source Inverter for Power Line Conditioning," in IEEE Industry Applications Society Annual Meetings, Vol.2, pp. 1073-1080, Oct. 7th –12th 1990.

[42] S. Fokuda and M. Yamaji, " Design and Characteristics of Active Power Filter Using Current Source Converter," in IEEE Industry Applications Society Annual Meetings, Vol.2, pp. 965-970, Oct. 7th –12th 1990.

[43] F. Z. Peng, H. Akagi and A. Nabae, "A New Approach to Harmonic Compensation in Power Systems—A Combined System of Shunt Passive and Series Active Filters," IEEE Trans. Industry Applications, 26(6), pp. 983-986, Nov./Dec. 1990.

[44] H. Fugita and H. Akagi, " A Practical Approach to Harmonic Compensation in Power Systems-Series Connection of Passive and Active Filters," IEEE Trans. Industry Applications, 27, pp. 1020-1025, 1991.

[45] N. Tokuda, Y. Ogihara, M. Oshima, and T. Miyata, "Active Filter with Series LC circuit," in Proc. 1994 IEEE/PES Int. Conf. Harmonics in Power Systems, 1994, pp. 242-249.

[46] A. van Zyl, J. H. R. Enslin and R. Spee, "A New Unified Approach to Power Quality Mangament," IEEE Trans. Power Electronics, 11(5), pp. 691-697, Sept.. 1996.

[47] A. van Zyl, J. H. R. Enslin and R. Spee, " Converter-Based Solution to Power Quality Problems on Radial Distribution Lines," IEEE Trans. Industry Applications, Vol. 32, No. 6, Nov./Dec 1996, pp. 1323-1330.

[48] H. Akagi, "New Trends in Active Filters for Power Conditioning," IEEE Trans. Industry Applications, Vol. 32, No. 6, Nov./Dec 1996, pp. 1312-1322.

[49] H. Fujita and H. Akagi, " The Unified Power Quality Conditioner: The Integration of Series- and Shunt-Active Filters," IEEE Transactions on Power Electronics, Vol. 13, No. 2, March 1998, pp. 315-322.

[50] M. Aredes, K. Heumann and E. H. Watanabe, " An Universal Active Power Line Conditioner," IEEE Trans. Power Delivery, vol. 13, No. 2, April 1998, pp. 545-551.

[51] T. A. Meynard and H. Foch, "Multilevel Converters and Drive Topologies for High Power Conversion," in proceedings of the IEEE 21st International Conf. on Industrial Electronics, Control, and Instrumentation, pp. 21-26, 1995.

[52] J-S Lai and F. Z. Peng, "Multilevel Converters --A New Breed of Power Converters," IEEE Trans. on Industry Applications, 32(3), pp. 509-517, May/June 1996.

[53] H. Akagi, Y. Tsukamoto, and A. Nabae, "Analysis and Design of an Active Power Filter Using Quad-Series Voltage Source PWM Converters," IEEE Trans. Industry Applications, Vol.26, pp. 93-98, Jan/Feb. 1990.

[54] Mohan, N., Underland, T., and Robbins, W., Power Electronics: Converters, Applications and Design, John Wiley & Sons, July 1995.

[55] X. Wang and B. T. Ooi, "A Unity Power Factor Current-Source Rectifier Based on Dynamic Tri-logic PWM," IEEE Trans. on Power Electronics, Vol.8 (3), pp.288-294, July 1993.

[56] G. R. Kamath and N. Mohan, "Series-Connected, All-Hybrid Converters for Utility Interactive Applications," Proceedings of the IECON'97 23rd International Conference on Industrial Electronics, Control, and Instrumentation, Vol. 2, pp. 726-731, 9-14 Nov, 1997.

[57] F. Z. Peng, J. W. McKeever and D. J. Adams "A Power Line Conditioner using Multilevel Inverters for Distribution Systems," IEEE Trans. on Industry Applications, Vol.34(6), pp. 1293-1298, Nov/Dec 1998.

[58] F. Z. Peng, H. Akagi and A. Nabae "A Study of Active Power Filters Using Quad-Series Voltage-Source PWM Converters for Harmonic Compensations," IEEE Trans. on Power Electronics, Vol. 5(1), pp. 9-14, Jan. 1990.

[59] R. El Shatshat, M. Kazerani, and M.M.A. Salama, "Modular Approach to Active Power-Line Harmonic Filtering," Proceedings of IEEE Power Electronics Specialists Conference (PESC 98), Japan, pp. 223-228, 1998.

[60] S. J. Huang and J. C. Wu, " Design and Operation of Cascade Active Power Filters for the reduction of Harmonic Distortions in A Power System," IEE Proc.-Gener. Transm. Distrib., Vol. 146, No. 2, pp. 193-199, March 1999.

[61] E. F. El-Saadany, R. El Shatshat, M.M.A. Salama, M. Kazerani, and A. Y. Chikhani, "Reactance One-Port Compensator and Modular Active Filter for Voltage and Current Harmonic Reduction in Non-Linear Distribution Systems: A Comparative Study," Electric Power Systems Research (52), 1999, pp. 197-209.

[62] Cooly, J. W., and Tukey J. W., " An Algorithm for Machine Calculation of Complex Fourier Series", Journal Math. Comput., Vol. 19, pp. 297-301, 1965.

[63] Harris, J., "On the use of window for harmonic analysis with DFT," Proc. IEEE, Vol. 66, pp. 51-83, 1978.

[64] E. Oran Brigham, "The fast fourier transformer and its applications," Prentice Hall International, 1988.

[65] Girgis, A.A. and Ham, F., "A quantitative Study of Pitfalls in FFT", IEEE Trans. Aerosp. Electron. Syst., Vol. 16, No. 4, pp. 434-439, 1980.

[66] W. M. Grady and G. T. Heydt, " Prediction of power system harmonics due to Gaseous Discharge Lighting," IEEE Trans. on Power Systems, Vol. 104, pp. 554-561, March 1985.

[67] M. Sharaf and P. K. Dash, "A Kalman Filtering Approach for estimating power System Harmonics," Proceeding of the Third International Conference on Power system Harmonics, pp. 34-40, 1989.

[68] Girgis, A.A., Chang, W.B., and Makram, E.B., "A Digital Recursive Measurement Sheme for On-Line Tracking of Power System Harmonics", IEEE Trans. Power Delivery, Vol. 6, No. 3, pp. 1153-1160, July 1991.

[69] Haili Ma, and Girgis, A. A., "Identification and tracking of Harmonic Sources in a Power System Using a Kalman Filter," IEEE Trans. Power Delivery, Vol. 11, No. 3, pp. 1659-1665, July 1996.

[70] Moreno Saiz, V., and Barros Guadalupe, J., "Application of Kalman Filtering for continous real time tracking of power system harmonics," IEE Proc. –Gener. Transm. Distrib., Vol. 144, No. 1, pp. 13-20, Jan. 1997

[71] D. J. Pileggi, N. H. Chandra and A. E. Emanuel, "Prediction of Harmonic Voltages in Distribution Systems," IEEE Trans. on Power Systems, Vol. 100, No. 3, March 1981.

[72] S. A. Soliman, G. S. Christensen, D. H. Kelly and K. M. El-Naggar, " A State Estimation Algorithm for Identification and Measurements of Power System Harmonics", Electric Power System Research Journal, Vol. 19, pp. 195-206, 1990.

[73] R. K. Hartana, and G. G. Richards, " Harmonic source monitoring and identification using neural networks", IEEE Trans. on Power Systems, Vol. 5, No. 4, pp. 1098-1104, Nov. 1990

[74] H. Mori, "An arificial neural network based method for power system voltage harmonics", IEEE Trans. on Power Delivery, Vol. 7, No. 1, pp. 402-409, 1992.

[75] S. Osowski, "Neural network for estimation of harmonic components in a power system", IEE Proceeding-C, Vol. 139, No.2, pp. 129-135, March 1992.

[76] N. Pecharanin, H. Mitsui and M. Sone, " Harmonic Detection by Using Neural Network," In IEEE Conf. Proceedings, Industry Applications Society Annual Meeting, pages 923-926, 1995

[77] P. K. Dash, D. P. Swain, A. C. Liew, and S. Rahman, "An adaptive linear combiner for on-line tracking of power system harmonics" IEEE Trans. on Power Systems, vol. 11, No. 4, pp. 1730-1735,Nov.1996.

[78] Dash, P.K., Panda, S.K., Mishra, B., and Swain, D.P., "Fast Estimation of Voltage and Current Phasors in Power Networks Using an Adaptive Neural Network", IEEE Trans. Power Systems, Vol. 12, No. 4, pp. 1494-1499, Nov. 1997.

[79] Bernard W., and Michael A. L., "30 years of adaptive neural networks: Perceptron, Madaline, and Backpropagation", Proceedings of the IEEE, Vol. 78, No. 9, pp. 1415-1442, Sep. 1990.

[80] T. A. George and D. Bones, "Harmonics Power Flow Determination Using The Fast Fourier Transform," *IEEE Trans. Power Delivery*, vol. 6, no. 2, pp. 530-535, April 1991.